THE ROLE OF P-REX2 PROTEIN IN THE DYSFUNCTION OF THE ENDOTHELIAL BARRIER

Inaugural Dissertation
submitted to the Faculty of Medicine
in partial fulfillment of the requirements
for the PhD-Degree
of the Faculties of Veterinary Medicine and Medicine
of the Justus Liebig University Giessen

by
Sevinç, Neslihan
of
Istanbul

Giessen 2022

From the University Hospital Giessen and Marburg,
Medical Clinic I, Cardiology and Angiology
Director: Prof. Dr. Christian W. Hamm
of the Faculty of Medicine of the Justus Liebig University Giessen

First Supervisor and Committee Member:

Dr. Muhammad Aslam

Second Supervisor and Committee Member:

Prof. Dr. Martin Diener

Committee Members:

Prof. Dr. Norbert Weissmann

Prof. Dr. Gabriela Krasteva-Christ

Date of Doctoral Defense: 06.02.2023

DECLARATION

I declare that I have completed this dissertation single-handedly without the unauthorized help of a second party and only with the assistance acknowledged therein. I have appropriately acknowledged and referenced all text passages that are derived literally from or are based on the content of published or unpublished work of others, and all information that relates to verbal communications. I have abided by the principles of good scientific conduct laid down in the charter of the Justus Liebig University of Giessen in carrying out the investigations described in the Dissertation.

Giessen, ……

Neslihan Sevinç

I TABLE OF CONTENTS

1 INTRODUCTION 1
1.1 The Endothelial Barrier and Its Dysfunction 1
1.2 Reactive Oxygen Species (ROS) and Endothelial Cells 3
1.2.1 Endothelial NADPH oxidases (NOXs) 6
1.3 Pathological Angiogenesis and Vascular Inflammation 7
1.4 Dual Role of the Rho Family of GTPase Rac1 on Endothelial Barrier 8
1.5 P-Rex2 10
2 AIM OF THE STUDY 13
3 METHODS 15
3.1 Cell Culture Techniques 15
3.1.1 Isolation of primary cells 15
3.1.2 Cultivation of cells 16
3.1.3 Treatments 16
3.1.4 Cell counting 17
3.1.5 Cryopreservation and thawing 17
3.2 Molecular Biology Techniques 17
3.2.1 RNA isolation and cDNA synthesis 17
3.2.2 Quantitative real time PCR (q-PCR) 19
3.2.3 Cloning 20
3.2.4 Transfection 21
3.3 Lentivirus-based Stable Gene Expression 22
3.3.1 Lentivirus production 23
3.3.2 Calculation of lentiviral titer 24
3.3.3 Lentiviral transduction 24
3.3.4 Kill curve generation 25
3.4 Protein Biochemistry 25
3.4.1 Protein sample preparation for western blot 25
3.4.1.1 Measurement of protein concentration 25
3.4.2 SDS-PAGE 26
3.4.3 Western blotting 27
3.4.4 Immunoprecipitation 28
3.5 Pull-Down Assay 29

3.6 Immunostaining 30
3.7 The *in vitro* Wound Healing Assay 31
3.8 The *in vitro* Spheroid-based Sprouting Assay 31
3.8.1 The spheroid cultures of endothelial cells 31
3.8.2 The *in vitro* sprouting assay 31
3.9 The Permeability Measurement of Endothelial Monolayers 32
3.10 ROS Measurements 32
3.11 Statistical Analysis 33
4 RESULTS 34
4.1 Molecular Validation of the Expression Vectors 34
4.2 Activation of Rac1 in Response to Inflammation 38
4.3 The Role of P-Rex2 Overexpression on Endothelial Barrier 40
4.3.1 Effect of P-Rex2 overexpression on EC permeability 40
4.3.2 Effect of P-Rex2 overexpression on AJs and actin cytoskeleton in response to TNF-α 41
4.4 The Role of P-Rex2 in the Pathological Angiogenesis 47
4.4.1 Effect of P-Rex2 overexpression on EC migration 47
4.4.2 Effect of P-Rex2 overexpression on *in vitro* sprouts in ECs 49
4.4.3 Effect of P-Rex2 overexpression on expression of cell adhesion molecules in ECs 50
4.4.4 Effect of P-Rex2 overexpression on expression of inflammatory cytokines in ECs 52
4.5 Effect of P-Rex2 Overexpression on ROS Generation in ECs 53
4.5.1 The role of P-Rex2 in NADPH oxidase-dependent ROS formation 56
5 DISCUSSION 59
5.1 Main Findings 59
5.2 TNF-α Induces P-Rex2-mediated Rac1 Activation 60
5.3 Overexpression of P-Rex2 Disrupts Endothelial Barrier 61
5.4 P-Rex2 Overexpression Triggers Pathological Angiogenesis 64
5.5 P-Rex2 Overexpression Triggers TNF-α-induced-NADPH oxidase-dependent ROS Formation 65
5.6 Conclusion 67
5.7 Future Perspective 69
6 SUMMARY 71
7 ZUSAMMENFASSUNG 73

8 REFERENCES 75
9 MATERIALS 89
9.1 Chemicals and Consumables 89
9.2 Antibodies 93
9.3 Enzymes and Inhibitors 93
9.4 Kits 94
9.5 Plasmids 94
9.6 Equipments 95
9.7 Software 96
10 LIST OF ABBREVIATIONS 97
11 ACKNOWLEDGMENT 103

1 INTRODUCTION

1.1 The Endothelial Barrier and Its Dysfunction

The endothelial cells (ECs), which are closely connected via adherens junctions (AJs) and tight junctional proteins of adjacent cells, cover the intima of blood vessels with a single layer. This monolayer functions as a dynamic semi-permeable barrier to control the passage of molecules between blood and surrounding tissues (Aghajanian et al., 2008; Mehta & Malik, 2006). The exchange of gases, water, ions, nutrients, leukocytes, and macromolecules across vessel walls is regulated via the vascular endothelium by following transcellular and paracellular pathways. Tightly integrated ECs losen their interaction and then recover again in a controlled way to open paracellular gaps for the transport of leukocytes and macromolecules across the endothelium (Küppers et al., 2014). Thus, the vascular endothelium has a crucial role in maintaining vascular tone, tissue homeostasis, and oxidative and inflammatory states of surrounding tissues (Bazzoni, 2006; Mehta & Malik, 2006). However, ECs may lose their function. That can result in barrier failure (Fig. 1.1). Loss of endothelial barrier integrity leads to gap formation between adjacent cells; hence, it causes uncontrolled leakage of small molecules and recruitment of leukocytes and other macromolecules in tissues (Komarova et al., 2017; Yuan et al., 2012). Thus, it has a pivotal role in the pathogenesis of human diseases such as atherosclerosis, diabetes, inflammatory diseases, acute lung injury, cancer, and other diseases (Chistiakov et al., 2015; Bonetti et al., 2003; Groeneveld, 2002; Kumar et al., 2009; Franses et al., 2013).

The function of the endothelium is precisely regulated via balancing forces generated by ECs contractile machinery. These forces are maintained by the actomyosin cytoskeleton dynamics, cell-cell adhesion molecules located at the surface of the adjacent cells, and the forces tethering ECs to the surrounding matrix (Gulino-Debrac, 2013; Liu et al., 2015). For instance, controlled polymerization/depolymerization of actin filaments regulates the integrity of cell-cell junctions as well as the formation of plasma membrane protrusions for cell migration and morphogenesis. Thus, the cytoskeletal dynamics also control endothelial barrier integrity and cell motility (Liu et al., 2015; Prasain & Stevens, 2009). Additionally, endothelial barrier integrity is strengthened by AJs. The interplay between cytoskeleton components and vascular endothelial cadherin (VE-cadherin)-based AJs supports the adhesion of ECs, and signaling pathways interfering with this

interaction may modulate endothelial barrier integrity (Potente et al., 2011; Vandenbroucke et al., 2008). The actin-binding proteins and members of the Rho family of small GTPases Ras homolog family member A (RhoA), Ras-related C3 botulinum toxin substrate 1 (Rac1), and Cell division control protein 42 homolog (Cdc42) are crucial mediators of the actin cytoskeleton dynamics and are thus involved in the regulation of AJs´ and endothelial barrier stability (Vouret-Craviari et al., 1998; Spindler et al., 2010; Tojkander et al., 2012). For instance, Rac1 was shown in the progression of various cardiovascular diseases by either rearranging cytoskeleton dynamics or overproducing reactive oxygen species (ROS) (Sawada et al., 2010).

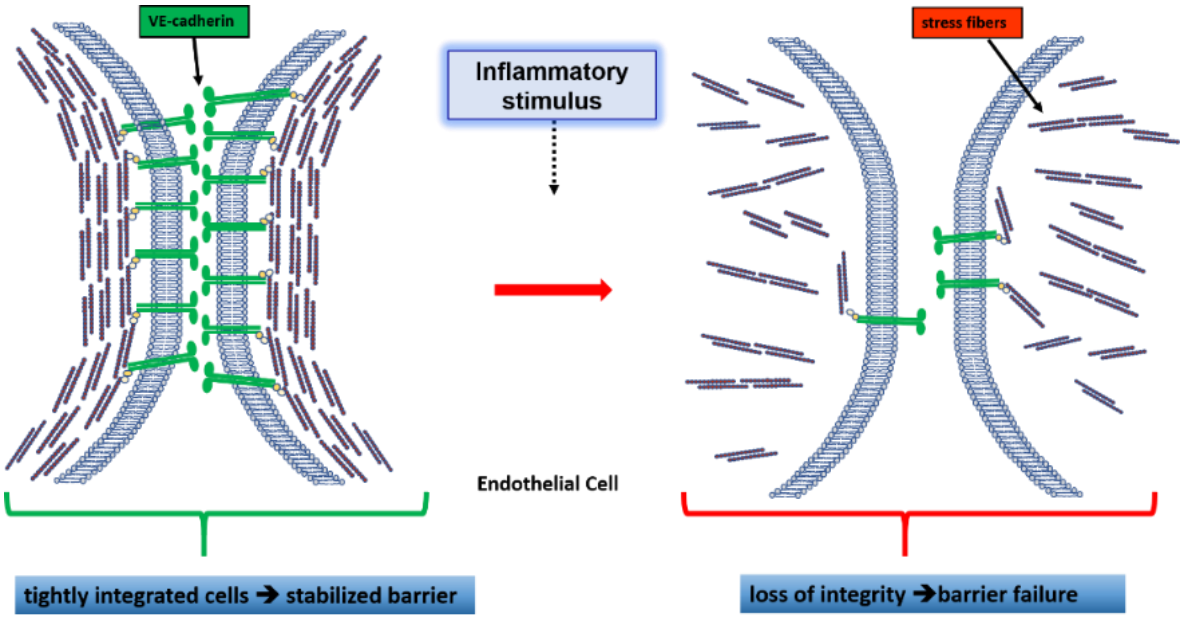

Figure 1.1: Schematic illustration of the mechanism of endothelial barrier dysfunction. Inflammatory mediators like Tumor necrosis factor-α (TNF-α) leads to loss of integrity of adjacent cells and thus barrier failure by regulating contractile machinery, AJs, and actin dynamics.

The factors regulating actin cytoskeleton dynamics are important mediators in regulating endothelial barrier function. Actin exists as globular actin (G-actin) in a monomeric form and as filamentous actin (F-actin) in a polymeric form, and both forms are present in a tightly balanced manner in ECs (Carlier & Pantaloni, 1997; Koestler et al., 2009). Nevertheless, this balance can be disrupted in favor of F-actin to regulate various cellular functions and maintain cell shape and polarity (Dominguez & Holmes, 2011). Additionally, inflammatory stimuli, growth factors, or

signaling cascades that occur through pathological conditions alter the F-actin level by activating cellular pathways such as RhoA/ROCK pathway (Deng et al., 2018). Increased F-actin forms stress fibers together with myosin filaments as a part of contractile machinery (Hotulainen & Lappalainen, 2006). The stress fibers consist of bundles of approximately 10 to 30 actin filaments crosslinked with alpha-actinin (α-actinin) and anchored to focal adhesions to serve as a bridge for the interaction of actin cytoskeleton with the extracellular matrix (ECM) (Tojkander et al., 2012). Bi-polar arranged myosin II bundles slide along these actin filaments, and this movement leads to the contraction of the actomyosin bundle (Pellegrin & Mellor, 2007). Thus, the increase in stress fibers leads to stretching throughout the cytoplasm causing loss of cell-cell contacts, thereby gap formation (Noria et al., 2004; Dudek & Garcia, 2001; Bogatcheva & Verin, 2008).

It was revealed that vascular endothelial growth factor (VEGF)-induced activation of Rac1 activates the nicotinamide adenine dinucleotide phosphate (NADPH) oxidases (NOXs) and thus increases the generation of ROS. The overproduction of ROS resulted in the re-arrangement of VE-cadherins and beta-catenins (β-catenins) by tyrosine phosphorylation, increased the endothelial permeability, and thereby endothelial barrier dysfunction (Monaghan-Benson & Burridge, 2009; Wildenberg et al., 2006). Similarly, Gavard and Gutkind showed that activation of Rac1 downstream of VEGF leads to internalization of VE-cadherin into clathrin-coated, resulting in cells losing their contact and permeability of the barrier increases (Gavard & Gutkind, 2006). On the contrary to that, the signaling cascade triggered by the increased level of cyclic adenosine 3′,5′-monophosphate (cAMP) via protein kinase A (PKA) activated Rac1 via its guanine nucleotide exchange factor (GEF) Vav2 and led to suppression of RhoA activity (Qiao et al., 2008; Birukova et al., 2008). The inhibition of RhoA activity increased the accumulation of α-catenin to the cell-cell contacts and its linking to α-actinin, which stabilizes VE-cadherin-based AJs, thereby the integrity of the EC barrier (Beckers et al., 2010). Identifying signaling cascades and pathways controlling endothelial barrier function/dysfunction is vital for managing critical disease conditions and developing therapeutic strategies.

1.2 Reactive Oxygen Species (ROS) and Endothelial Cells

Free radicals and various molecules derived from molecular oxygen that has two unpaired electrons in the outer shell are called ROS (Turrens, 2003). In the vascular cells, various types of ROS, especially superoxide ($O_2^{-\cdot}$), hydrogen peroxide (H_2O_2), and nitric oxide ($NO^{\cdot}$), are

produced. Although NO· has a vasodilatory effect and shows anti-inflammatory characteristics, its interaction with O_2^{-}· produces peroxynitrite ($ONOO^{\cdot-}$) (Papaharalambus & Griendling, 2007). Physiological levels of ROS are involved in several biological functions, such as signal transduction, controlling vascular tone, maintenance of redox homeostasis, sensing of oxygen tension, regulation of oxygen concentration-related cellular functions, and others (Dröge, 2002). On the other hand, excessive or uncontrolled production of ROS generates oxidative stress leading to oxidation of deoxyribonucleic acid (DNA), protein, carbohydrates, and lipids, thereby leading to pathological conditions, such as atherosclerosis, hypertension, diabetes, heart failure, asthma and acute lung injury (Cai & Harrison, 2000; van der Vliet & Cross, 2000; Burtenshaw et al., 2019).

ECs are known as the leading vascular source of ROS such as O_2^{-}·, H_2O_2, NO·, $ONOO^{\cdot-}$ and hydroxyl radicals (·OH) (Li & Shah, 2004). Indeed, it was shown that the production of ROS is accelerated in EC monolayers upon treatment with known inducers of ROS such as Interleukin-1 beta (IL-1β), interferon-gamma (IFN-γ), vasoactive peptides, and hypoxia/reoxygenation (Boueiz & Hassoun, 2009). To date, several enzymatic systems are defined as an endogenous source of ROS in ECs, which are the NADPH oxidases (NOXs), xanthine oxidase (XO), mitochondrial electron-transport chain, cytochrome P450 (CYP), and uncoupled endothelial NO synthase (eNOS) (Dröge, 2002).

Mitochondrial ROS production serves as one of the important sources of intracellular ROS in ECs. ROS generation can be triggered upon stimulation in mitochondria, besides its physiological production (Bretón-Romero & Lamas, 2014; Du et al., 2000; Pearlstein et al., 2002; Yamagishi et al., 2001). In mitochondria, molecular oxygen is either completely reduced to H_2O or partially reduced to O_2^{-}· by the one-electron reduction with electrons derived from nicotinamide adenine dinucleotide (NADH) or dihydroflavine-adenine dinucleotide ($FADH_2$) (Finkel, 2011; Sena & Chandel, 2012). Generated O_2^{-}· is further converted to H_2O_2 with mitochondrial superoxide dismutase (MnSOD). The uncharged H_2O_2 is more stable and can pass through the membrane, unlike O_2^{-}· (Zhang & Gutterman, 2007).

NADPH oxidases are the major known source of ROS in vascular endothelium (Bretón-Romero & Lamas, 2014). Moreover, unlike their main function in phagocytic cells as a part of the host defense mechanism to kill microorganisms, NADPH oxidases are involved in various cellular

functions in vascular cells. Hence, they are described as vascular NADPH oxidases (Babior, 2000; Dupré-Crochet et al., 2013). The main subunit of the NADPH oxidase complex gp91phox was initially discovered in phagocytes (Babior et al., 1973; Babior, 1999). Later, the identified homologs of gp91phox (NOX2) in different tissues were named as NOX1, NOX3, NOX4, NOX5, dual oxidase-1 (DUOX1), and dual oxidase-2 (DUOX2) (Suh et al., 1999; Cheng et al., 2001; Edens et al., 2001). Until now, only NOX1, NOX2, NOX4, and NOX5 isoforms were identified in ECs (Frey et al., 2009) (Fig. 1.2).

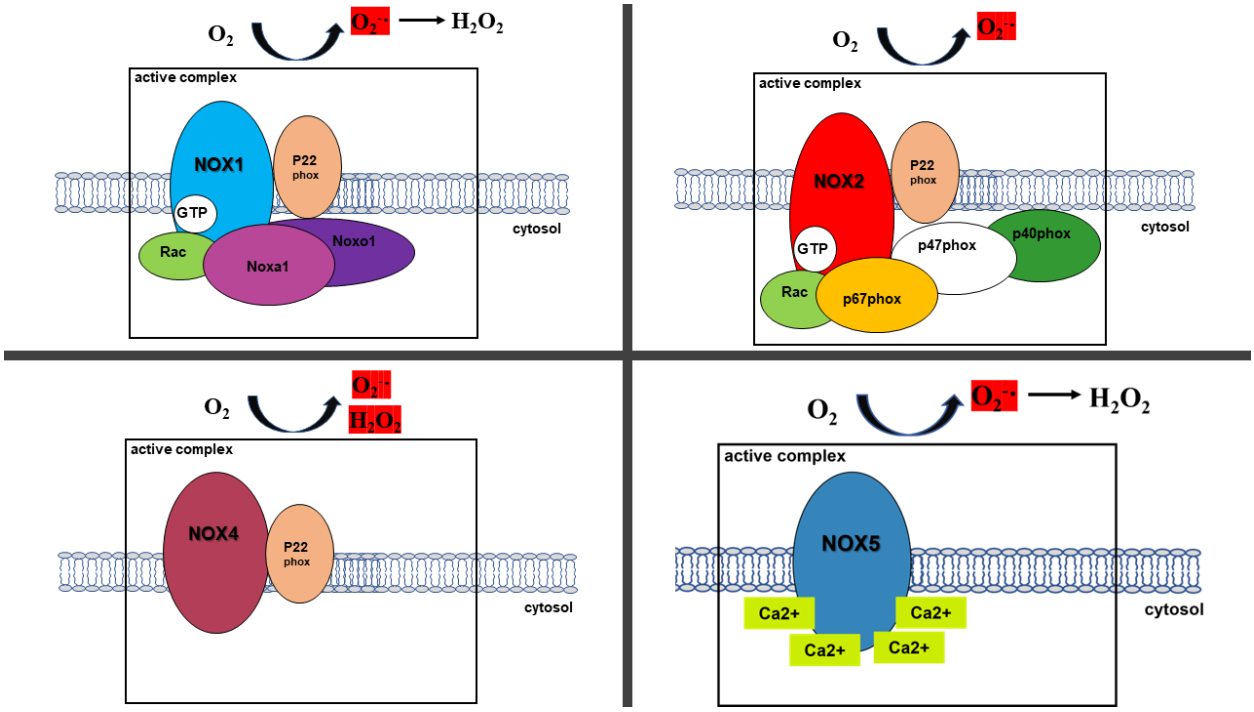

Figure 1.2: Endothelial NADPH oxidases. NADPH oxidases are membrane-bound proteins and have six transmembrane spanning α-helices with cytosolic N and C-termini (Altenhöfer et al., 2012). On this transmembrane domain, there are two heme domains that are bound to the conserved histidine residues. Two irons in heme domains act as an electron carrier to provide a channel for the passage of electrons, which are initially transferred from NADPH to FAD and from FAD to heme domains. In a final reaction, molecular oxygen is reduced to $O_2^{-\cdot}$ (Lambeth, 2004). While NOX 1,2, and 4 are consisting of NADPH and FAD-binding domains at the cytoplasmic C-terminus, NOX5 includes an additional calmodulin-like Ca^{2+}-binding domain at the N-terminus (Dworakowski et al., 2008b). The third extracytosolic loop (E-loop) of NOX4 has additional amino acids to provide protons for dismutation of $O_2^{-\cdot}$ to generate H_2O_2 (Takac et al., 2011). *Adapted from (Frey et al., 2009).*

The assembly of different components regulates the activity of the NADPH oxidase complexes; gp91phox, p22phox, p47phox, p40phox, p67phox, Rac, and heat shock protein 90 (Hsp90) (Altenhöfer et al., 2012). In ECs, NOX1 and NOX2 require guanosine triphosphate (GTP)-bound active Rac1 to show activity (Abo et al., 1991; Cheng et al., 2006). While gp91phox and p22phox exist as membrane-bound in the cells, other components are thought to be present in the cytosol under basal conditions (Babior, 1999). Upon induction, cytosolic components translocate to the membrane to form the NADPH oxidase enzyme complex (Cheng et al., 2001).

It is a fact that NADPH oxidases have been largely studied in various cell types for decades; however, physiological and pathological roles still need to be clarified since they are differentially regulated and distributed about the cell type. The complexity of NADPH oxidases makes them the main focus of studies investigating oxidative stress-related EC barrier dysfunction and the pathogenesis of human diseases that occurred through either oxidative stress or EC barrier dysfunction. Indeed, numerous stimuli enhance the NADPH activity, leading to increased vascular permeability, hypertension, atherosclerosis, diabetes, and acute lung injury/sepsis (Frey et al., 2009).

1.2.1 Endothelial NADPH oxidases (NOXs)

NOX1, NOX2, NOX4, and NOX5 are known isoforms in ECs (Frey et al., 2009). They differ in structural-based and subcellular localizations and in terms of generated ROS products (Schröder, 2010) (Fig. 1.2). For instance, NOX1 and NOX2 are localized lipid rafts and are related to the receptor-mediated signaling in the non-phagocytic cells (Mumbengegwi et al., 2008; Oakley et al., 2009). NOX4 was detected in the focal adhesions, nucleus, and endoplasmic reticulum (ER) (Brown & Griendling, 2009). Furthermore, NOX5 was observed in internal membranes; however, its interaction with Phosphatidylinositol 4,5-bisphosphate (PIP_2) leads to translocation of NOX5 to the plasma membrane (Kawahara & Lambeth, 2008). NOX4, which is constitutively active, is the most abundantly expressed form among all isoforms, followed by NOX2 (Ago et al., 2004). Guzik *et al.* stated that NOX4 has higher expression than NOX2 in arteries at the mRNA level, whereas this phenomenon changes in veins in favor of NOX2 (Guzik et al., 2004). Furthermore, gene expression analysis has revealed that all complex components are expressed in phagocytic cells; gp91phox, p22phox, p47phox, p40phox, p67phox, and Rac1, were also detectable in ECs in both mRNA and protein levels (Bedard & Krause, 2007).

Despite sharing identical components at a molecular level, endothelial NOXs differ from phagocytic NOXs in the mechanism of action. Endothelial NOXs are activated after translocation of cytosolic components to the membrane upon stimulation as in leukocytes. Nevertheless, unlike their phagocytic isoforms, endothelial NOXs continuously show basal activity without requiring any stimulation, which is thought to be related to the different subcellular localization of enzyme components in ECs (Li & Shah, 2002; Abid et al., 2007). Another specific difference of the vascular NOXs is their perinuclear localization in ECs that provide an intracellular ROS influx (Abid et al., 2007).

The upstream signaling pathways regulating the NOX activity still require further analysis in ECs. TNF-α, one of the critical signaling molecules in vascular inflammation, leads to the activation of NOX1, NOX2, and NOX4 in ECs (Konior et al., 2014). In addition to that, p47phox and Rac1 components of NOXs are also critical mediators of the enzyme activity. In ECs, GTP-bound active Rac1 controls the activity of the NOXs; NOX1 and NOX2 (Holmström & Finkel, 2014), besides its various distinct functions, especially in the cytoskeleton. However, mechanisms by which Rac1 is directed to different pathways are still poorly understood. So far, several regulators, protein modification sites, and stimuli have been identified on Rac1 (Dworakowski et al., 2008; Ray & Shah, 2005). Although NOX1 and NOX2 require binding of active Rac1 to show activity, NOX4 and NOX5 are known as Rac1 independent isoforms (Montezano et al., 2011). It was shown that NOX4 NADPH oxidase activity was not altered by either overexpression or downregulation of Rac1 (Meng et al., 2008).

1.3 Pathological Angiogenesis and Vascular Inflammation

Angiogenesis is a process that requires endothelial proliferation, sprouting, migration, and differentiation to generate new blood vessels from existing vessels (Muñoz-Chápuli et al., 2004). It is essential during embryonic development, regeneration, or wound healing. Angiogenesis begins with endothelial activation and is regulated by various signals acting on EC function, but migration and proliferation rates of ECs are restricted to basal levels under physiological conditions (Potente et al., 2011). Developmental angiogenesis is controlled by various signals, such as angiopoietins, VEGF, and Notch signaling (Imhof & Aurrand-Lions, 2006). The Rho family of GTPases and their regulatory proteins GEFs were also found in the regulation of the angiogenesis (Hasan & Siekmann, 2015; Niu et al., 2003; Soga et al., 2001; van Nieuw Amerongen

et al., 2003). Notably, Tan *et al.* revealed that the deletion of Rac1 in primary ECs using the Cre/Flox approach prevented migration and permeability *in vitro* while being lethal in the development of the embryo of mice *in vivo* (Tan et al., 2008).

Highly complex signaling mechanisms regulating angiogenesis may also lead to uncontrolled growth and cause various pathological conditions. This phenomenon is known as pathological angiogenesis. Since EC activation is a critical step in angiogenesis, there is a link between signaling cascade leading to EC barrier dysfunction and pathological angiogenesis (Goveia et al., 2014). Vascular inflammation and oxidative-stress caused by inflammation are found to be related to pathological angiogenesis with mechanisms that are not fully understood yet (Kim et al., 2013). The NOXs, the primary source of ROS in ECs, were shown among the important regulators of angiogenesis (Prieto-Bermejo & Hernández-Hernández, 2017). NOX2 activity, which requires the binding of Rac1-GTP, was detected at the leading edge of ECs during the migration, indicating its role in angiogenesis (Ushio-Fukai, 2006).

1.4 Dual Role of the Rho Family of GTPase Rac1 on Endothelial Barrier

Rac1, which is a Rho family of GTPases, stabilizes endothelial AJs and the EC barrier. On the other hand, Rac1, as part of the enzyme complex NADPH oxidase, regulates ROS production, of which uncontrolled overproduction leads to disruption of the endothelial barrier. The mechanisms by which Rac1 undergoes distinct downstream functions are not well understood yet (Fig. 1.3). The activity of Rac1, so as the Rho family of GTPases, is regulated by GEFs, GTPase activating (GAP) factors, and guanine dissociation inhibitors (GDIs). To bring Rac1 into an active state, Rac1 GEFs exchange guanosine diphosphate **(**GDP) to GTP, while GAP replaces GTP to GDP to inactivate Rac1. Additionally, the binding of GDI stabilizes the inactive state (Beckers et al., 2010). To date, various Rac1 GEFs have been identified in different cell types. Among 20 different Rho-GEFs highly expressed in ECs, Tiam1 (T-cell lymphoma invasion and metastasis 1**)**, Vav2, P-Rex1 (Phosphatidylinositol (3,4,5)-trisphosphate-dependent Rac exchanger 1), P-Rex2 (Phosphatidylinositol (3,4,5)-trisphosphate-dependent Rac exchanger 2), and β-PIX (β-p21-activated kinase (PAK)-interacting exchange factor) mainly regulate Rac1 activity (van Buul et al., 2014). Numerous studies point to the fact that different GEFs regulate Rac1 downstream signaling in response to various upstream signals; nevertheless, under which conditions the

downstream signaling cascade is regulated is poorly understood yet (Buchsbaum et al., 2002; Connolly et al., 2005; Manser et al., 1998; Zhou et al., 1998).

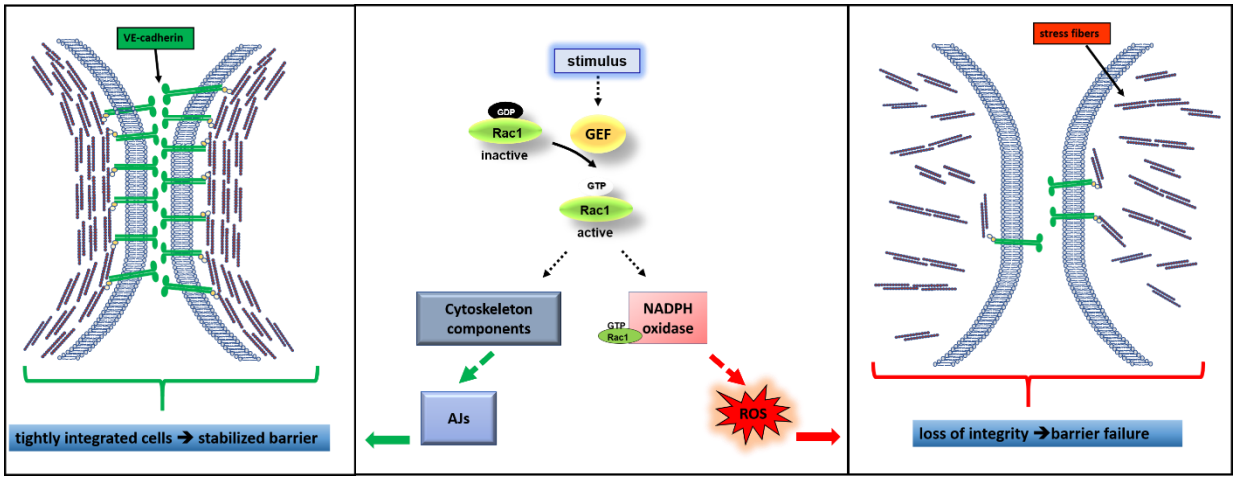

Figure 1.3: Dual role of Rac1 on the endothelial barrier. Activation of Rac1 in response to various stimuli directs it to two distinct functions. It can either stabilize the barrier via activating cytoskeleton components or causes barrier failure by activating NADPH oxidase-dependent excessive ROS production.

Various studies have provided robust data supporting the role of Rac1 as a barrier disrupting agent. Knezevic *et al.* stated that platelet-activating factor (PAF) triggers the translocation of Rac1 and its GEF Tiam1 towards membrane fraction where they interact with the PAF receptor, the interaction of which in turn activates Rac1, thereby increasing permeability via re-arranging actin polymerization and cell-cell junctions (Knezevic et al., 2009). Additionally, It was stated that VEGF stimulation phosphorylates VEGFR-2, which later activates Rac1 via its GEF Vav2 and triggers the loss of cell contacts and migration of ECs (Gavard & Gutkind, 2006; Eriksson et al., 2003). Consistent with these findings, Garrett *et al.* demonstrated that targeting endogenous Vav2 in ECs results in attenuation of both VEGF-induced Rac1 activation and cell migration (Garrett et al., 2007). Liao *et al.* stated that Vav2 selectively activates Rac1 in response to UTP via signaling cascade, which is triggered by activation of G_q protein-coupled P2Y2 nucleotide receptor (P2Y2R) and its interaction with VE-cadherin and VEGF receptor 2 (VEGFR-2) (Liao et al., 2014). Moreover, VEGF-induced Rac1 activity enhances ROS production via NADPH oxidases, ultimately leading to barrier dysfunction (Monaghan-Benson & Burridge, 2009). Similarly, it was shown that shear stress-induced activation of Rac1 directs it towards the NADPH oxidase for ROS

production in a process in which two different GEFs of Rac1 are involved. Interestingly, while initial activation of Rac1 requires Vav2, Tiam1 acts as an adaptor protein instead of a GEF to stabilize the interaction of activated Rac1 in NADPH oxidase with VE-cadherin, indicating complex regulatory roles of GEFs on the EC barrier (Liu et al., 2013).

Sphingosine-1-phosphate (S1P) is known as a barrier stabilizing agent by decreasing permeability in ECs. Singleton *et al.* found that S1P-induced actin rearrangement leading to increased barrier integrity occurs through activation of phosphoinositide-3-kinase (PI3K), which in turn activates Rac1 via its GEF Tiam1 (Singleton et al., 2005). In parallel to that, activation of Rac1 by anti-inflammatory ligands reduces permeability and stabilizes the endothelial barrier. It was shown that cAMP-induced activation of Rac1 via its GEFs Tiam1 and Vav2 stabilizes the barrier both *in vivo* and *in vitro* by regulating the arrangement of AJs (Schlegel & Waschke, 2014). It was suggested that selective activation of regulatory proteins of Rac1 based on the type of the signal directs it to distinct downstream pathways (Marei & Malliri, 2017). In this context, it was indicated that while Tiam1 expression is promoting localization of actin and epithelial-cadherin (E-cadherin) towards the cell periphery of epithelial cells, the lack of Tiam1 expression diminishes this effect. In contrast, over-expression of another Rac1 GEF P-Rex1 gives rise to loss of cell-cell contacts, besides increasing migration (Marei et al., 2016b; Marei et al., 2016a). Indeed, the interaction of P-Rex1 with flightless-1 homolog (FLII), which is an important mediator of actin dynamics and cell migration, triggers Rac1-mediated cell migration (Marei et al., 2016b).

1.5 P-Rex2

P-Rex2 is one of the GEFs that regulate the small GTPase Rac1 activity (Fig. 1.4). The full-length human P-Rex2 protein is 183kDa in size and encoded by the gene *P-REX2* located on chromosome 8, q 13.2. There are two P-Rex2 isoforms; P-Rex2 (P-Rex2a) and P-Rex2b (Donald et al., 2004; Rosenfeldt et al., 2004). Both P-Rex1 and P-Rex2 proteins share the same domain structure with the %59 identity (Donald et al., 2004). P-RRex2b is generated from P-Rex2a with alternative splicing and has no C-terminal inositol polyphosphate-4 phosphatase (IP4P) domain (Rosenfeldt et al., 2004). Other domains present in all isoforms are N-terminal DH (Diffuse B-cell lymphoma homology) domain, PH (pleckstrin homology) domain, two DEP (disheveled, EGL-10, and pleckstrin homology) domains, and two PDZ domains (Postsynaptic density protein of

95 kDa (PSD95), *Drosophila* disc large tumor suppressor (DlgA), and Zonula occludens-1 protein (Zo-1)) (Welch, 2015). The DH domain is the catalytic domain that presents in Dbl-type GEFs regulating the Rho-family of GTPases. The PH domain is linked to the DH domain. It contributes to the catalytic activity of the DH by binding to Phosphatidylinositol 3,4,5-bisphosphate (PIP_3) and allosteric protein interactions (Rossman et al., 2005; Cook et al., 2014). DEP and PDZ domains provide protein-protein interaction and have weak homology to the C-terminal domain (Welch, 2015). Northern blot analysis has shown that P-Rex2 is expressed in the heart, lung, skeletal muscle, small intestine, and placenta (Donald et al., 2004; Rosenfeldt et al., 2004; Pandiella & Montero, 2013), whereas P-Rex1 is mainly expressed in leukocytes and neurons (Machin et al., 2021). In the activation of P-Rex1 and P-Rex2 proteins, G protein-coupled receptors (GPCRs) and PI3K-coupled receptors are shown as upstream regulators (Welch et al., 2015) (Fig. 1.4). Cash *et al.* showed structural differences in the PH domain of P-Rex2 in comparison to the PH domain of P-Rex1, enabling P-Rex2 to be less dependent on PIP3 in terms of protein activation and membrane localization (Cash et al., 2019).

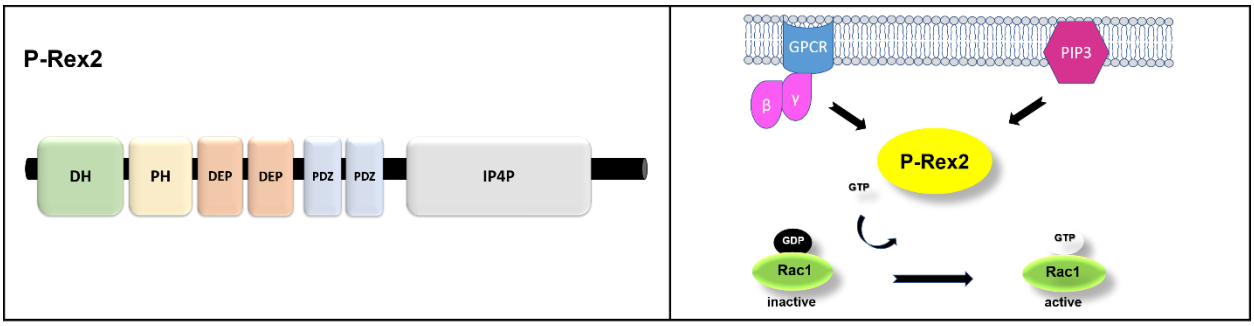

Figure 1.4: Molecular structure and activation of P-Rex2 protein.

Studies have shown that P-Rex2 has a role in cancer pathogenesis and glucose metabolism, which is altered in cancer cells (Hodakoski et al., 2014). For instance, P-Rex2 was identified as a frequently mutated protein in breast cancer based on whole-genome sequencing data of 107 human melanomas (Berger et al., 2012). In xenograft tumors, truncating P-Rex2 mutations in N-terminus increased tumor formation, GEF activity, and proliferation (Lissanu Deribe, 2016). Furthermore, P-Rex2 was determined as a target of miR-338-3p, of which inhibition leads to enhancement of

the progression of cancer (Chen et al., 2013; Guo et al., 2014). Even though the molecular mechanism is not fully understood yet, studies have revealed that the PI3K/PTEN/Akt pathway is critical to understanding the role of P-Rex2 in cancer. It was identified that P-Rex2 interacts with phosphatase and tensin homolog on chromosome 10 (PTEN) to inhibit its lipid phosphatase activity (Gogolla et al., 2009). PTEN is a tumor suppressor, in the absence of which PIP_3 accumulates inside the cells, leading to an increase in the activity of Akt, consequently enhancing the survival rate of cancer cells (Cully et al., 2006). P-Rex2-mediated inhibition of PTEN occurs through the interaction of the PH domain of P-Rex2 with the phosphorylated C-terminal tail of PTEN (Hodakoski et al., 2014). Moreover, PTEN also inhibits P-Rex2 GEF activity and reduces cell movement in breast cancer cells (Mense et al., 2015).

2 AIM OF THE STUDY

The main aim of the current study was to investigate the Role of P-Rex2 directed Rac1-activation in endothelial barrier dysfunction under inflammatory conditions. In the present study, TNF-α was used as an inflammatory mediator together with VEGF to activate the signaling cascade directing Rac1 to its role as a barrier disrupting agent. It has already been known that Rac1 has distinct functions in the regulation of the endothelial barrier. The activation of Rac1 can either stabilize the endothelial barrier or can activate the barrier disrupting mechanisms.

It was hypothesized in the present study that in the presence of inflammation, activation of Rac1 via its GEF-P-Rex2 triggers excessive ROS production, and ultimately barrier dysfunction.

The objective of the study was specifically to fulfill the following points:

1) To investigate whether P-Rex2 activates Rac1 in response to inflammatory mediators.
2) To elucidate whether activation of P-Rex2 leads to endothelial barrier dysfunction.
3) To elucidate with which mechanisms P-Rex2 leads to endothelial barrier dysfunction.
4) To examine the role of ROS production in P-Rex2 mediated endothelial barrier dysfunction.

3 METHODS

3.1 Cell Culture Techniques

3.1.1 Isolation of primary cells

Human umbilical vein endothelial cells (HUVECs) were isolated from umbilical cords obtained from the gynecology department of the University Hospital Giessen after informed consent from donors.

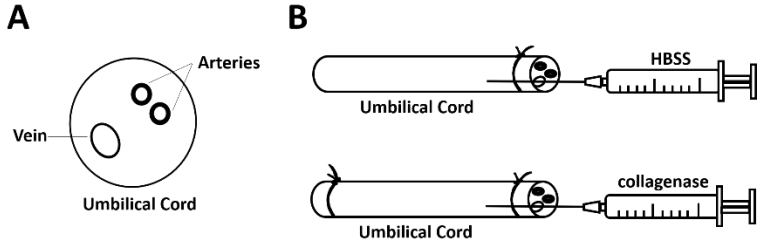

Figure 3. 1: Schematic illustration of the isolation of HUVECs. **A.** Represents arteries and veins in an umbilical cord. The umbilical cord consists of two arteries and one vein. Arteries have a smaller diameter and thicker walls than the vein. **B.** Represents isolation of HUVECs. First, the vein is cannulated with an iron stick, and the stick is stabilized with a plastic cable. Next, the remaining blood is removed by washing with HBSS through the iron stick using a syringe. The other end is also closed tightly with another plastic cable, and the collagenase solution is given to separating endothelial cells from the vessel walls.

Firstly, the umbilical vein was cannulated with a cannula and washed twice with pre-warmed (37 °C) Hank's balanced salt solution (HBSS) to remove blood from the vein. Next, it was filled with collagenase solution (200 IU/mL) to detach ECs from the vessel wall and incubated for 20 minutes (min) at 37 °C in an incubator. Afterward, collagenase solution containing the cells was collected in a 50 mL Falcon tube. The vein was washed with HBSS twice to collect the remaining cells. Collagenase was inactivated by adding 1 mL of fetal calf serum (FCS). HUVECs were precipitated by centrifugation at 250 x g for 10 min, resuspended in PromoCell^{TM} EC growth medium, seeded in a T75 cell culture flask, and incubated in a CO_2 (5 %) cell culture incubator for 2 hours (h) at 37 °C. Finally, the cells were washed twice with pre-warmed phosphate-buffered saline (PBS), and a fresh growth medium was added.

3.1.2 Cultivation of cells

HUVECs culture was maintained in PromoCell™ EC growth medium supplemented with 2 % (vol./vol.) FCS, 100 units/mL penicillin and 100 µg/mL streptomycin in a humidified atmosphere at 37 °C and 5 % CO_2. Cells were used from passages one to six.

Human endothelial cell line Hu-ARLT cells were a gift from Prof. Dr. Dagmar Wirth. Hu-ARLT were maintained in PromoCell™ endothelial cell growth medium supplemented with 5 % (vol./vol.) FCS, 100 units/mL penicillin, 100 µg/mL streptomycin, and 2 mg/mL doxycycline (Dox) in a humidified atmosphere at 37 °C and 5 % CO_2. Cell culture plates were coated with 0.5 % gelatin before cell seeding.

Human embryonic kidney 293 (HEK-293) and HEK-293 FT cells were maintained in high glucose-containing Dulbecco's Modified Eagle Medium (DMEM) supplemented with 10 % (vol./vol.) FCS, 100 units/mL penicillin, 100 µg/mL streptomycin and 1 mM sodium pyruvate in a humidified atmosphere at 37 °C and 5 % CO_2.

For sub-culturing, 70-90 % confluent cells were trypsinized in PBS supplemented with 0.05 % (wt./vol.) trypsin, and 0.02 % (wt./vol.) ethylenediaminetetraacetic acid (EDTA). The reaction was stopped by adding 1 mL FCS. Cell suspensions were centrifuged at 250 x g for 10 min. Collected cells were resuspended and seeded at a density of 15 x $10^3/cm^2$ (HUVECs), 10 x $10^3/cm^2$ (Hu-ARLT), and 3 x $10^4/cm^2$ (HEK-293 and HEK-293 FT).

3.1.3 Treatments

In all experiments, if not specified, long-term stimulations were performed in Opti-MEM reduced serum medium supplemented with 2 % FCS and 1 % penicillin/streptomycin. For short-term stimulations, HBSS supplemented with $CaCl_2$ (1.3 mM) and $MgCl_2$ (1.2 mM) was used. All short-term stimulations except ROS measurements were performed on a heating plate at 37 °C. The cells were incubated in a humidified atmosphere at 37 °C and 5 % CO_2 in the ROS measurements. Prior to short-term stimulations, cells were preincubated 20 min in HBSS supplemented with $CaCl_2$ and $MgCl_2$, and then agents were added as indicated. All agents were prepared freshly from stock solutions prior to use. In the experiments performed with inhibitors, cells were preincubated with optimized concentrations of inhibitors as indicated in the figure legends. As a solvent, dimethyl sulfoxide (DMSO) was used to prepare stock solutions of 2',7'-

dichlorofluorescein diacetate (DCF-DA), N-Acetyl-L-cysteine (NAC), and VAS2870. NSC23766 was solved in deionized water. Then, the agents were used at following concentrations: H_2DCF-DA (10 µM), NSC23766 (50 µM), NAC (1 mM), and VAS2870 (2 µg/mL and 5 µg/mL).

3.1.4 Cell counting

The number of viable cells was counted by staining with 0.4 % trypan blue solution to determine the number of cells before seeding. The cell suspension was diluted 1:1 with staining solution, incubated for 1 min at room temperature (RT), and only viable cells were counted using a hemocytometer.

3.1.5 Cryopreservation and thawing

Cells were harvested, and one million cells/mL were resuspended in their respective growth medium containing 10 % DMSO without antibiotics in Cryo-tubes. For short-term storage no longer than a week, cells were transferred to -80 °C. For long-term storage, cells were transferred to a liquid nitrogen container.

Cell suspensions were warmed to 37 °C in a water bath for thawing the cells and immediately transferred to 10 mL of growth medium of corresponding cell type. In order to remove toxic DMSO from the cell culture medium, cells were centrifuged at 250 x g for 10 min. After centrifugation, the medium was discarded, and cells were resuspended in a pre-warmed growth medium for seeding. The medium was exchanged after 24 h incubation in a humidified atmosphere at 37 °C and 5 % CO_2.

3.2 Molecular Biology Techniques

3.2.1 RNA isolation and cDNA synthesis

The column-based ribonucleic acid (RNA) extraction method was used to obtain high purity RNA. For that, RNA isolation was performed using a direct-zol RNA Miniprep Plus Kit (Zymo Research; Irvine, USA). All samples were prepared in TRI Reagent® solution (peqGOLD; Leighton Buzzard, UK) as described below and loaded into columns for total RNA isolation.

For sample preparation, cells were washed twice with PBS, and then TRI Reagent® solution (peqGOLD) was added into cell culture plates. Next, each sample was collected with a cell scraper into a 1.5 mL Eppendorf tube. After that, all samples were incubated at RT for 3 min to homogenize the samples and then immediately placed onto the ice. Then, centrifugation was performed at 4 °C to remove cell debris, and the supernatant was transferred in an RNase-free tube for total RNA isolation.

For RNA isolation, ethanol (100 %) in an equal volume to samples in TRI Reagent® was added in each sample tube, briefly vortexed, and spined down. Next, each sample was transferred into a column placed in a collection tube. After that, centrifugation was performed at 10000 x g for 30 sec at RT. Collection tubes containing flow-through were discarded, and columns containing nucleic acids were transferred in a new collection tube. Then, DNase treatment was applied according to the manufacturer's instructions for 15 min at RT to remove deoxyribonucleic acid (DNA) from RNA samples. Columns were washed by adding wash buffer and centrifuging as previously. Before the elution step, empty columns were centrifuged for 1 min to completely remove remaining wash buffer from columns. Finally, columns were transferred in an RNase-free tube and elution of the total RNA from the columns was performed with pre-warmed (55 °C) Dnase/Rnase-free water by centrifugation. Following the isolation, the concentration of each sample and the purity were determined spectrophotometrically using a nanodrop (Thermo Fisher Scientific; Waltham, USA).

For reverse transcription polymerase chain reaction (PCR), All-in-One cDNA Synthesis SuperMix (Bimake; Houston, USA) was used to convert 200 ng of total RNA template to complementary DNA (cDNA) according to the manufacturer's instructions (Table 3.1 & 3.2).

Table 3.1 Reverse transcription PCR components for cDNA synthesis.

Component	**Volume**
Total RNA	200 ng
5 x qRT SuperMix	2 µL
RNase-free water	up to 10 µL

Table 3.2 Reverse transcription PCR conditions for cDNA synthesis.

Conditions	
25 °C	10 min
42 °C	30 min
85 °C	5 min

3.2.2 Quantitative real time PCR (q-PCR)

Quantitative real-time polymerase chain reaction (q-PCR) was performed using 2X SYBR Green q-PCR Master Mix (Bimake) in a total volume of 10 µl using CFX96 Touch™ (Bio-Rad; Hercules, USA) q-PCR instrument as shown in Table 3.3 and Table 3.4. All samples were assayed in duplicates and normalized to the *GAPDH* gene to assess relative gene expression levels. The melting curve was subjected to each reaction sample. A list of used primers is given in Table 3.5.

Table 3.3 Q-PCR master mix composition.

Component	**Volume**
cDNA (eq to 4 ng total RNA)	4 µL
2 x SYBR Green Master Mix	5 µL
Forward primer (10 mM)	0.25 µL
Reverse primer (10 mM)	0.25 µL
DNase/RNase-free water	up to 10 µL

Table 3.4 Q-PCR cycling conditions.

Conditions		
95 °C	5 min	1 cycle
95 °C	30 sec	40 cycles
59-61 °C	30 sec	
72 °C	30 sec	
95 °C	10 sec	1 cycle
Melt curve analysis: 65 °C to 95 °C Increment 0.5 °C for 5 sec		

Table 3.5 Sequences of primers used in q-PCR gene expression level analysis.

Target gene	Primer sequences
P-Rex2	F: GTCCGGACTCTTGCTCAGAA R: GGAGCTGTGTCTCACTATCTGAA
GAPDH	F: TGCACCACCAACTGCTTAGC R: GGCATGGACTGTGGTCATGAG
I-CAM1	F: TGTGACCAGCCCAAGTTGTT R: TGGAGTCCAGTACACGGTGA
V-CAM1	F: ATGCCTGGGAAGATGGTCG R: CCTCCAGAGGGCCACTCA
IL-6	F: TTCGGTCCAGTTGCCTTCTC R: TACATGCTCCTTTCTCAGGGC
IL-8	F: GCTCTGTGTGAAGGTGCAGTT R: ACCCAGTTTTCCTTGGGGTC

The threshold cycle (Ct) values of samples were exported to excel software (Microsoft, 2010) to calculate fold change ($2^{-\Delta\Delta Ct}$) to determine relative gene expression levels. Briefly, mean Ct values from technical replicates of each biological replicate were calculated. After that, delta Ct (ΔCt) and fold change values are calculated as:

$$\Delta Ct = Ct_{\text{mean}} \text{ of target gene} - Ct_{\text{mean}} \text{ of GAPDH} \quad \text{(a)}$$

$$\Delta\Delta Ct = \Delta Ct \text{ of treatment} - \Delta Ct \text{ of control} \quad \text{(b)} \qquad [3.1]$$

$$\text{Fold change} = 2^{-\Delta\Delta Ct} \quad \text{(c)}$$

3.2.3 Cloning

The Gateway cloning technology was used to generate entry clones for all genes used in the study, which were further used to produce expression vectors for both transient and stable gene expression systems using LR recombinase. For the generation of the transient gene expression system, entry vectors were recombined with Gateway pcDNA3.1/nV5-DEST destination vector (Invitrogen™, 12290010) using Gateway™ LR Clonase™ II Enzyme mix. For the generation of lentivirus-based stable gene expression systems, entry vectors were recombined either with pLenti-CMV-Blast-DEST (Addgene plasmid, #17451) (Campeau et al., 2009) or the pLenti-CMV-Puro-DEST (Addgene plasmid, #17452) (Campeau et al., 2009) destination vectors using Gateway™ LR Clonase™ II Enzyme mix. The pcDNA3.1-P-Rex2-V5-6xHis was a gift from Ramon Parsons

(Addgene plasmid, #41555) (Fine et al., 2009). The R777-E189 Hs.PREX2 was a gift from Dominic Esposito (Addgene plasmid, #70473).

To generate *the pcDNA3.1/nV5-control* and *the pcDNA3.1/nV5-Rac1-WT*, the pENTR-D-TOPO and the pENTR-Rac1-WT entry vectors were recombined with the pcDNA3.1/nV5-DEST destination vector. To generate *the pLenti-CMV-hP-Rex2* plasmid, the R777-E189 Hs.PREX2 entry vector was recombined with pLenti-CMV-Blast-DEST. To generate *the pLenti-CMV-blast-control* or *the pLenti-CMV-puro-control* plasmids, the pENTR-D-TOPO-control entry vector was used. To generate *the pLenti-CMV-Rac1-CA* and *the pLenti-CMV-Rac1-DN* plasmids, the pENTR-Rac1-CA and the pENTR-Rac1-DN entry vectors were recombined with both pLenti-CMV-Blast-DEST and pLenti-CMV-Puro-DEST vectors, respectively.

Briefly, for each recombination reaction, 75 ng of entry vector, 125 ng of destination vector, 2 µL of Tris-EDTA (TE) buffer (pH 8.0), and 1 µL of the Gateway™ LR Clonase™ II Enzyme mix were added into a reaction tube with a final volume of 5 µL. The reaction was carried out at RT for 4 h, and then it was terminated by adding 1 µL of Proteinase K solution at 37 °C for 10 min. After that, recombined products were transformed into either the One Shot® Stbl3™ electrocompetent *E.coli* cells (pLenti-vectors) or Top10 electrocompetent *E.coli* cells (pENTR-vectors, pcDNA3.1-vectors) with electroporation and seeded on selection antibiotic containing agar plates. The growth colonies were picked from agar plates and cultured for miniprep. After overnight incubation, miniprep of the recombinant plasmids was performed using the peqGOLD Plasmid Miniprep Kit I according to the manufacturer's instructions. Initial confirmation of the plasmids was performed by enzymatic restriction digestion. Final confirmation of the plasmids was done by Sanger sequencing. After confirmation of the plasmids by sequencing, midiprep cultures were grown overnight, and then midiprep was performed using the PureLink™ HiPure Plasmid Midiprep Kit (Invitrogen; Waltham, USA). After determining the concentrations and purities of plasmids with nanodrop, they were stored at -20 °C until required.

3.2.4 Transfection

Transfection experiments were performed based on the lipid-mediated transfection approach using jetPRIME® Transfection reagent (Polyplus transfection), which is applicable in adherent cultures of various cell types to deliver DNA and small-interfering RNA (siRNA) molecules.

Briefly, cells were seeded the day before to be 70-80 % of cell confluency at the day of transfection. To prepare the transfection solution, 10 µg plasmid DNA was diluted in 500 µL jetPRIME® buffer according to the manufacturer's instructions. After mixing briefly by vortexing, 10 µL of jetPRIME® transfection reagent was added to the solution. Then, the transfection solution was mixed properly by brief vortexing and spinning down and incubated 10 min at RT. Next, transfection was performed by adding transfection solution dropwise onto cells in a serum containing cell growth medium. Approximately 5 h after post-transfection, cells were washed with pre-warmed PBS, a fresh growth medium was added, and cells were cultured until reaching the required growth for the following experiments.

3.3 Lentivirus-based Stable Gene Expression

Lentiviruses which were developed from the human immunodeficiency virus (HIV) as replication-incompetent, are valuable tools to transfer a gene of interest into various cell types for stable gene expression (Naldini et al., 1996). In the experiments, 3rd generation lentivirus production system was used to transfer plasmids carrying the open reading frame (ORF) to lentiviral particles. Experimental steps are summarized in Fig. 3.2. Lentiviruses produced with 3rd generation vectors require co-transfection of four plasmids into a producer cell-line like HEK-293 FT (Vargas et al., 2016). Briefly, the transgene plasmid is generated by cloning the gene of interest into a lentiviral construct between long terminal repeats (LTRs). The other plasmids consist of viral genes that are split into three plasmids. While two of them carry packaging genes, *GAG*, *POL*, and *Rev*, one of them usually encodes the *VSV-G* gene for the envelope (Dull et al., 1998). After transfection, cells carrying four plasmids produce viruses, which are later collected from the medium (see section 3.3.1). These viruses are later used to express the transgene in the target cells by transduction (see section 3.3.3). The required amount for an efficient infection is determined by calculating the virus titer as given in section 3.3.2. The required concentration and time for the selection of the cells that stably express the transgene are determined by generating a kill curve (see section 3.3.4).

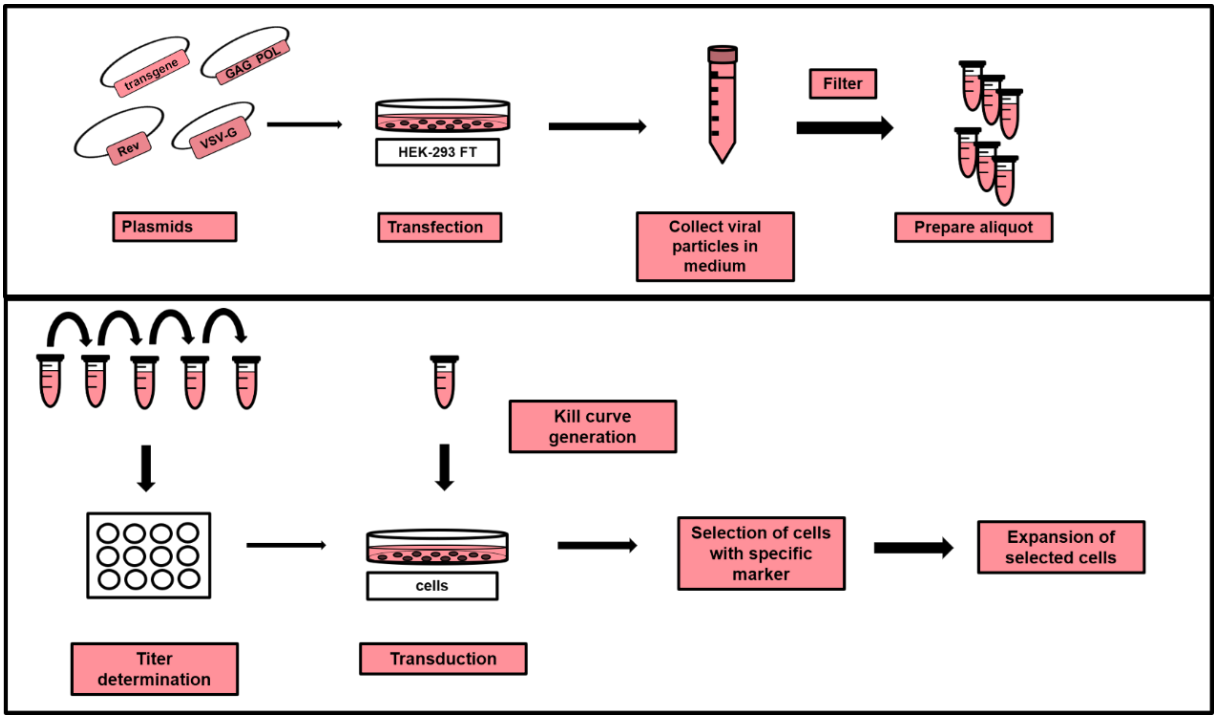

Figure 3.2: Schematic illustration of the generation of lentiviral-based stable expression systems. In the figure above, lentivirus production steps were described. In the figure below, steps required for stable expression of a transgene in mammalian cells using produced viruses were summarized.

3.3.1 Lentivirus production

Lentiviruses were produced in HEK-293 FT cells with reverse transfection. The 3rd generation lentivirus production system, Invitrogen™ ViraPower™ Lentiviral Packaging Mix, was used to produce lentiviruses. Equimoles of all 4 plasmids (pLP1, pLP2, pLP/VSVG, and lentiviral vector containing ORF) were co-transfected using jetPRIME® transfection reagent according to manufacturer's instructions. Transfection was performed in an antibiotic-free high glucose-containing DMEM medium containing G418 (100 µg/mL) and 10 % FCS. After the transfection, cells were incubated overnight. The next day, the medium was replaced with a fresh complete growth medium for HEK-293 FT cells containing antibiotics. Finally, lentiviruses were collected at 48 h post-transfection, filtered through a low-binding polyvinylidene fluoride (PVDF) 0.45 µm filter, and stored at -80 °C.

3.3.2 Calculation of lentiviral titer

Titers of the viral stocks were calculated for each cell type used for lentiviral transduction. The experiment was performed in a 6-well plate. One day before the transduction, 25.000 cells per well were seeded. Virus stocks were diluted with a growth medium for the transduction, as shown in Table 3.6. Polybrene was added into each dilution at a final concentration of 8 µg/mL to increase transduction efficiency. After transduction, cells were incubated overnight at 37 °C and 5 % CO_2. Then, cells were washed twice with PBS, and 2 mL of the complete growth medium was added. The selective antibiotic was added at 48 h post-transduction, and the selection was continued until colonies were formed.

Table 3.6 The composition of transduction medium for calculation of virus titers.

Well number	**1**	**2**	**3**	**4**	**5**	**6**
Virus amount (µL)	100	10	10	1	1	0
Medium amount (µL)	850	940	940	949	949	950
Total volume (µL)	950	950	950	950	950	950

Crystal violet staining was applied to calculate viral titers. Prior to staining, cells were washed twice with PBS and then fixed with 4 % paraformaldehyde (PFA) for at RT 20 min. After fixation, cells were washed twice with PBS and stained with a 0.5 % crystal violet solution at RT for 20 min. The staining solution was removed from the wells, each well was washed carefully with distilled water, and the colonies were counted. Viral titers were calculated in terms of transduction units per milliliter (CFU/mL) as:

(number of colonies x dilution factor) / (volume of virus containing medium) [3.2]

3.3.3 Lentiviral transduction

Lentiviral transduction was performed in the presence of 8 µg/mL polybrene. For infection, 1 x 10^5 cells per well seeded in a 6-well plate. Cells were incubated until attachment to the surface at 37 °C and 5 % CO_2. Afterward, the medium was replaced with the polybrene-containing basal medium, and viruses were added to the culture at the required amount. Then, the cells were incubated overnight. The next day, cells were washed twice with PBS, and the virus-containing

medium was replaced with complete growth medium. Cells were passaged at 48 h post-infection and then seeded with the selection marker to select stable clones. The selection medium was replaced every two days until the selection was completed. Finally, the stable clones were expanded and frozen until required.

3.3.4 Kill curve generation

The required amount of antibiotic concentrations for the selection of stable clones was determined for each cell type and selection marker by generating kill curves. For this purpose, cells were seeded in a 12-well plate at a density of 5 x 10^4 per well. Then, different concentrations of the selection antibiotics were added into the medium after 24 h. Each concentration was maintained in triplicates. The viability of cells was monitored every day. The selection medium was replaced with a fresh medium every two days until the cells were completely dead. HUVECs were selected with either 2 µg/mL of puromycin or 4 µg/mL of Blasticidin S hydrochloride over 5 days. Hu-ARLT cells were selected with either 0.0625 µg/mL of puromycin or 5 µg/mL of Blasticidin S hydrochloride over 7 days.

3.4 Protein Biochemistry

3.4.1 Protein sample preparation for western blot

For total protein extraction, cells were washed twice with cold PBS and lysed with protein lysis buffer (Table 3.7). After that the lysed cells were scratched with a cell scraper and transferred into 1.5 mL Eppendorf tubes. Before determining protein concentration, samples were treated with DNase (Benzonase® supplemented with 120 mM $MgCl_2$) for 30 min at 4 °C.

3.4.1.1 Measurement of protein concentration

Protein concentration was determined using the Pierce™ BCA protein assay kit (Thermo Fisher Scientific) according to the manufacturer's instructions. Each sample was diluted in deionized water with a ratio of 1:10 and 1:20 and assayed in duplicate in a 96-well plate. As protein standards, different bovine serum albumin (BSA) concentrations between 0.125 mg/mL and 2 mg/mL were prepared. After 30 min incubation of proteins with bicinchoninic acid (BCA) reagent

at 37 °C, the measurement was performed with a Tecan Microplate reader using Tecan's Magellan Microplate Reader Software (Tecan; Männedorf, Switzerland).

After protein measurement, protein samples were prepared for sodium dodecyl sulfate–polyacrylamide gel electrophoresis (SDS-PAGE). For that, each sample was mixed with the loading buffer given in Table 3.7 and then boiled for 5 min at 95 °C for denaturation in the presence of 10 mM 1,4-dithiothreitol (DTT).

Table 3.7 Compositions of protein lysis buffer and gel loading buffer.

	Components	**Concentrations**
Protein lysis buffer	Tris/HCl (pH 6.8)	120 mM
	SDS (wt/vol)	4 %
	Glycerol (vol/vol)	20 %
	NaF	20 mM
	Na-orthovanadate	1.5 mM
	Protease inhibitor cocktail	1:100
Gel loading buffer	Tris/HCl (pH 6.8)	300 mM
	SDS (wt/vol)	10 %
	Glycerol (vol/vol)	50 %
	NaF	50 mM
	Bromophenol blue	0.02 %

3.4.2 SDS-PAGE

Proteins from cell lysates were separated with SDS-PAGE using self-made gels as indicated in Table 3.8. Mini-PROTEAN gel electrophoresis chamber (Bio-Rad) system used for the SDS-PAGE experiment. All samples mixed with loading buffer and boiled were placed on ice, and proteins (20 µg - 30 µg) were loaded into the gel with a molecular weight marker. Electrophoresis was performed in 1X running buffer (Table 3.9) initially at 80 volt (V) for 30 min, and then voltage was increased to 120 V.

Table 3.8 The composition of the SDS-gels based on a percentage.

Components	**Resolving gel**			**Stacking gel**
	7.5 %	**10 %**	**12.5 %**	**6 %**
Tris-HCl (pH 8.8; 120 mM)	4.5 mL	4.5 mL	4.5 mL	-
Tris-HCl (pH 6.8; 120 mM)	-	-	-	0.5 mL
Acrylamide/Bisacrylamide (1:19) 40 % (wt./vol)	2.25 mL	3 mL	3.75 mL	0.5 mL
Water	5.05 mL	4.3 mL	3.55 mL	2.95 mL
SDS 10 % (wt/vol)	120 µL	120 µL	120 µL	40 µL
APS 10 % (wt/vol)	100 µL	100 µL	100 µL	25 µL
TEMED	10 µL	10 µL	10 µL	5 µL

Table 3.9 The composition of 1X Gel Running Buffer.

Component	**Concentration**
Tris	25 mM
Glycine	200 mM
SDS (wt/vol)	0.1 %

3.4.3 Western blotting

Separated proteins were transferred from SDS-gel to a nitrocellulose membrane using the wet electro-blotting system (Mini Trans-Blot, Bio-Rad) at constant 120 V for 60 min in 1 X transfer buffer (Table 3.10). Then, membranes were blocked for 1 h at RT with 5 % non-fat dry milk solved in tris buffered saline containing 0.02 % Tween 20 (TBS-T) and 20 mM sodium fluoride (NaF). Afterward, membranes were washed twice with TBS-T for 5 min and were incubated overnight at 4 °C with primary antibodies against the protein of interests. All primary antibodies were diluted in 5 % BSA and 20 mM NaF in TBS-T at given concentrations in Table 3.11. Following the incubation, membranes were washed three times for 10 min with TBS-T followed by incubation with secondary antibodies for 1 h at RT. Horseradish peroxidase (HRP)-conjugated secondary antibodies were diluted in 5 % non-fat dry milk in TBS-T (Table 3.11). After

incubation, membranes were washed three times with TBS-T for 5 min. Next, bands were visualized by adding the Clarity™ western ECL substrate (Bio-Rad) according to the manufacturer's instructions. Finally, generated signals were detected using ChemiDoc™ MP (Bio-Rad) instrument, and band intensities were quantified by volume densitometry via Image Lab software. For further analysis, the values were transferred to the Microsoft Excel software, and then relative protein expression levels were quantified by normalizing to the protein level of the reference protein.

Table 3.10 The composition of the 1X transfer buffer.

Component	**Concentration**
Tris	25 mM
Glycin	200 mM
Methanol	20 %
SDS	0.1 %

Table 3.11 The list of used antibodies and their concentrations.

Primary antibodies	**Dilution factor**	**Manufacturer**
P-Rex2 (Rabit IgG, polyclonal)	1:500	Thermo Fisher Scientific
Rac1 (Mouse IgG, monoclonal)	1:1000	Thermo Fisher Scientific
GAPDH (Rabit IgG, polyclonal)	1:1000	Cell Signaling Technolgies
Histidine tag (Mouse IgG, monoclonal)	1:500	Thermo Fisher Scientific
V5 tag (Mouse IgG, monoclonal)	1:1000	Thermo Fisher Scientific
Secondary antibodies	**Dilution factor**	**Manufacturer**
Anti-Rabit IgG, HRP-linked	1:1000	Santa-Cruz Biotechnology
Anti-Mouse IgG, HRP-linked	1:1000	Santa-Cruz Biotechnology

3.4.4 Immunoprecipitation

HEK-293 cells were seeded at a density of 2 x 10^6 in a 10 cm cell culture dish. After 24 h of incubation, the HEK-293 cells were transfected with 4 µg plasmid DNA using jetPRIME® Transfection reagent. The immunoprecipitation (IP) experiments were performed at 48 h post-

transfection using Dynabeads® Protein G (Thermo Fisher Scientific). Firstly, transfected cells were washed twice with cold PBS and lysed in freshly prepared 600 µL of ice-cold IP lysis buffer (Table 3.12). The lysed cells were scratched and collected into 1.5 mL Eppendorf tubes and placed on ice. After that, the cells lysed by passing through a 26G needle several times to achieve complete lysis of the cells. The cell lysates were centrifuged at 4 °C for 5 min to remove cell debris. As an input, 10 % of supernatants were separated into separate tubes. The remaining samples were incubated overnight with either an immunglobulin G (IgG) antibody or an antibody specific to the protein of interest at 4 °C. Dynabeads® were washed twice in a magnetic rack with cold PBS containing 0.01 % tween 20. After the washing, beads were dissolved in the IP lysis buffer, added into the antibody-protein mixture, and incubated at 4 °C for 30 min. Afterward, the beads bound to protein/antibody complexes were washed three times with cold PBS containing 0.01 % tween 20 in a magnetic rack. The immunoprecipitants were dissolved from beads at RT for 15 min in 30 µL of the protein lysis buffer (Table 3.7).

Table 3.12 The composition of IP lysis buffer.

Components	**Concentrations**
Tris/HCl (pH 7.4)	25 mM
NaCl	150 mM
NP-40	1 %
Triton X 100	0.5 %
Na-orthovanadate	1.5 mM
EDTA	1 mM
NaF	20 mM
Protease inhibitor cocktail	1:100
PMSF	50 µg/mL
$MgCl_2$	1 mM

3.5 Pull-Down Assay

According to the manufacturer's instructions, a Pull-Down assay was performed to determine the level of GTP-bound Rac1 using the active Rac1 Pull-Down and detection kit (Thermo Scientific). Briefly, cells were seeded on 10 cm dishes and allowed to grow until they reached the

required confluency. After that, cells were treated with TNF-α (10 ng/mL) for the indicated times. Following treatment, cells were washed once with ice-cold TBS and immediately lysed with 0.3 mL of lysis buffer provided with the kit supplemented with protease inhibitor cocktail and 1.2 mM $MgCl_2$. For each assay, 400 µL of cell lysate was loaded into the 20 µg of GST-human Pak1-PBD containing spin cups, and the reaction mixtures were incubated at 4 °C for 1 h with constant rocking. Then, the spin cups were washed three times with washing buffer, and samples were eluted with β-mercaptoethanol and 2X SDS sample buffer (1:20) by heating at 95 °C for 3 min. All steps were performed under cold conditions, and then the eluted samples were stored at -80 °C until use.

3.6 Immunostaining

HUVECs were cultured with a complete growth medium in 6-well plates on coverslips. After the cells reached the required confluency, they were treated as indicated in the figure legends and then fixed for further experiments. Similarly, Hu-ARLT cells were cultured with a growth medium on coverslips but in the absence of Dox. Each Hu-ARLT cell type expressing different transgenes was seeded with a density of 2.5 x 10^5 per well in a 12-well-plate. After 48 h, they were stimulated as indicated in the figures and then fixed for staining.

For VE-cadherin staining, first, cells were fixed with cold methanol for 10 min at -20 °C. After that, methanol was removed entirely, and cells were washed with PBS for 10 min at RT with constant shaking. For actin staining, the cells were fixed with 4 % PFA for 15 min at RT and then the same procedure was followed. Next, cells were permeabilized with PBS plus 0.2 % Triton X for 15 min at RT on the shaker and washed with PBS three times for 10 min of each at RT. Then, they were blocked in PBS containing 5 % goat serum and 1 % BSA for 1 h at RT. Following blocking, for VE-cadherin staining, cells were stained with an overnight incubation for the primary antibody (mouse anti-human VE-cadherin (CD144), 1:100) at 4 °C. Afterward, they were washed with PBS three times for 10 min of each at RT on the shaker and incubated with secondary antibody (goat anti-mouse IgG Alexa Fluor® 488 (FITC), 1:200) for 1 h at RT in a dark environment. For actin staining, cells were incubated with 50 µM Phalloidin-TRITC for 1 h at RT. Finally, cells were washed with PBS five times for 3 min each at RT on the shaker, and then coverslips were mounted on glass slides in Mowiol solution containing 4′,6-diamidino-2-phenylindole (DAPI)

(1:1000). The images were taken with fluorescence microscopy (Biorevo BZ-9000, KEYENCE; Neu-Isenburg, Germany).

3.7 The *in vitro* Wound Healing Assay

HUVECs were plated in a 12-wells plate containing rectangular silicone inserts (to generate gaps) and then were grown until reaching 90% confluency. Next, the medium was replaced with the basal EC medium without supplement. After incubation for 24 h, the inserts were removed, and the medium was replaced with the stimulation medium. In the experiments with Hu-ARLTs, the cells that previously were grown in the presence of Dox. were cultured without Dox. at a density of 3 x 10^5 cells per well in a 12-wells plate. After 24 h, the medium was replaced with the treatment medium, and the inserts were removed. The photographs were taken at 0 h, 24 h, and 48 h time points after treatment. Phase contrast inverted microscope was used for visualizing, and migrated distance was measured using the Cell D Software (Olympus Life Science; Hamburg, Germany).

3.8 The *in vitro* Spheroid-based Sprouting Assay

3.8.1 The spheroid cultures of endothelial cells

The hanging-drop method was used to generate 3D spheroid cultures. For that, healthy cultures of HUVECs (400 cells/well) and Hu-ARLT cells (200 cells/well) were used. Prior to experiments, Hu-ARLT cells were grown in the presence of Dox. Briefly, cells were trypsinized, counted, and added into 20 % Methocel (Sigma-Aldrich) containing EC growth medium. Next, 100 µL of cell suspensions were re-seeded in 96-well non-adherent cell culture plates. After incubation for 24 h at 37 °C and 5 % CO_2, the spheroid formation was observed under microscopy. The spheroids were generated with at least 90 % efficiency in the experiments for further analysis.

3.8.2 The *in vitro* sprouting assay

An *in vitro* sprouting assay was performed using spheroid cultures to observe the angiogenetic properties of the cells. Briefly, the spheroids were collected and centrifuged at 600 x g for 6 min. After discarding the supernatant, firstly, 40 % FCS containing Methocel was slowly added into the spheroids containing tubes. Next, rat-tail-collagen in 10X M199 medium (1:1) was

added into the tubes. The suspension was slowly mixed and cultured in 24-well plates. Meanwhile, the treatment solution was prepared in the endothelial cell growth medium. Following 1 h incubation, spheroids were treated and then returned to the incubator. The *in vitro* sprout formations were monitored after 24 h and 48 h under the microscope, and the length of sprouts was measured using the Cell D software (Olympus Life Science).

3.9 The Permeability Measurement of Endothelial Monolayers

The permeability of ECs was measured by monitoring the passage of Trypan blue-labeled albumin molecules across endothelial monolayers as described previously (Aslam et al., 2014). Briefly, ECs were cultured on a Transwell® filter membrane with 0.4 μm pore size and 6.5 mm diameter until the cells formed a tight monolayer. Next, ECs growth medium was discarded, and both compartments of the Transwell® filter were fulfilled with a modified Tyrode medium consisting of 150 mM NaCl, 2.7 mM KCl, 1.2 mM KH_2PO_4, 1.2 mM $MgSO_4$, 1 mM $CaCl_2$, 30 mM N-2-hydroxyethyl piperazine-N'-2-ethane sulfonic acid (HEPES) (pH 7.4), and 2 % FCS. Then, 2.5 mL of Tyrode medium containing Trypan blue (60 μM) was added to the upper compartment, and 7.2 mL of Tyrode medium was added into the lower compartment to maintain equal hydrostatic pressure among compartments of the Transwell® filter. In order to measure endothelial permeability, the passage of the labeled albumin from the upper compartment to the lower compartment was continuously monitored by pumping the liquid through a spectrophotometer (Specord 600, Analytik Jena, Jena, Germany).

3.10 ROS Measurements

The intracellular ROS level was determined using DCF-DA. For microplate-based measurements, an equal number of cells from each Hu-ARLT cell type was grown in a black 96-well plate with a density of 4×10^3 per well in the presence of doxycycline. After 24 h in the incubator, cells were washed once with PBS, basal cell medium was added, and then cell plates were incubated an additional 12 h for starvation. Before the DCF-DA treatment, cells were washed with HBSS. Then, the DCF-DA was diluted in HBSS and added into the wells in a final concentration of 10 μM. After that, plates were incubated for 30 min in the incubator. Then, cells were rewashed with HBSS, and ROS production was stimulated with TNF-α (10 ng/mL) in HBSS buffer for one h. While HBSS buffer was used as a negative control, 10 μM H_2O_2 in HBSS was

used as a positive control. Additionally, the inhibitor was added 30 min prior to stimulation in the measurements performed with an inhibitor. In order to determine the ROS level, the DCF-DA signal was measured immediately with a Tecan Microplate reader using Tecan´s Magellan Microplate Reader Software. For the analysis, the background DCF-DA signals obtained from wells without cells were subtracted from the signals generated by cells. The normalization of the signals was done based on the protein levels of each well. Initially, each well was washed with PBS, and then protein levels were determined using the Bradford protein assay (Bio-Rad).

3.11 Statistical Analysis

All statistical analysis was performed using GraphPad Prism 9 Software. An unpaired Student's t-test was applied to determine statistical differences between the two groups. For comparison of more than two groups, one-way ANOVA was used. All data were given as mean ± standard error of the mean (S.E.M.). The significance of statistical analysis was determined based on calculated *p*-values, and $p < 0.05$ was considered significant.

4 RESULTS

4.1 Molecular Validation of the Expression Vectors

At first, molecular interactions between P-Rex2 and Rac1 were investigated via transiently overexpressing these proteins in HUVECs and endothelial cell line Hu-ARLT. For this, wild type *RAC1* gene was cloned into the pcDNA3.1 expression vector to generate *the pcDNA3.1/Rac1-WT*. The final recombinant product was confirmed initially with restriction enzyme digestion (Fig. 4.1) and then with Sanger sequencing. For transient overexpression of P-Rex2, pcDNA3.1-P-Rex2-V5/His (Addgene plasmid, #41555) plasmid was confirmed with Sanger sequencing (Fig. 4.2).

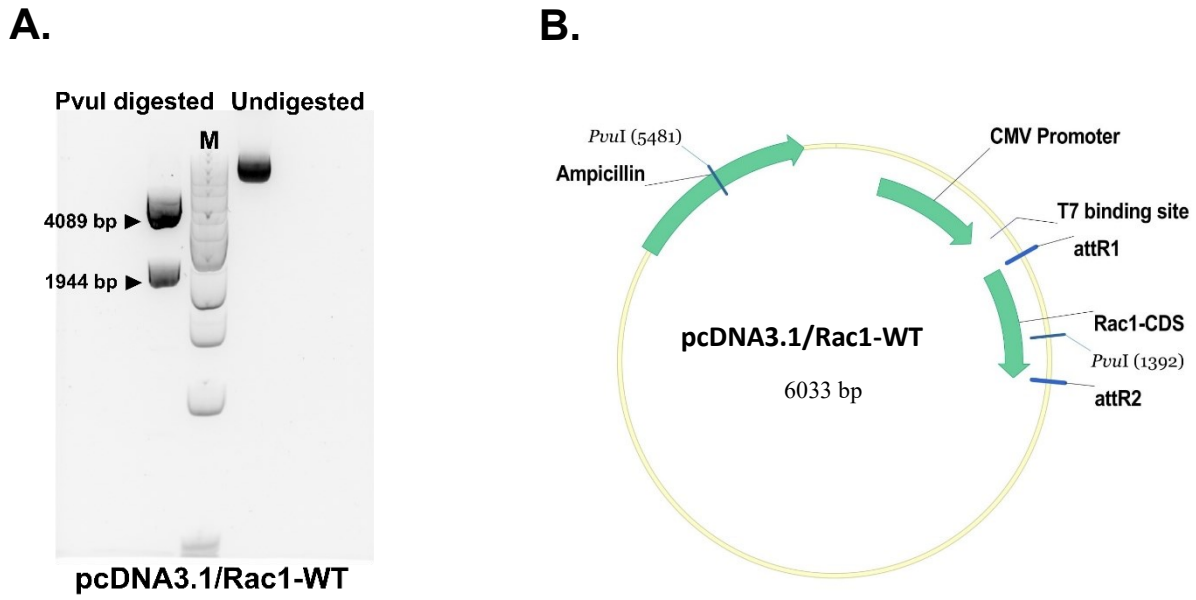

Figure 4.1: Transient overexpression vector; pcDNA3.1/Rac1-WT. **A.** Plasmid DNA of pcDNA3.1/Rac1-WT was digested with PvuI enzyme. The expected band size of positive clone after digestion was 4089 bp and 1944 bp. *M.* 1kb DNA Ladder (NEB N0552). **B.** The plasmid map of pcDNA3.1/Rac1-WT.

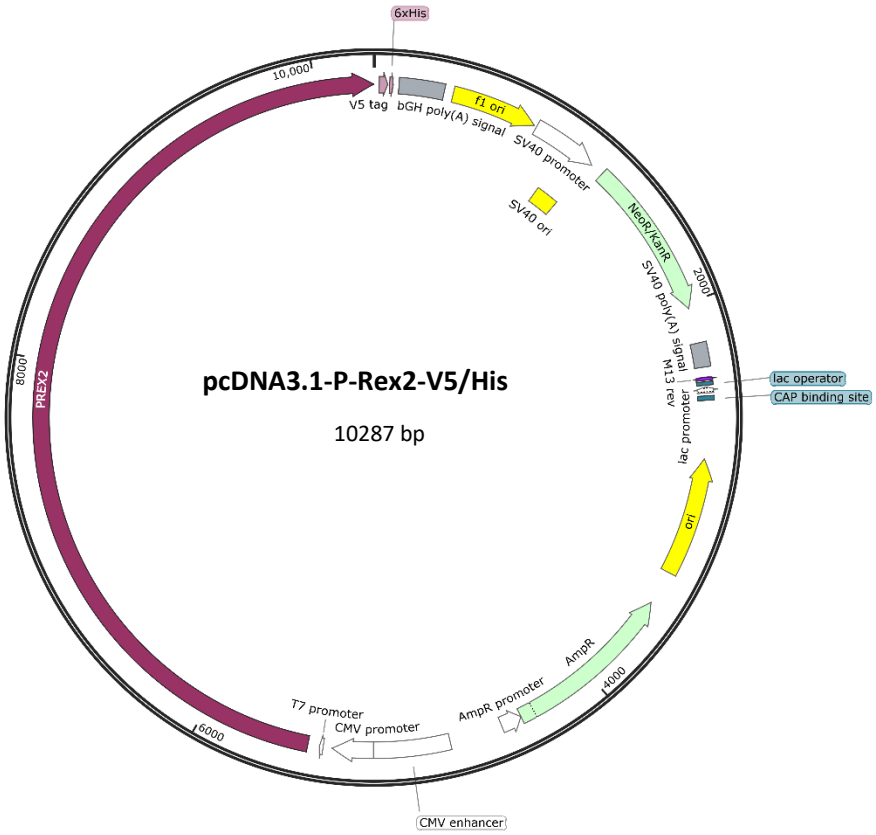

Figure 4.2: Plasmid map of transient overexpression vector; pcDNA3.1-P-Rex2-V5/His (Addgene plasmid, #41555).

To study the role of *P-REX2* and *RAC1* genes in ECs barrier dysfunction, lentivirus-based stable gene expression systems were generated. For this, either the pLenti-CMV-Blast-DEST or the pLenti-CMV-Puro-DEST vectors were used as an expression vector. For stable overexpression of the *P-REX2* gene in ECs, *the pLenti-CMV-hP-Rex2* plasmid was generated and confirmed initially with restriction enzyme digestion, and then final verification was done with Sanger sequencing. The plasmid map was given in Fig. 4.3.

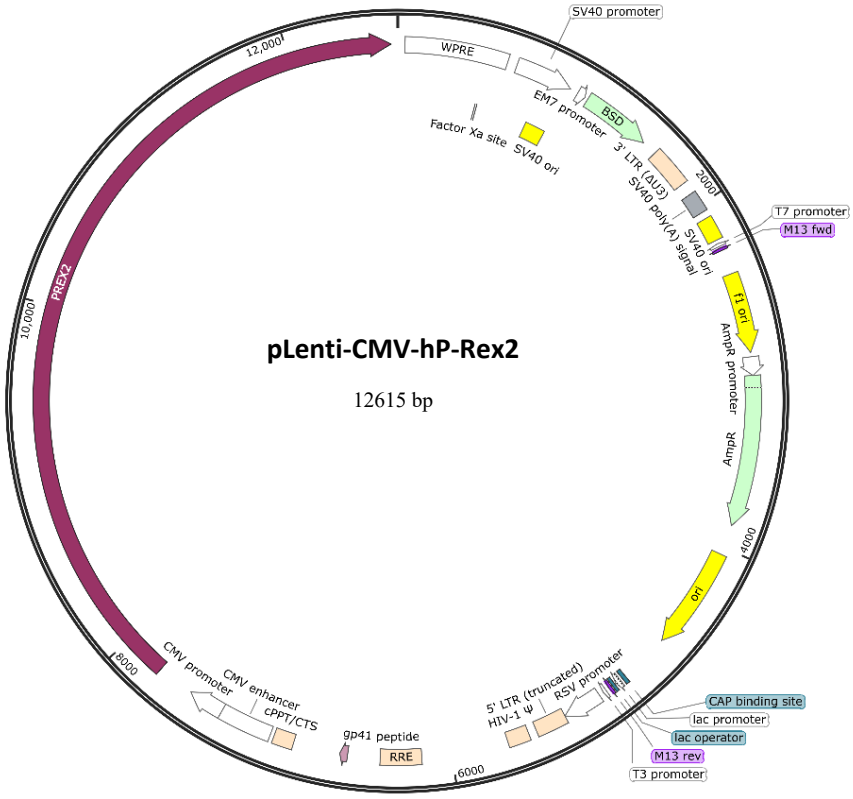

Figure 4.3: Plasmid map of pLenti-CMV-hP-Rex2. For molecular validation, it was cut by SacII enzyme. The expected band size of positive clones after digestion were 7121 bp, 5375 bp, and 64 bp.

To regulate Rac1 activity, *pLenti-CMV-Rac1-WT*, *pLenti-CMV-puro-Rac1-DN*, expressing dominant negative form of Rac1 (Rac1-DN), and *pLenti-CMV-puro-Rac1-CA*, expressing constitutively active form of Rac1 (Rac1-CA) were generated and verified similarly (Fig. 4.4). Additionally, to use as a control, *the pLenti-CMV-control-blast* or *the pLenti-CMV-control-puro* plasmids were generated with HA tag.

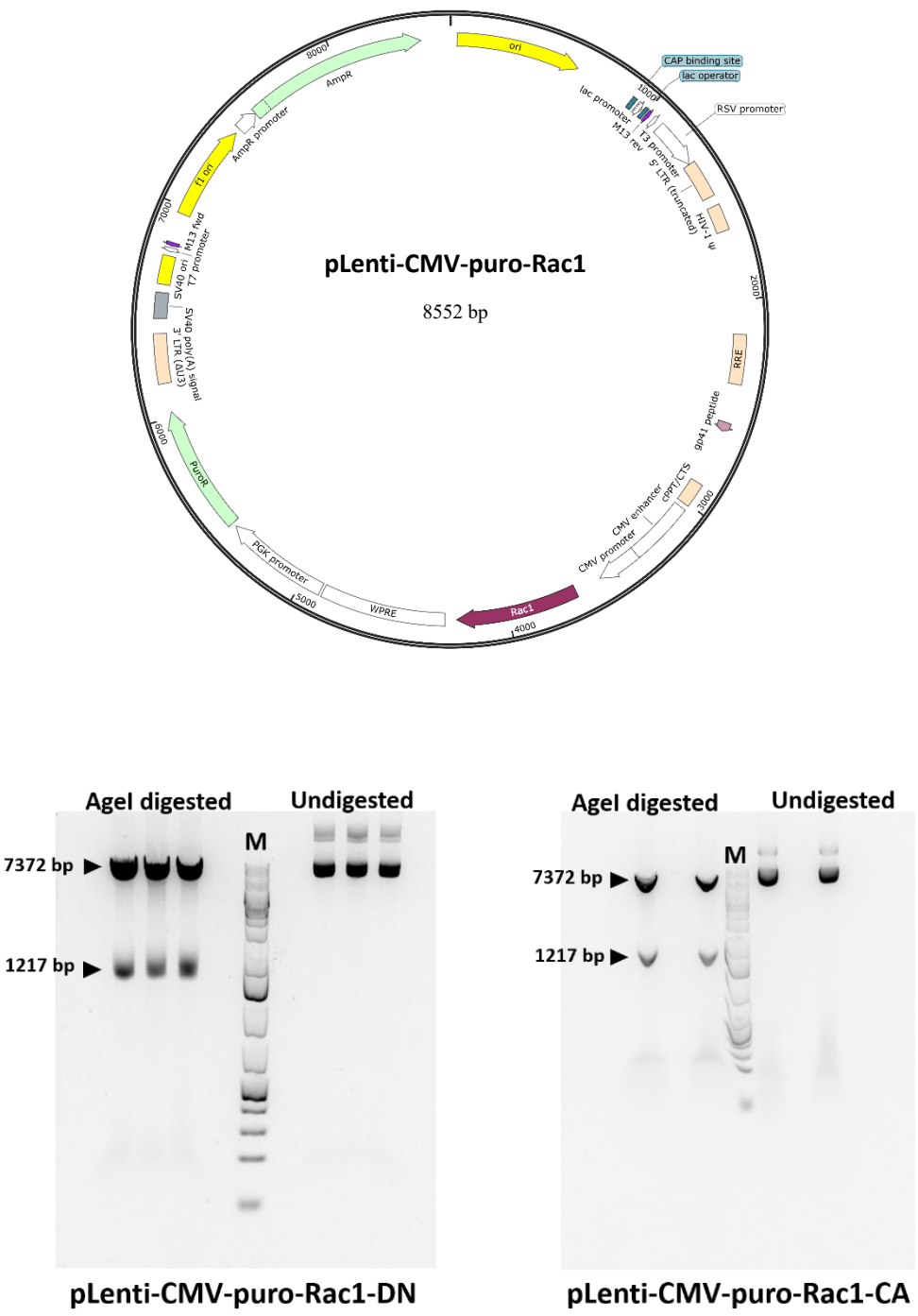

Figure 4.4: Plasmid map of pLenti-CMV-puro Rac1. Plasmid DNA was digested with AgeI enzyme into 7372 bp and 1217 bp fragments by insertion of Rac1-DN or Rac1-CA. *M.* GeneRuler 1kb Plus DNA Ladder. Each lane represents a clone.

4.2 Activation of Rac1 in Response to Inflammation

It has been known that the Rac1, a major mediator of the endothelial barrier, plays a crucial role in endothelial barrier dysfunction in response to inflammation. Since P-Rex2 was shown as a GEF that activates Rac1, as a first instance, the interaction of P-Rex2 with Rac1 was investigated. To this end, firstly, P-Rex2 and Rac1 were exogenously overexpressed in HEK-293 cells and co-immunoprecipitated with either an anti-Rac1 antibody or an anti-histidine (His) antibody targeting His tagged-P-Rex2 protein. As shown in Fig. 4.5A, Rac1 was co-immunoprecipitated with His tagged-P-Rex2, similarly, P-Rex2 was also co-immunoprecipitated with Rac1, indicating the interaction of Rac1 with P-Rex2.

Then, it was asked that whether TNF-α-induced P-Rex2 expression correlates with increased activity of Rac1 in ECs. It was found that *P-REX2* over-expression was significantly increased in the presence of TNF-α (Fig. 4.5B), which also caused robust activation of Rac1 in cultured HUVECs (Fig. 4.5C). Consistently, overexpression of P-Rex2 enhanced Rac1 activity in response to TNF-α (Fig. 4.5D). Together, these data demonstrate that TNF-α induced-Rac1 activation is upregulated with P-Rex2 overexpression.

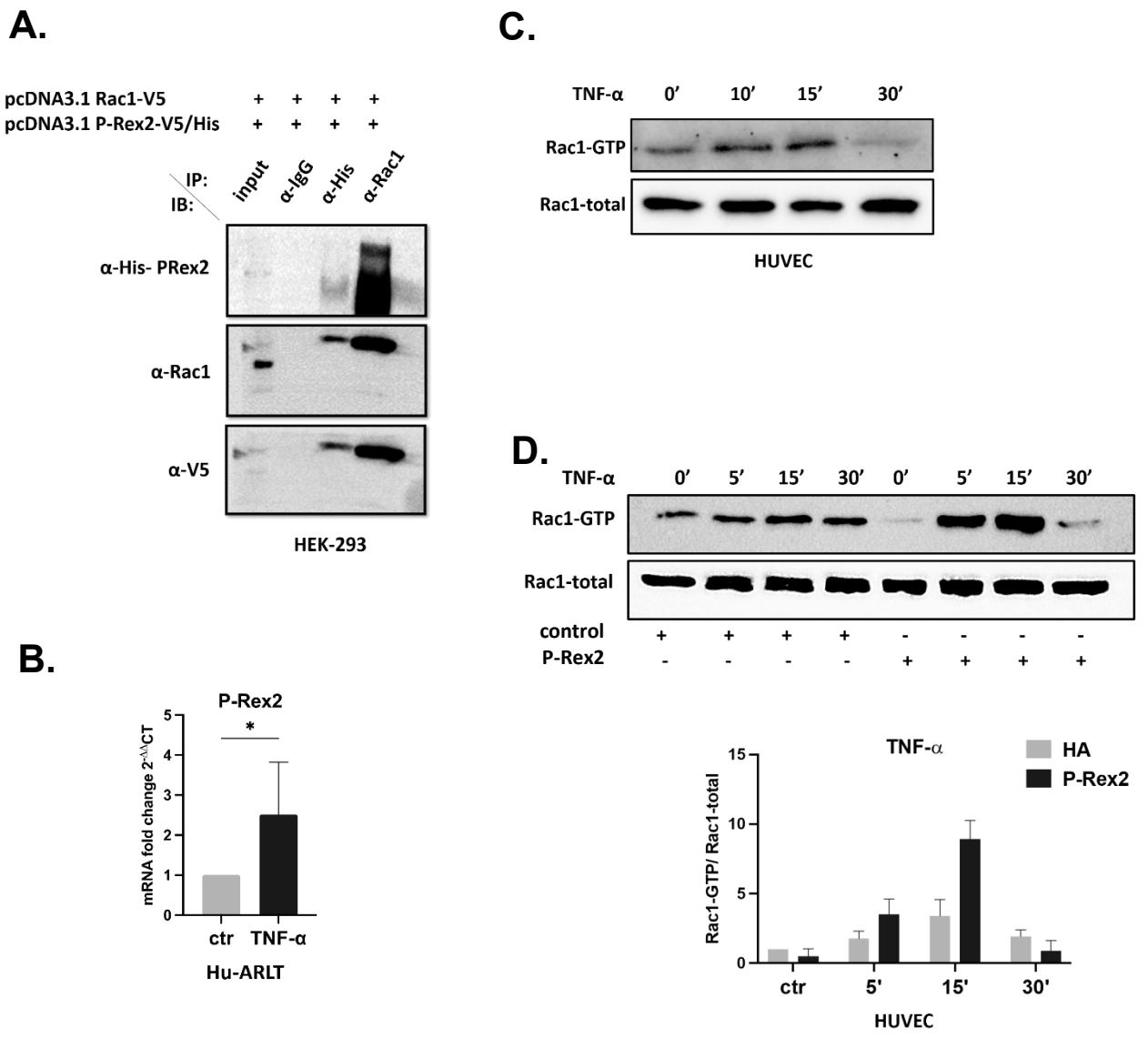

Figure 4.5: Activation of Rac1 in response to TNF-α. **A.** Co-immunoprecipitation of Rac1 and P-Rex2 in HEK-293 cells. P-Rex2 protein was immunoprecipitated with anti-His antibody, and Rac1 protein was immunoprecipitated with anti-Rac1 antibody. Next, precipitated proteins were analyzed with western blotting using an anti-P-Rex2 antibody to detect P-Rex2 and anti-Rac1 and anti-V5 antibodies to detect Rac1. To detect Rac1 protein, the membrane initially was blotted with anti-V5 antibody, and then the membrane was stripped and reblotted with anti-Rac1 antibody to show presence of Rac1 in the input sample. **B.** mRNA expression analysis of *P-REX2* gene in response to 12h TNF-α (1 ng/mL) in Hu-ARLT cells that infected with pLenti-CMV-hP-Rex2-WT vector to overexpress *P-REX2*. GAPDH is used as an internal control, data are expressed as fold change of untreated control (N=5). **C.** Rac1 activity that analyzed by pulldown assay. Representative blots of Rac1-GTP and Rac1-total from HUVECs that exposed to TNF-α (10 ng/mL) at different time points (min.) (N=3). **D.** Rac1 activity; HUVEC monolayers were infected with lentiviruses containing either pLenti-CMV-control vector or pLenti-CMV-hP-Rex2-WT vector. Then, cells were exposed to TNF-α (10 ng/mL) at different time points (min.) and Rac1 activity analyzed by pulldown assay (N=3). *Values are represented as the mean ±S.E.M. of independent experiments indicated as N. Data was analyzed using an unpaired student's t-test. *p< 0.05 is accepted as significant.*

4.3 The Role of P-Rex2 Overexpression on Endothelial Barrier

4.3.1 Effect of P-Rex2 overexpression on EC permeability

The P-Rex2 is a GEF that activates Rac1 GTPase via exchanging GDP to GTP. It has already been shown in various studies that Rac1 regulates EC barrier permeability. To better understand upstream mechanisms regulating Rac1 activity and EC barrier function, the Rac1 GEF P-Rex2 was overexpressed in HUVECs by using lentiviral expression vector (p-Lenti-CMV-hP-Rex2) (Fig. 4.6A). The role of P-Rex2 on EC barrier permeability was investigated *in vitro* by monitoring albumin permeability across endothelial monolayers. It was observed that overexpression of the P-Rex2 in HUVECs increased the permeability. Moreover, the presence of inflammatory cytokine TNF-α (10 ng/mL) enhanced P-Rex2-mediated EC barrier permeability (Fig. 4.6B).

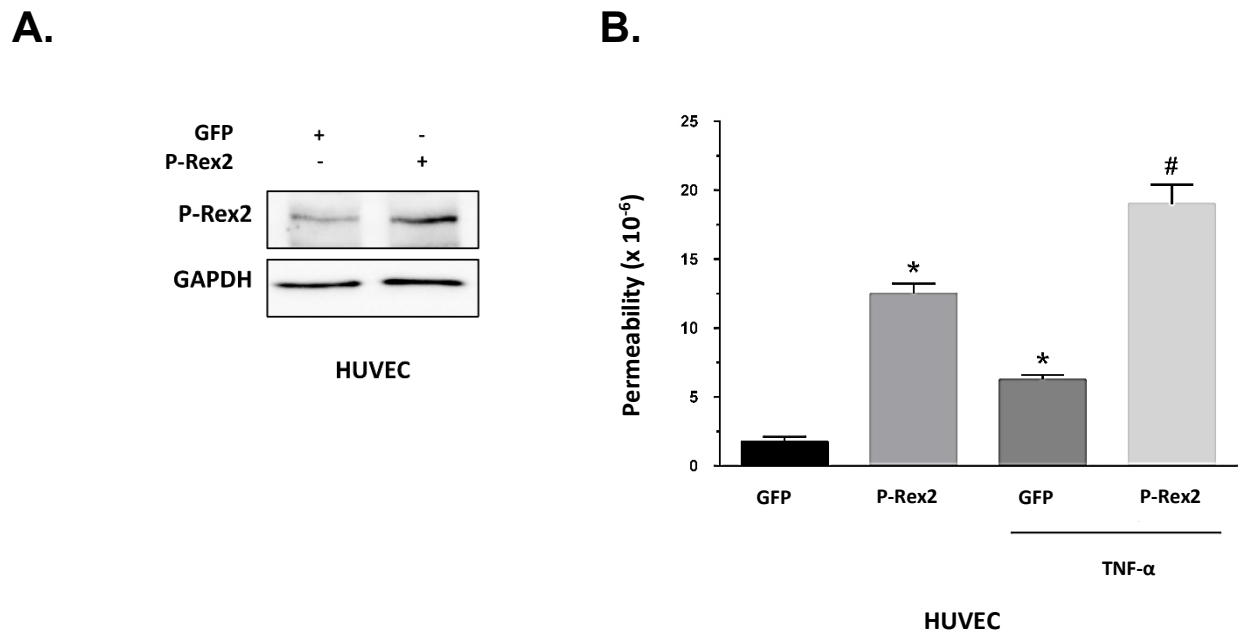

Figure 4.6: Effect of Rac1 GEF P-Rex2 overexpression on EC barrier permeability. HUVECs were infected with lentiviruses either containing p-Lenti-CMV-hP-Rex2-WT vector to overexpress P-Rex2 protein or pLenti-CMV-GFP vector as a control. **A.** Protein expression analysis of P-Rex2 in infected HUVECs by western blotting. GAPDH is used as an internal control. **B.** Endothelial permeability was defined as measuring albumin flux across the EC monolayer (N=3). *Values are represented as the mean ±S.E.M. of independent experiments indicated as N. Data was analyzed using an unpaired student's t-test. *p< 0.05 is accepted as significant.*

4.3.2 Effect of P-Rex2 overexpression on AJs and actin cytoskeleton in response to TNF-α

It has been shown that the integrity of the endothelial barrier is regulated by actin cytoskeleton dynamics and the arrangement of VE-cadherin-based AJs (Aslam et al., 2013). Therefore, firstly, it was asked whether overexpression of P-Rex2 alters the rearrangement of VE-cadherin at cell-cell junctions under basal and inflammatory conditions. The localization of VE-cadherin in HUVEC monolayers overexpressing the P-Rex2 was examined in response to different concentrations of TNF-α (Fig. 4.7). It was shown that although under basal conditions, VE-cadherin is accumulated at the cell-cell junctions, P-Rex2 overexpression reduces the density of VE-cadherin at junctions. Furthermore, exposure of HUVECs to TNF-α caused loss of VE-cadherin localization at cell-cell junctions in a concentration-dependent manner. Moreover, in the presence of P-Rex2 overexpression, TNF-α stimulation drastically enhanced the loss of VE-cadherin from the cell surface, indicating barrier destabilizing effect of P-Rex2 overexpression in ECs.

Similar to VE-cadherin, which localizes at the cell periphery under basal conditions, the filamentous actin (F-actin) also localizes at the cell periphery. When ECs lose their integrity, localization of actin at the cell periphery decreases, followed by an increase in stress fiber formation (Gündüz et al., 2010). Thus, as a next step, it was investigated whether P-Rex2 overexpression leading to rearrangement of the actin cytoskeleton to alter the integrity of the endothelial barrier. As shown in Fig. 4.8, in comparison to control, where actin localized at the cell periphery, P-Rex2 overexpression resulted in a loss of peripheral actin localization and enhanced actin stress fiber formation on treatment with low TNFα concentrations. However, at high TNFα concentrations (10-20 ng/mL) hardly any difference was seen probably due to activation of other actin regulatory pathways such as RhoA/Rock signaling.

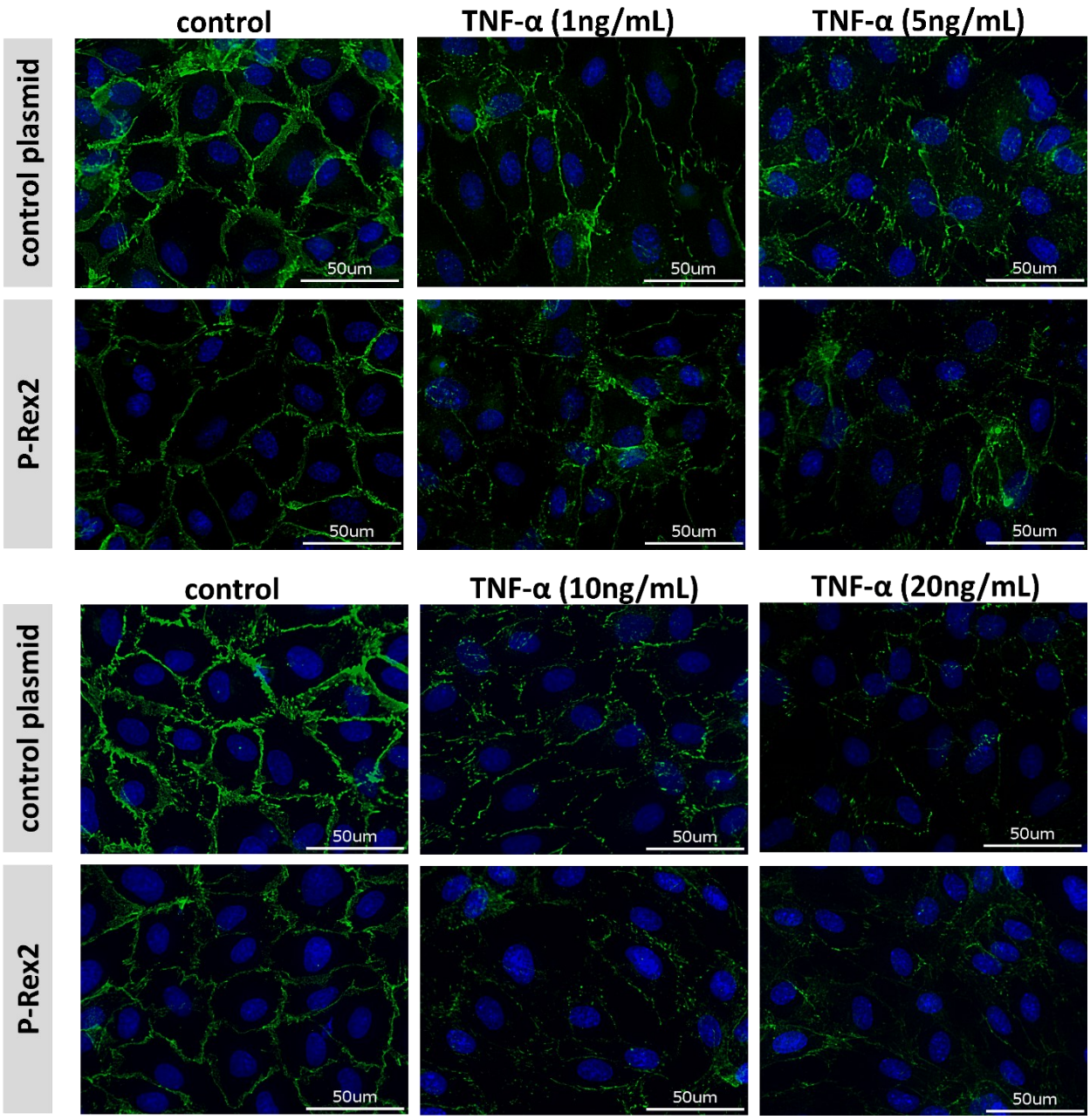

Figure 4.7: Effect of P-Rex2 overexpression and TNF-α on localization of VE-cadherin in EC monolayers. HUVEC monolayers were infected with lentiviruses carrying either pLenti- CMV-hP-Rex2 or pLenti-CMV-control plasmids, were selected for stable clones, were grown on coverslips, and immunostained for VE-cadherin after methanol fixation. DAPI was used for nuclear staining. HUVECs were exposed to TNF-α as indicated concentrations for 12 h in the starving medium. Images were taken with fluorescence microscopy with 40x objective. Representative images from three experiments of independent cell preparations (Scale bar: 50 μm).

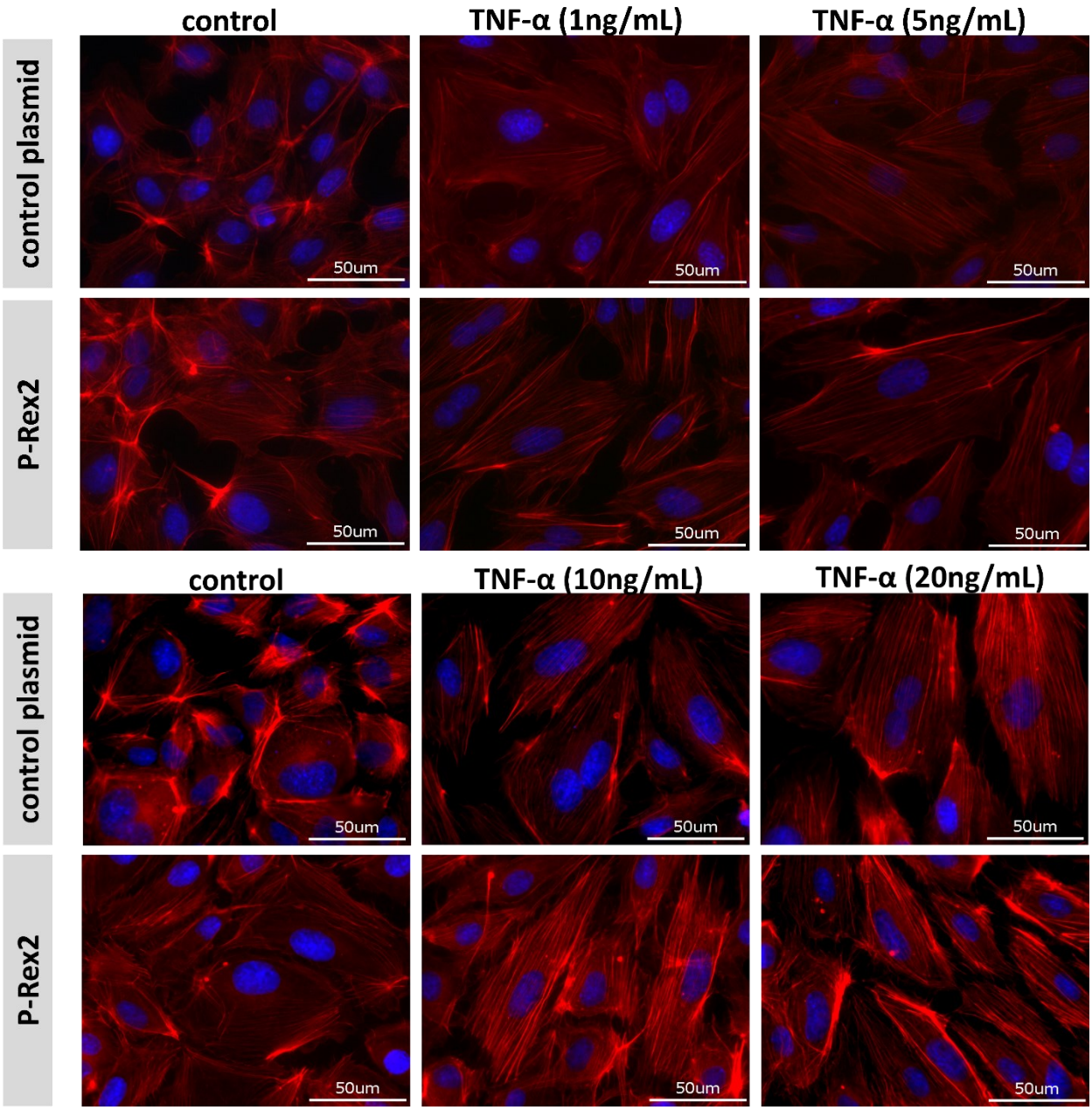

Figure 4.8: Effect of P-Rex2 overexpression and TNF-α on actin cytoskeleton dynamics in EC monolayers. Cells were stained for actin with phalloidin-TRITC after 4% PFA fixation. DAPI was used for nuclear staining. HUVECs were exposed to TNF-α as indicated concentrations for 12 h in the starving medium. Images were taken with fluorescence microscopy with 40x objective. Representative images from three experiments of independent cell preparations (Scale bar: 50 µm).

Since P-Rex2 is a GEF that activates Rac1, it was also analyzed that whether inhibition of Rac1 can protect endothelial barrier against P-Rex2 mediated loss of VE-cadherin and actin localization at cell-cells junctions in response to TNF-α. To this end, Rac1 inhibitor, NSC23766, was used to inhibit Rac1 pharmacologically in HUVEC monolayers.

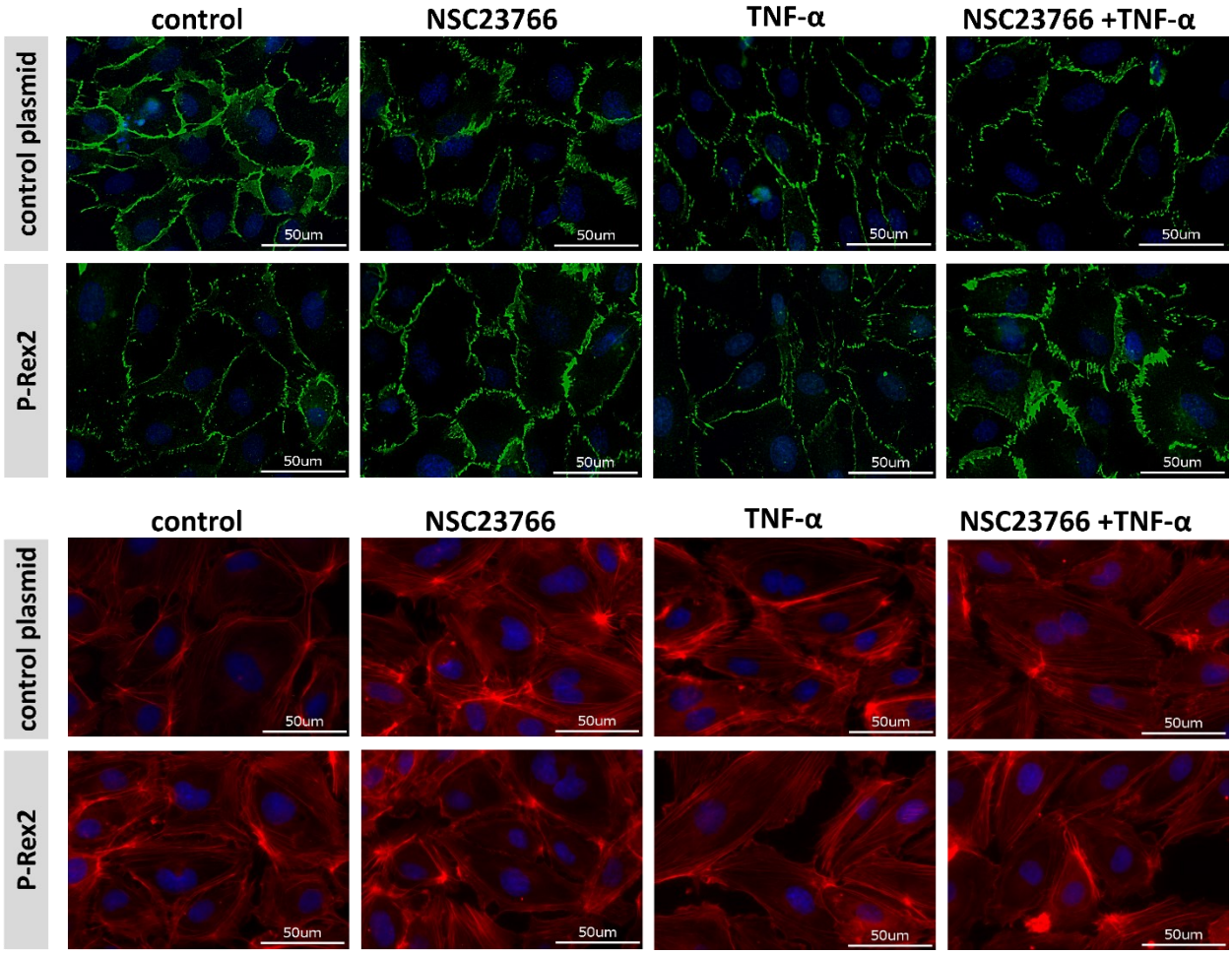

Figure 4.9: Effect of inhibition of Rac1 on localization of VE-cadherin and actin cytoskeleton dynamics in EC monolayers. Cells were stained for VE-cadherin and actin. DAPI was used for nuclear staining. HUVECs were exposed to TNF-α for 6 h in the presence or absence of NSC23766. The Rac1 inhibitor NSC23766 were applied before TNF-α treatment. Images were taken with fluorescence microscopy with 40X objective. Representative images from three experiments of independent cell preparations (Scale bar: 50 μm).

It was shown in Fig. 4.9 that preincubation of EC monolayers with NSC23766 (50 μM) for 2 h partially protected TNF-α-induced loss of VE-cadherin from cell-cell junctions while slightly reducing actin stress fibers. On the other hand, pharmacological inhibition of Rac1 in P-Rex2 overexpressing ECs reversed the loss of peripheral localization of VE-cadherin and actin. Moreover, Rac1 inhibition in P-Rex2 overexpression EC monolayers prevented TNF-α-induced stress fiber formation and maintained assembly of VE-cadherin at cell-cell junctions (Fig. 4.9).

For further analysis, Hu-ARLT cells stably expressing P-Rex2 were double-infected with either dominant-negative or constitutively active Rac1 containing lentiviruses. Consistent with pharmacological inhibition of Rac1, biological inhibition of Rac1 (Rac1-DN) also prevented TNF-α-induced rearrangement of actin cytoskeleton in P-Rex2 overexpressing cells but not in cells expressing control plasmid (Fig. 4.10). Moreover, in comparison to control, in which constitutively active Rac1 (Rac1-CA) protected ECs against TNF-α-induced stress fiber formation, expression of Rac1-CA in P-Rex2 overexpressing cells caused opposite effects. It resulted in the loss of peripheral actin localization and increased stress fiber formation in response to TNF-α. Taken together, these data indicate that under inflammatory conditions, P-Rex2-induced rearrangement of AJs and actin cytoskeleton dynamics are Rac1 dependent in ECs.

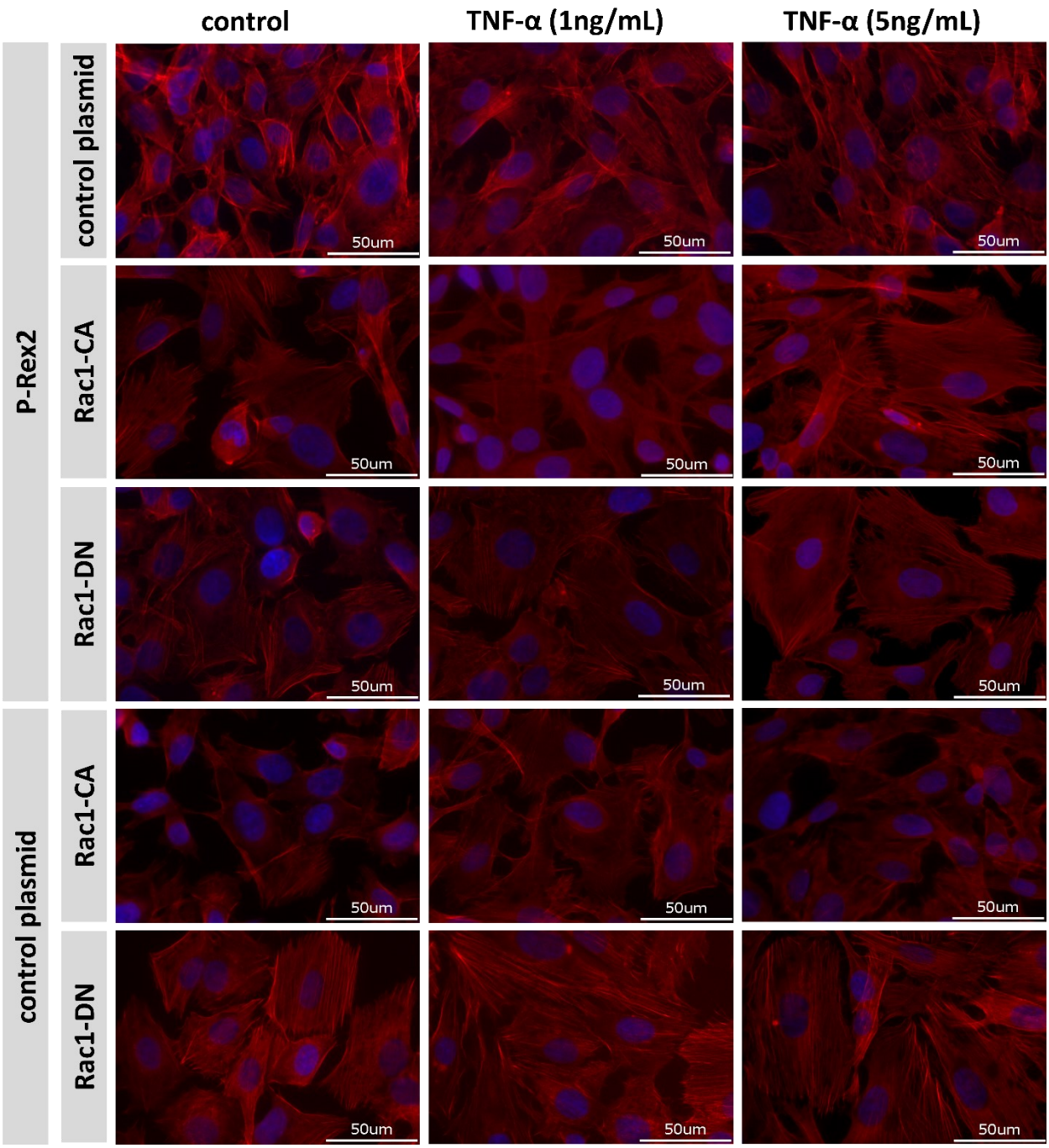

Figure 4.10: Effect of inhibition of Rac1 on actin cytoskeleton dynamics in EC. Hu-ARLT cells were double-infected as indicated with lentiviruses carrying pLenti-CMV-hP-Rex2, pLenti-CMV-control, pLenti-CMV-Rac1-CA, and pLenti-CMV-Rac1-DN plasmids. Cells were stained for actin. DAPI was used for nuclear staining. Exposed to TNF-α for 12 h at given concentrations. Images were taken with fluorescence microscopy with 40x objective. Representative images from three experiments of independent cell preparations (Scale bar: 50 µm).

4.4 The Role of P-Rex2 in the Pathological Angiogenesis

Various diseases, including cancer, arteriosclerosis, and hypoxia, require activating cellular pathways to trigger pathological angiogenesis. This process begins in ECs with loss of barrier integrity, followed by increased migration, proliferation, and capillary tube formation (Sawada et al., 2010). Since Rac1 is a well-known regulator of angiogenesis in ECs and expression of truncated forms of its GEF P-Rex2 in various tumor tissues show increased proliferative and migratory effects (Lissanu Deribe et al., 2016), it was investigated whether P-Rex2 is a mediator regulating pathological angiogenesis in ECs.

4.4.1 Effect of P-Rex2 overexpression on EC migration

It was investigated by using *in vitro* wound healing assay that whether overexpression of the P-Rex2 protein has a migratory effect on ECs. In comparison to GFP expressing controls, the P-Rex2 overexpression induced a significant increase in the wound closure rate of HUVEC monolayers, the effect of which enhanced in the presence of VEGF (10 ng/mL) (Fig. 4.11). Consistently, in Hu-ARLT endothelial cell line generated from immortalized HUVECs, P-Rex2 overexpression also induced faster wound healing; furthermore, TNF-α stimulation enhanced the migratory effect of P-Rex2 overexpression (Fig. 4.12).

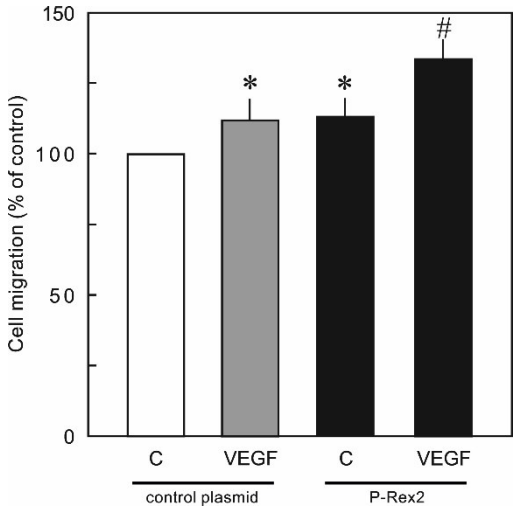

Figure 4.11: Effects of P-Rex2 and VEGF on migration of ECs. HUVECs were infected with recombinant lentiviruses to overexpress either GFP as control or P-Rex2. Wound healing assay was performed with starving medium in the presence or absence of VEGF for 24h and quantified as described in detail in wound healing assay (Methods, section 3.7). Values are represented as the mean ±S.E.M. *p< 0.05 is accepted as significant (N=3).

As a next step, it was investigated whether the observed effect of P-Rex2 overexpression on ECs is mediated by the activation of Rac1. To test that, confluent monolayers of Hu-ARLT cells, overexpressing either HA as a control group or P-Rex2 as a study group, were incubated with the Rac1 inhibitor NSC23766 (50 μM) as given in Fig. 4.12, and then well inserts were removed to monitor wound closure rate. It was found that pharmacological inhibition of Rac1 attenuates EC migration in the P-Rex2 overexpressing cells but not in the control group, indicating P-Rex2 mediated EC migration is Rac1 dependent.

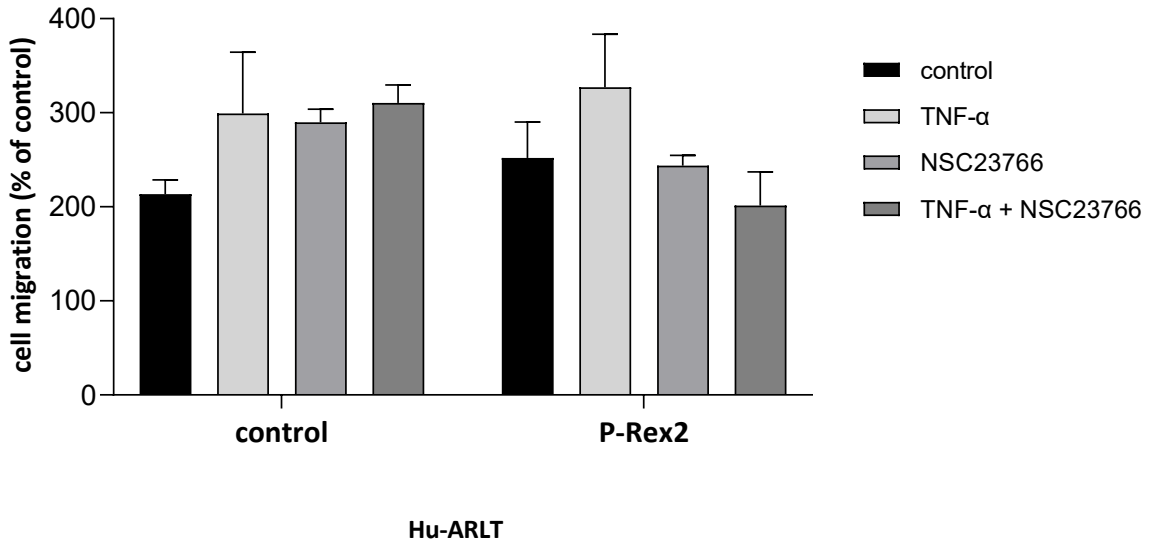

Figure 4.12: ECs migration in response to TNF-α (10 ng/mL), P-Rex2 overexpression, and Rac1 inhibition with NSC23766 (50 μM). Hu-ARLT cells were infected with recombinant lentiviruses to overexpress either HA tag as control or *P-REX2* gene. Wound healing assay was performed with starving medium in the presence or absence of TNF-α. To inhibit Rac1 activity, cells were preincubated with NSC23766 for 30 min. and then well inserts were removed, cells were induced with TNF-α, and gap closure were quantified after 48 h.

4.4.2 Effect of P-Rex2 overexpression on *in vitro* sprouts in ECs

To determine whether P-Rex2 overexpression induces angiogenesis, 3D cultures of ECs were generated, and *in vitro* sprout formation was monitored under different conditions. As a positive control to induce sprout generation, Fluvastatin (1 μM) was used in each experiment (Gündüz et al., 2015). As shown in Fig 4.13, P-Rex2 overexpression led to sprout formation significantly longer in comparison to GFP expressing controls in cultured primary ECs; HUVECs. The length of sprouts was stimulated more upon treatment with VEGF (10 ng/mL).

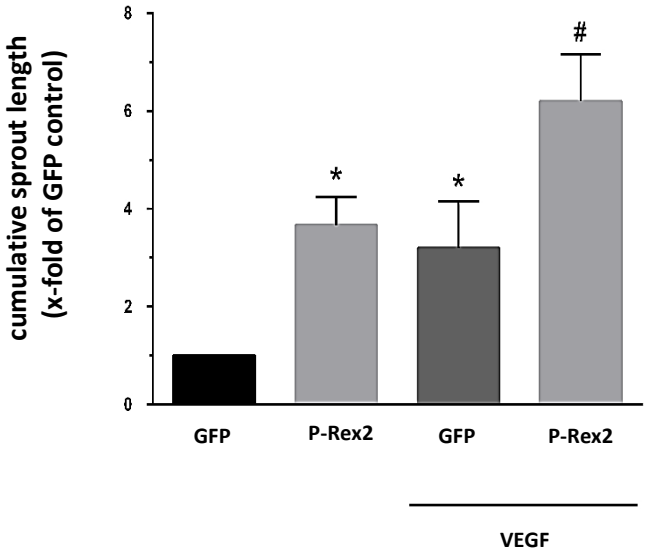

Figure 4.13: Effects of P-Rex2 and VEGF (10 ng/mL) on EC sprouting in HUVECs. Quantitative analysis of cumulative sprout length calculated from photographs of three independent experiments. In each experiment, eight spheroids were used to calculate sprout length. Values are represented as the mean ±S.E.M. (N=3). *$p < 0.05$ is accepted as significant.

On the other hand, in the endothelial cell line Hu-ARLT, while P-Rex2 overexpression caused a significant increase in sprout formation similar to HUVECs, different concentrations of VEGF stimulation did not enhance P-Rex2-mediated sprout formation (Fig 4.14A & C). However, in the presence of TNF-α, longer sprouts were measured (Fig 4.14B & D).

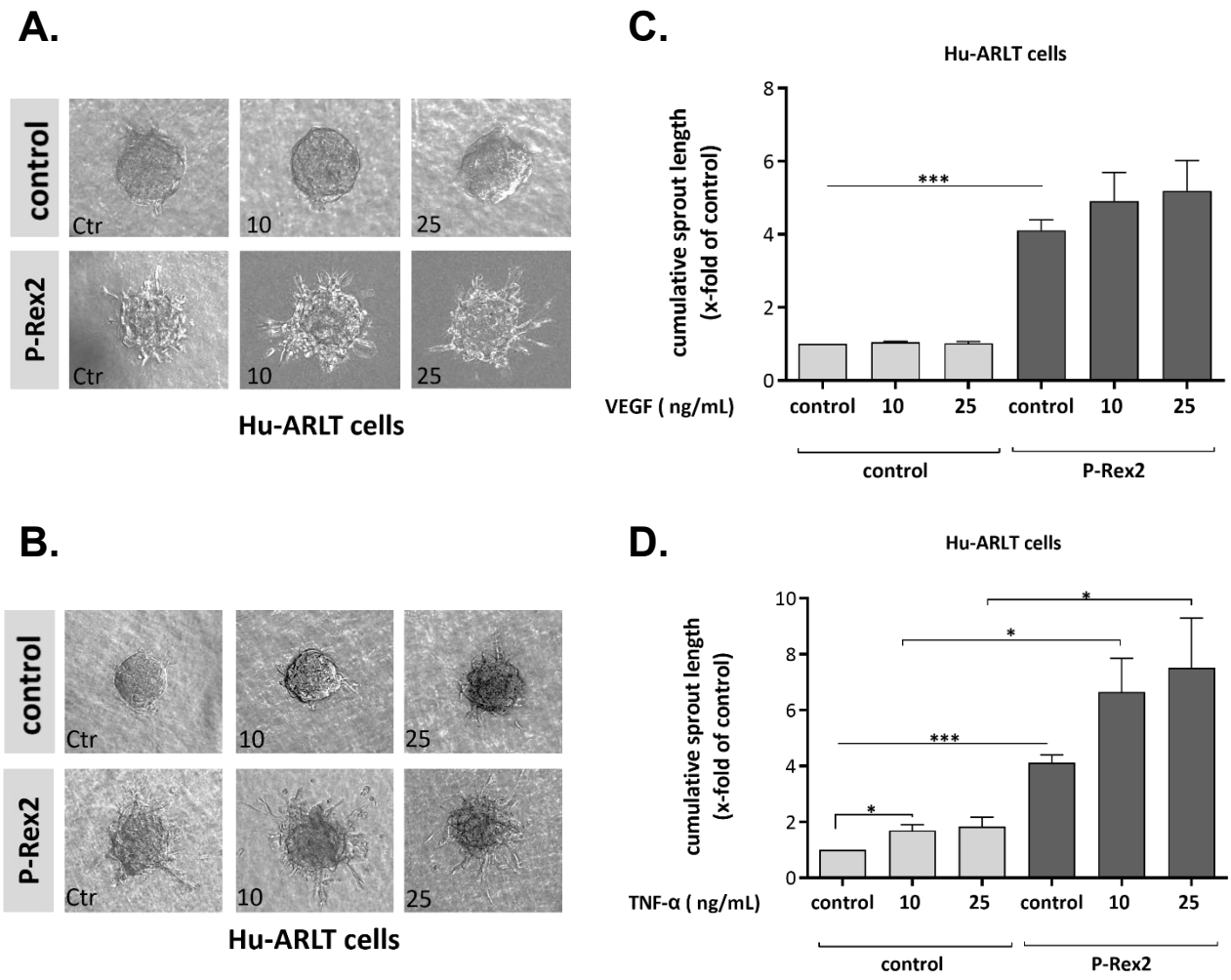

Figure 4.14: Effects of P-Rex2, VEGF, and TNF-α on EC sprouting in Hu-ARLT cells. **A & B.** Representative images of EC sprouts in response to different concentrations of VEGF (ng/mL) (A) and TNF-α (ng/mL) (B). **C & D.** Quantitative analysis of cumulative sprout length calculated from photographs of N=3 independent experiments. In each experiment, N=8 spheroids were used to calculate sprout length. Values are represented as the mean ±S.E.M. Data was analyzed using an unpaired student's t-test. *p< 0.05 is accepted as significant.

4.4.3 Effect of P-Rex2 overexpression on expression of cell adhesion molecules in ECs

It has been known that vascular inflammation and angiogenesis trigger various signaling mechanisms that result in the activation of ECs, which includes an increase in expression levels of ICAM-1 and VCAM-1. Since endothelial barrier dysfunction is also an outcome of vascular inflammation and pathological angiogenesis, it was investigated that whether P-Rex2 overexpression alters the expression pattern of cell adhesion molecules in response to

inflammation. As seen in Fig 4.15, it was shown that P-Rex2 overexpression increased the expression of cell adhesion molecules, ICAM-1 and VCAM-1; however, the observed differences between control group and P-Rex2 overexpressing cells were not significant in most of the groups.

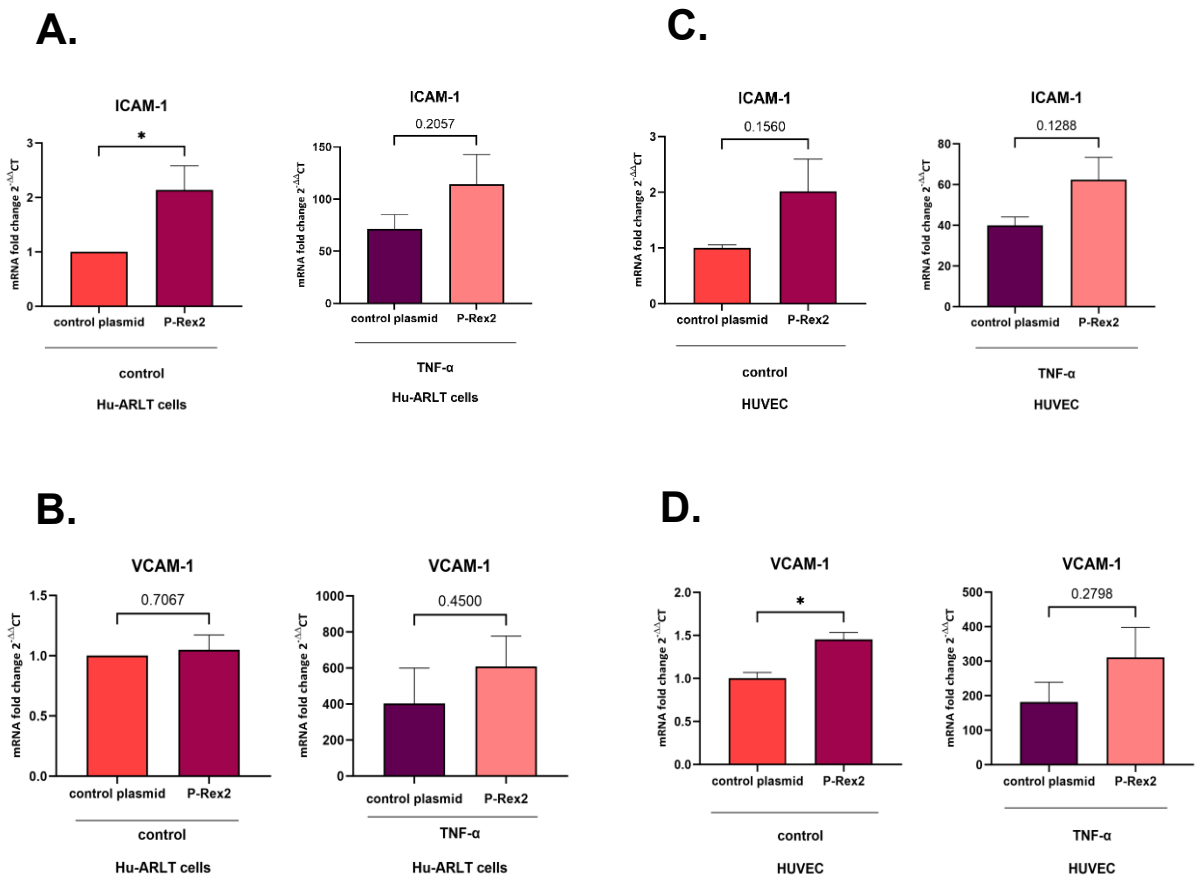

Figure 4.15: Effect of P-Rex2 overexpression on ICAM-1 and V-CAM1 expression levels in ECs in the presence and absence of TNF-α. ECs were treated with TNF-α (10 ng/mL) in starvation medium for 12 h. **A & B.** Hu-ARLT cells. Values are the mean ±S.E.M. of N=6 (ICAM-1) and N=5 (VCAM-1) independent experiments. **C & D.** HUVECs. Values are the mean ±S.E.M. of N=3 from independent infections. In all experiments, GAPDH is used as an internal control, data are expressed as fold change of control and were analyzed using an unpaired student's t-test. *p< 0.05 is accepted as significant.

4.4.4 Effect of P-Rex2 overexpression on expression of inflammatory cytokines in ECs

The inflammatory cytokines are involved in endothelial barrier dysfunction, hence, the pathogenesis of various diseases. It was investigated whether increased expression of P-Rex2 alters the expression of inflammatory cytokines, IL-6 and IL-8, in ECs. It was observed that P-Rex2 overexpression significantly upregulates the expression of IL-6 and IL-8 (Fig. 4.16A & B) in Hu-ARLT cells. However, although the presence of TNF-α amplified expression level of cytokines, no significant differences was observed between control group and P-Rex2 overexpressing cells (Fig.4.16).

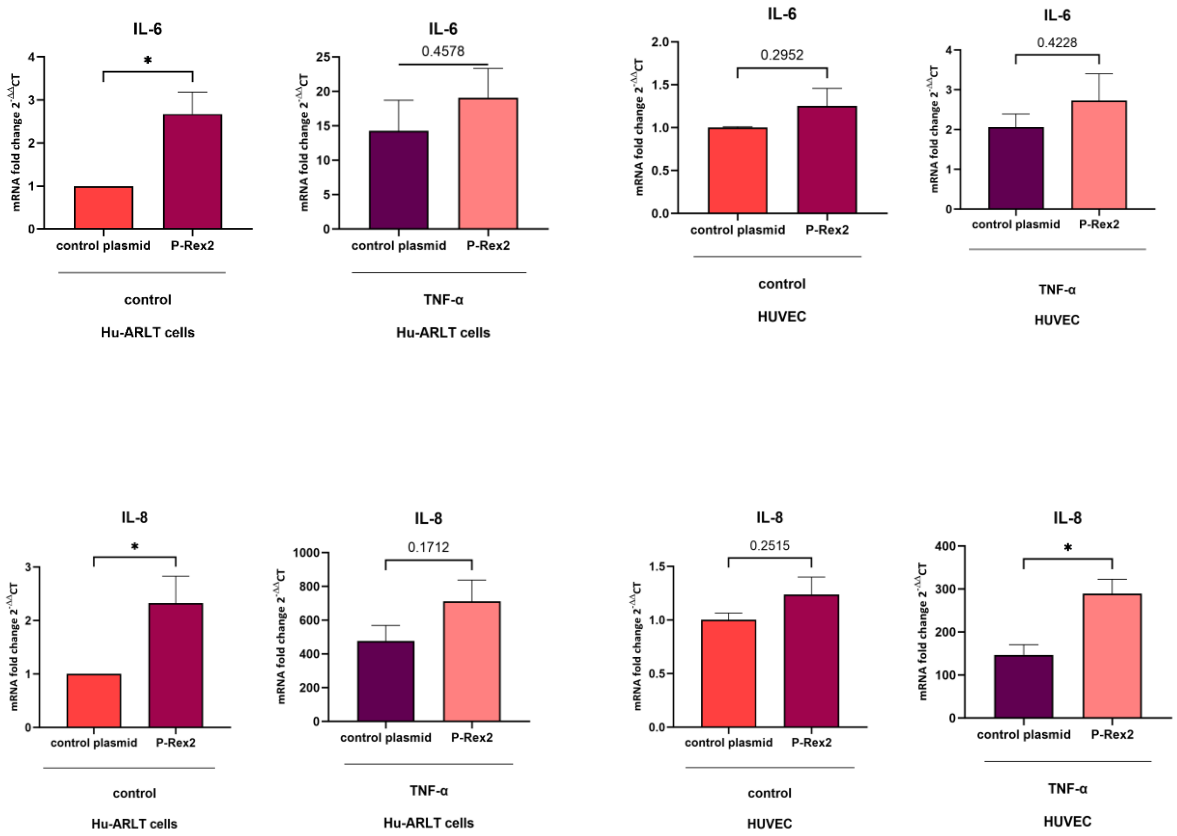

Figure 4.16: Effect of P-Rex2 overexpression on IL-6 and IL-8 expression levels in the presence and absence of TNF-α. ECs were treated with TNF-α (10 ng/mL) in starvation medium for 12 h. **A & B.** Hu-ARLT cells. Values are the mean ±S.E.M. (N=5). **C & D.** HUVECs. Values are the mean ±S.E.M. of N=3 from independent infections. GAPDH is used as an internal control, data are expressed as fold change of control and were analyzed using an unpaired student's t-test. *p< 0.05 is accepted as significant.

4.5 Effect of P-Rex2 Overexpression on ROS Generation in ECs

It was reported that Rac1-mediated endothelial barrier dysfunction is related to excessive generation of ROS in ECs. Therefore, it was investigated that whether the Rac1 GEF P-Rex2 has a role in the regulation of ROS generation in ECs. To this end, molecular probe DCF-DA was used to determine intracellular ROS production due to P-Rex2 overexpression and TNF-α stimuli in the Hu-ARLT cells stably expressing P-Rex2, as well as in the control. As given in Fig. 4.17, P-Rex2 overexpression significantly upregulated intracellular ROS production under basal conditions, while no significant difference was observed in TNF-α (10 ng/mL)-induced ROS production in ECs.

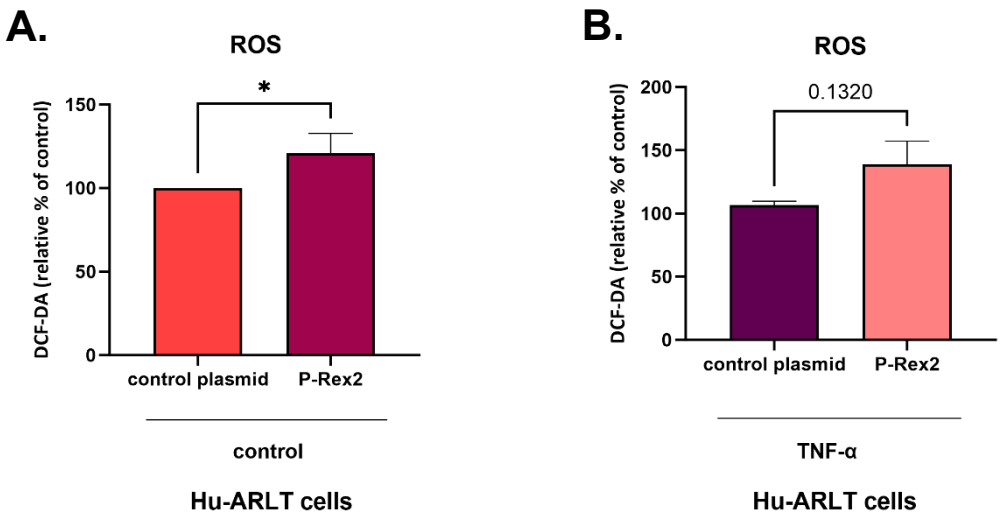

Figure 4.17: Effect of P-Rex2 on intracellular ROS production of ECs in the presence and absence of TNF-α. The generation of ROS was measured in black-coated 96-well plates using DCF-DA (10 µM). Following 30 min. incubation with DCF-DA, cells were stimulated with TNF-α (10 ng/mL) for 1h. Values are represented as the mean ±S.E.M. of N=6 independent experiments in which each group was assayed as N=16. Data normalized to protein levels in each well, presented as relative % of control, and analyzed using an unpaired student's t-test. *p< 0.05 is accepted as significant.

Consistently, inhibition of ROS using ROS scavenger N-Acetyl-L-cysteine (NAC) (1 mM) not only reversed P-Rex2 mediated loss of VE-cadherin from cell-cell junctions (Fig. 4.18) but also increased localization of actin at the cell periphery (Fig. 4.19). Moreover, preincubation of cells with NAC (1 mM) partially protected cells against increased concentrations of TNF-α. Notably, inhibition of ROS with NAC reduced TNF-α-induced loss of VE-cadherin at cell

periphery accompanied by decrease in stress fiber formation and increase in accumulation of actin at cell-cell junctions (Fig. 4.18 & Fig. 4.19). Taken together, these data indicate that P-Rex2 mediated loss of AJs and rearrangement of actin dynamics are associated with generation of ROS in ECs.

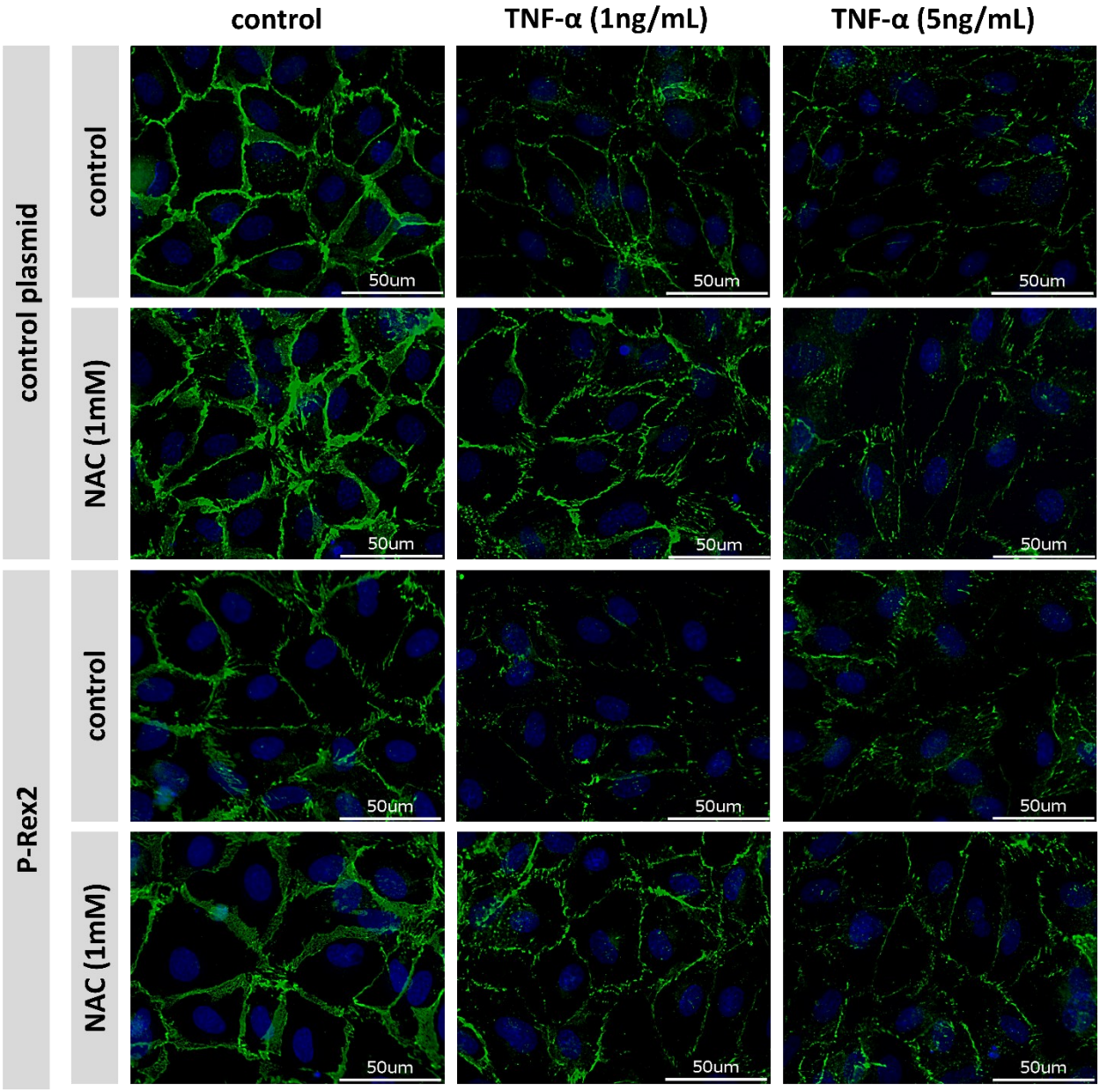

Figure 4.18: Role of ROS on localization of VE-cadherin in EC monolayers. HUVEC monolayers were stained for VE-cadherin. DAPI was used for nuclear staining. HUVECs were exposed to TNF-α at different concentrations for 12 h in the presence or absence of NAC (1 mM). NAC was applied 2 h before TNF-α treatment. Images were taken with fluorescence microscopy with 40X objective. Representative images from three experiments of independent cell preparations (Scale bar: 50 µm).

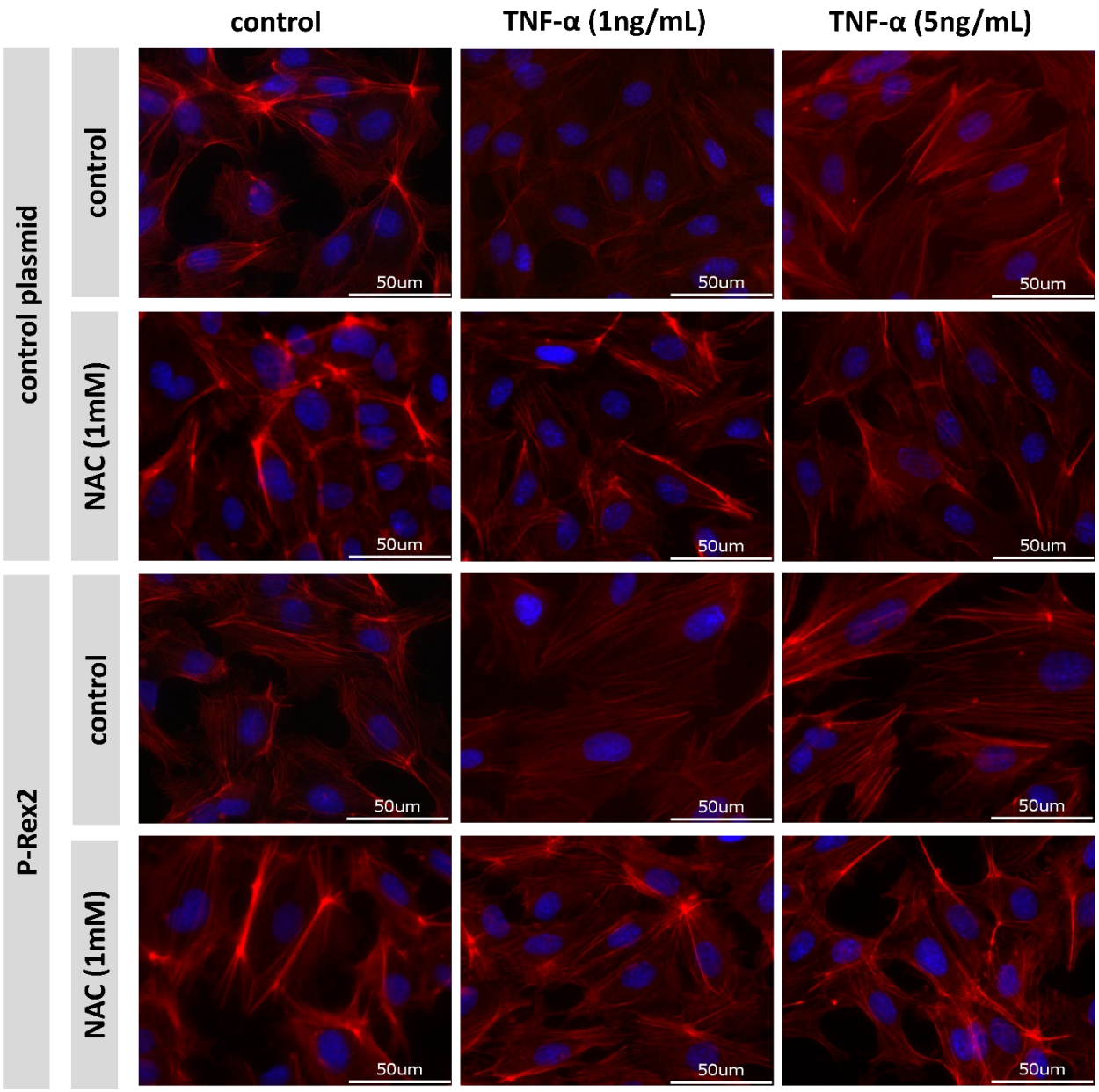

Figure 4.19: Role of ROS on localization of actin in EC monolayers. HUVEC monolayers were stained for actin. DAPI was used for nuclear staining. HUVECs were exposed to TNF-α at different concentrations for 12 h in the presence or absence of NAC (1 mM). NAC was applied 2 h before TNF-α treatment. Images were taken with fluorescence microscopy with 40X objective. Representative images from three experiments of independent cell preparations (Scale bar: 50 μm).

4.5.1 The role of P-Rex2 in NADPH oxidase-dependent ROS formation

It was asked whether P-Rex2-induced loss of AJs and rearrangement of actin caused by excessive ROS generation is due to NADPH oxidase activity. To this end, HUVECs overexpressing either P-Rex2 or control were preincubated with different concentrations of VAS2870, and further ROS production was induced with increased concentrations of TNF-α. The effect of P-Rex2 overexpression on AJs and actin dynamics were attenuated in the presence of VAS2870 in a concentration-dependent manner (Fig. 4.20 & Fig. 4.21). Interestingly, it was observed that in P-Rex2 overexpressing cells, incubation with VAS2870 protected ECs against TNF-α-induced loss of both VE-cadherin (Fig 4.20) and actin from cell periphery and prevented stress fiber assembly (Fig. 4.21) but not in control. These data not only support ROS mediated loss of cell-cell junctions but also indicate that P-Rex2 leads to TNF-α-induced NADPH oxidase dependent ROS production in ECs.

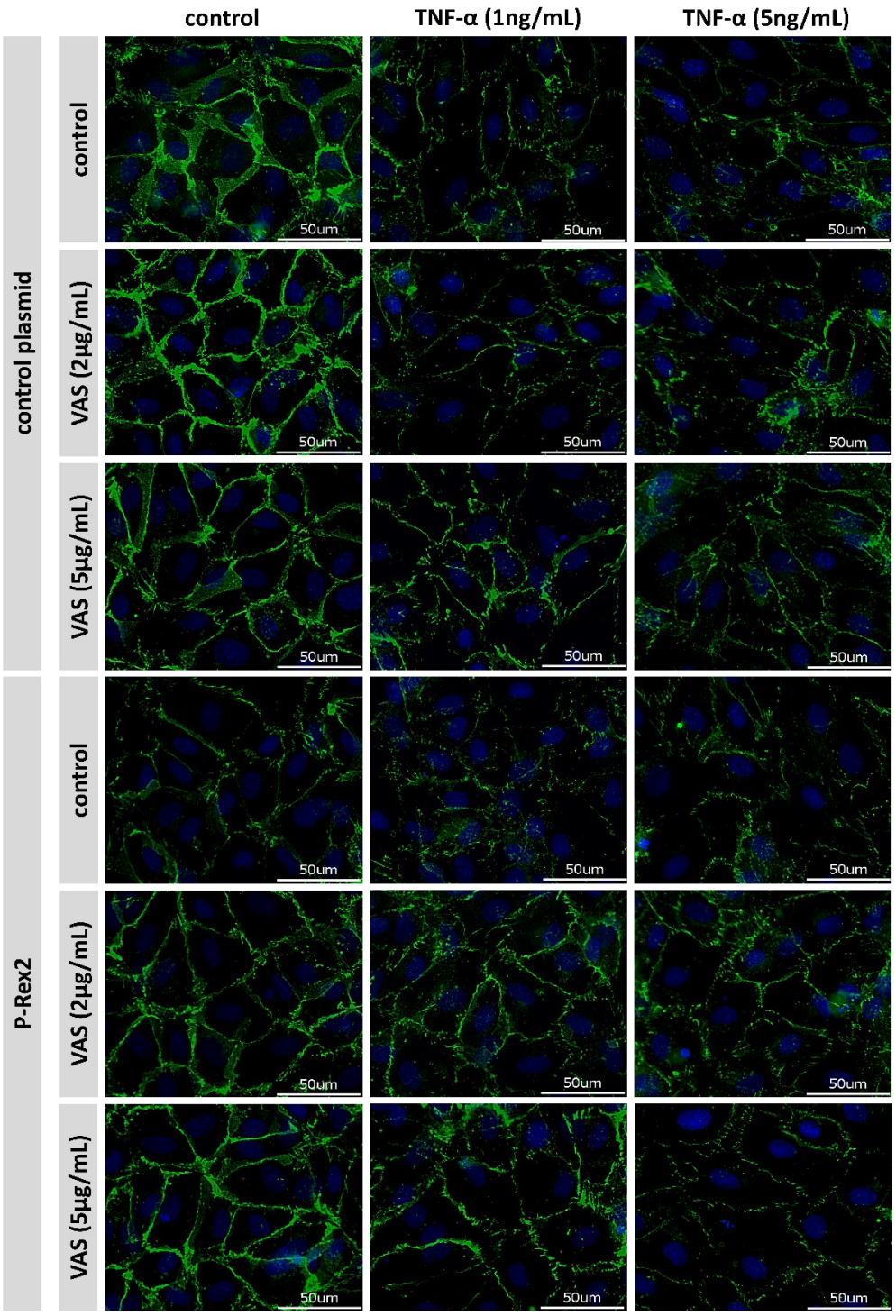

Figure 4.20: Role of NADPH oxidases on localization of VE-cadherin. HUVEC monolayers were infected with lentiviruses to overexpress control or P-Rex2. Cells were stained for VE-cadherin. DAPI was used for nuclear staining. HUVECs were exposed to TNF-α at different concentrations for 12 h in the presence or absence of VAS2870 at given concentrations. VAS2870 was applied 2 h before TNF-α treatment. Images were taken with fluorescence microscopy with 40X objective. Representative images from three experiments of independent cell preparations (Scale bar: 50 µm).

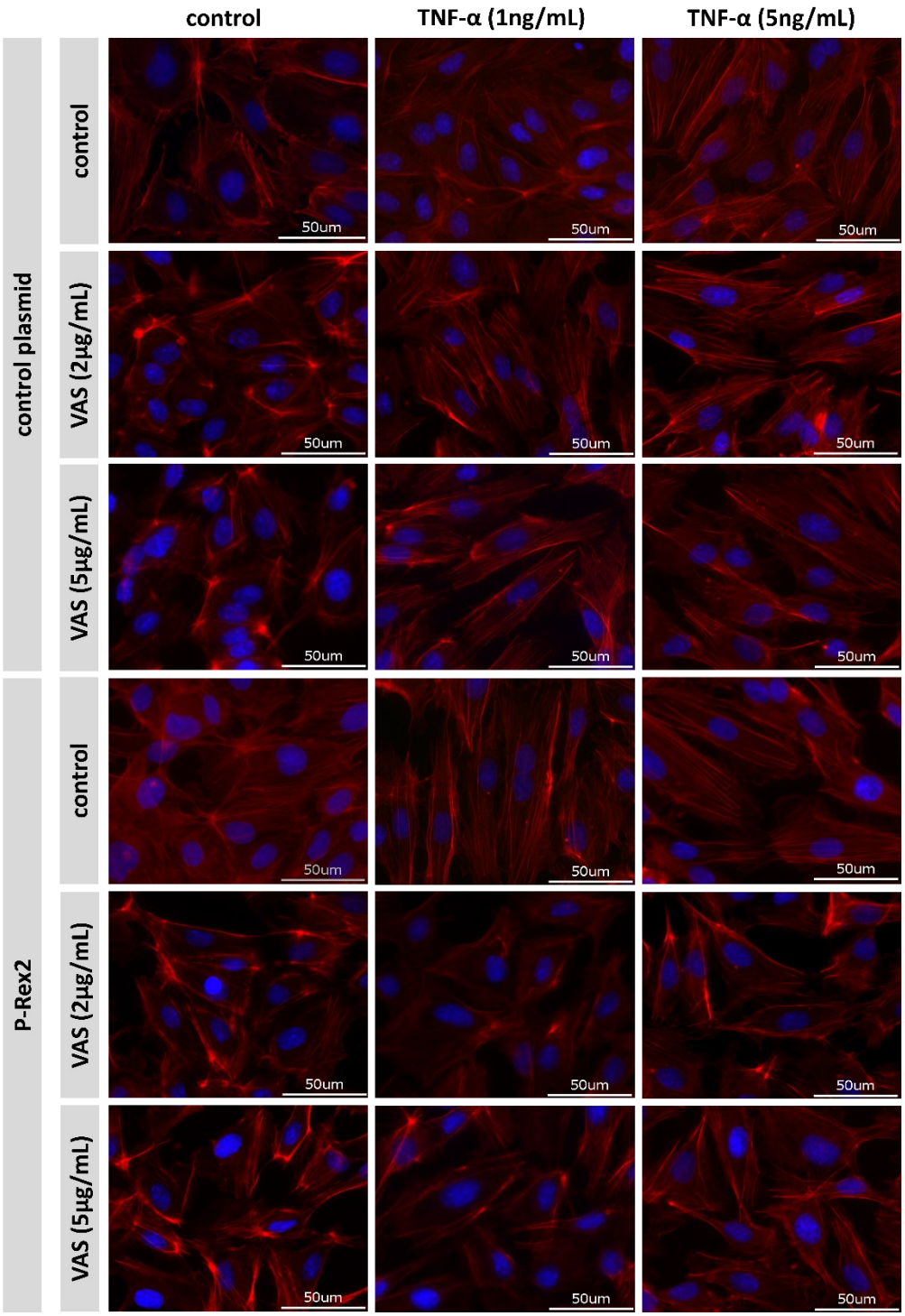

Figure 4.21: Role of NADPH oxidases on actin dynamics. HUVEC monolayers were infected with lentiviruses to overexpress control or P-Rex2. Cells were stained for actin. DAPI was used for nuclear staining. HUVECs were exposed to TNF-α at different concentrations for 12 h in the presence or absence of VAS2870 at given concentrations. VAS2870 was applied 2 h before TNF-α treatment. Images were taken with fluorescence microscopy with 40X objective. Representative images from three experiments of independent cell preparations (Scale bar: 50 µm).

5 DISCUSSION

5.1 Main Findings

In the present study, it was aimed to investigate P-Rex2 as an upstream regulator of Rac1-mediated dysfunction of the endothelial barrier.

The main findings of the presented study are as following:

(1) P-Rex2 overexpression increases basal endothelial permeability and potentiates TNF-α-induced hyperpermeability.
(2) P-Rex2 overexpression causes delocalization of both AJs and actin at the cell periphery while enhancing F-actin stress fibers formation in a Rac1-dependent manner.
(3) P-Rex2 expression increases ROS production by activating Rac1-dependent-NADPH oxidase in response to TNF-α.
(4) P-Rex2 induces Rac1-dependent migration while triggering in vitro sprouting in ECs.
(5) P-Rex2 upregulates gene expression levels of cell adhesion molecules, ICAM-1 and VCAM-1, besides inflammatory cytokines, IL-6 and IL-8.

It was shown that activation of Rac1 by P-Rex2 under inflammatory conditions directs it to trigger NADPH oxidase-dependent excessive ROS generation, consequently leading to loss of the integrity of the cells, increased permeability, and migration, thereby the dysfunction of the endothelial barrier.

Vascular inflammation is the leading cause of many cardiovascular diseases in the pathogenesis of which oxidative stress leading to endothelial barrier dysfunction plays an important role (Steven et al., 2019). In the presented study, TNF-α was used to mimic inflammation in *in vitro* cell culture models of ECs; HUVECs and Hu-ARLT cells. TNF-α is not only associated with long-term inflammatory responses but also has an important role in both initiation and termination of the inflammation (Marcos-Ramiro et al., 2014). TNF-α triggers a signaling cascade, which causes expression of the various inflammatory cytokines in cells (Zhang, 2008). Furthermore, its involvement in diverse functional mechanisms was shown, for instance, activation of Rho family GTPases, cell migration, proliferation, permeability, and expression of cell adhesion molecules (Kim et al., 2008; Xu et al., 2008; Wolczyk et al., 2016). All these findings point out TNF-α as a considerable candidate to simulate inflammation in our EC culture models.

Studies demonstrated contradictory results regarding the role of Rac1 on the endothelial barrier. It was reported by our group that cAMP recovers endothelial barrier integrity after thrombin challenge by activating Rac1. This activation, in turn, triggered the localization of both AJs and actin dynamics on the cell periphery to increase the barrier integrity (Aslam et al., 2014). In contrast to that, the involvement of active Rac1 in excessive ROS generation, which leads to endothelial barrier dysfunction, has been well studied. Barth *et al.* reported that inflammatory mediators, TNF-α and interleukin-1 beta (IL-1β), induce a signaling cascade in which increased ROS production caused by Rac1 mediated-NADPH oxidase activity results in rearrangement of the actin cytoskeleton into lamellipodia structure and promotes cell spreading (Barth et al., 2009). Taken together, these findings indicate the dual role of Rac1 in the regulation of the endothelial barrier function; however, the mechanism behind that still needs to be elucidated. Since Rac1 follows different pathways based on the type of the signal, it is likely that at the upstream of Rac1, different GEFs are activated to regulate Rac1 activity in response to various signals regulating the endothelial barrier. Thus, revealing mechanisms linking upstream and downstream signaling of Rac1 will provide a better understanding of how endothelial barrier function is regulated.

5.2 TNF-α Induces P-Rex2-mediated Rac1 Activation

The role of inflammatory cytokine TNF-α on the activation of Rho family GTPases has been well-studied. The Rac1 protein is also one of the Rho family of GTPase being activated by TNF-α induced cellular response in ECs (Wang et al., 2015). Consistently, the data of the presented study confirmed the activation of Rac1 in response to TNF-α stimuli within minutes by using the EC culture model, HUVECs (Fig. 4.5). However, the level of Rac1-GTP decreased after 30 min stimuli, which demonstrates time-dependent control of TNF-α signaling on Rac1 activity.

The molecular pathways activating Rac1 in response to TNF-α still need to be investigated. It is a fact that the activation of Rac1 requires the binding of the GTP molecule by GEF proteins in response to various signals (Marei & Malliri, 2017). It was confirmed by co-immunoprecipitation analysis that the P-Rex2 protein, which is identified as a Rac1 specific GEF in previous studies (Donald et al., 2004), interacts with Rac1 under basal conditions. Moreover, it was found that TNF-α elevates the gene expression level of *P-REX2* gene in ECs. Increased expression of P-Rex2 upregulated TNF-α induced Rac1 activation in a time-dependent manner. Taken together, these findings demonstrate that P-Rex2 activates Rac1 upon TNF-α stimuli.

However, it does not exclude the involvement of other Rac1 GEFs in TNF-α induced Rac1 activation.

5.3 Overexpression of P-Rex2 Disrupts Endothelial Barrier

The role of both Rac1 and TNF-α in the disruption of endothelial barrier is a known phenomenon; however, both the upstream signaling cascade of Rac1 and downstream signaling of TNF-α still need to be elucidated. In the current study, it was found that P-Rex2-mediated activation of Rac1 triggers disruption of the endothelial barrier via rearranging AJs and actin cytoskeleton, and effects of P-Rex2 are accelerated in the presence of long-term TNF-α stimuli. Moreover, while inhibition of Rac1 prevented TNF-α-induced loss of cell-cell junctions in P-Rex2 overexpressing cells, constitutive Rac1 expression enhanced the disruption of the barrier.

It was shown in our study by monitoring albumin permeability in HUVECs that endothelial permeability increases with P-Rex2 overexpression. Furthermore, P-Rex2-mediated endothelial permeability was upregulated in the presence of TNF-α (10 ng/mL). Although the role of TNF-α in endothelial permeability is known, the regulatory pathways still need to be investigated. Previously, the role of both RhoA activation and myosin light chain (MLC) phosphorylation were identified in endothelial permeability (van Nieuw Amerongen et al., 1998). Despite the fact that these mechanisms are mainly involved in thrombin-induced barrier hyperpermeability, Petrache *et al.* stated that TNF-α triggers MLC phosphorylation accompanied by increased permeability, stress fibers, and paracellular gap formation. However, in spite of decreasing stress fibers, inhibition of MLC phosphorylation was not alone enough to diminish TNF-α-mediated changes in the endothelial permeability (Petrache et al., 2001). These findings were supported by Mckenzie and Ridley that in the presence of prolonged TNF-α stimulation, the inhibition of MLC phosphorylation prevented neither actin stress fiber formation nor increased permeability, indicating the existence of an MLC independent way (McKenzie & Ridley, 2007).

The Rac1 activity could also involve in the regulation of endothelial permeability. Although it was mainly pointed out as a protective mechanism by stabilizing AJs, it is also the fact that activated Rac1 can involve in opposite roles in ECs (Sukriti et al., 2014; Shao et al., 2013). It was demonstrated by Tan *et al.* that deletion of *RAC1* in primary ECs results in attenuation of both S1P and VEGF-induced endothelial permeability by triggering alignment of AJs, tight junctions (TJs),

and actins at the cell borders, thereby preventing gap formation (Tan et al., 2008). Consistently, Gavard *et al.* suggested a regulatory mechanism in which Rac1 mediated phosphorylation; hence, internalization of VE-cadherin, in response to VEGF signaling, increases endothelial permeability (Gavard et al., 2008). The activation of Rac1 downstream of TNF-α signaling also has a role in the regulation of endothelial integrity, hence permeability. It was stated that TNF-α alters the organization of the actin cytoskeleton, which increases the amount of stress fiber followed by intracellular gaps formation; however, inhibition of Rac1 expression by generating dominant-negative mutants of Rac1 (N17Rac1) prevents TNF-α-mediated cellular response on the regulation of endothelial barrier, while expression of constitutively active Rac1 (V12Rac1) is enhancing actin rearrangement into lamellipodia structures, thereby promoting the loss of cell-cell junctions (Wójciak-Stothard et al., 1998; Barth et al., 2009). Cain *et al.* found that PI3K subunit p110α contributes to the regulation of the endothelial permeability through recruiting Rac1 GEF Tiam1 to the VE-cadherin complex, where Rac1 is activated and caused elongation of ECs, increased permeability, and trans-endothelial migration (TEM) of leukocytes (Cain et al., 2010). The role of the PI3K pathway was also shown in the regulation of the P-Rex protein activity. It was found that both P-Rex1 and P-Rex2 are regulated by Class I PI3K product PIP_3 and beta-gamma (βγ) subunit of heterotrimeric G protein coupled receptors (Donald et al., 2004; Welch et al., 2002).

Previously, it was demonstrated by Naikawadi *et al.* that P-Rex1 protein regulating Rac1 activity upregulates permeability in response to TNF-α signaling in the lung vascular ECs. In the study, it was shown using *in vitro* and *in vivo* models that silencing of P-Rex1 protein protects endothelial barrier integrity against TNF-α-induced barrier disruption, reduces ROS generation, expression of cell adhesion molecules, and TEM of leukocytes (Naikawadi et al., 2012). Interestingly, Amado-Azevedo *et al.* showed in HUVEC cultures that recovery of the EC barrier following thrombin-induced hyperpermeability is delayed with the knock-down of P-REX1 (Amado-Azevedo et al., 2018). The regulatory pathways of P-Rex proteins have been not fully understood yet. Abiko *et al*. found that mechanical force-induced reorganization of actin dynamics leads to perpendicular reorganization of stress fiber to the stretch axis, the mechanism of which attenuated with knock-down of P-REX2 (Abiko et al., 2015). In the presented study, to reveal the role of P-Rex2 protein in the regulation of Rac1-mediated barrier disruption, P-Rex2 protein expression was upregulated in *in vitro* models of ECs, together with inhibiting and enhancing Rac1 activity. In a functional endothelial barrier under basal conditions, VE-cadherin and actin

molecules were localized at the cell periphery, which provide a strong junctional connection among adjacent cells, thereby supporting barrier integrity (Aslam et al., 2013). In accordance with barrier disrupting effects of TNF-α on the endothelial barrier, present data showed that prolonged TNF-α stimulation leads to concentration-dependent loss of peripheral localization of both actin and VE-cadherin, together with increased stress fiber formation. Moreover, P-Rex2 protein overexpression was alone enough to weaken endothelial barrier integrity by decreasing the assembly of VE-cadherin and actin at cell-cell junctions (Fig. 4.7 & Fig. 4.8). In the presence of P-Rex2 overexpression, TNF-α-induced effects on the loss of junctional assembly and stress fibers were dramatically enhanced. It was shown in our study that P-Rex2-mediated barrier disruption in response to TNF-α signaling is maintained via Rac1 activation. In P-Rex2 overexpressing cells, the pharmacological intervention of Rac1 activation using NSC23766 not only recovered the endothelial barrier via reassembly of AJs and peripheral actin but also protected cells against TNF-α induced barrier disruption. In contrast to that, under basal conditions, NSC23766 caused gap formation and failed to protect the endothelial barrier against TNF-α (Fig. 4.9). These findings could be explained by the dual role of Rac1 on the endothelial barrier function (Birukova et al., 2008). Under basal conditions, Rac1 activity stabilizes the endothelial barrier via supporting junctional connections and peripheral actin assembly. Thus, inhibition of Rac1 activity results in loss of VE-cadherin from cell-cell junctions accompanied by increased F-actin formation. Besides pharmacological inhibition of Rac1, these findings are also supported by our data in which we generated constitutively active Rac1 (Rac1-CA) and dominant negative Rac1 (Rac1-DN) mutants to enhance and inhibit Rac1 activity biologically. It was observed that increased Rac1 activity prevents stress fiber formation in response to TNF-α; however, loss of Rac1 activity results in a dramatic increase in the number of stress fibers even under basal conditions. On the other hand, P-Rex2 overexpression directs Rac1 to an opposite role and triggers endothelial barrier dysfunction via disrupting junctional integrity. In P-Rex2 overexpressing cells, both pharmacological and biological attenuation of Rac1 activity was protective against TNF-α induced stress fiber formation. Interestingly, expression of Rac1-CA in P-Rex2 overexpressing ECs dramatically enhanced actin stress fibers, supporting the role of Rac1 in the barrier disruption downstream of P-Rex2 (Fig. 4.10).

In summary, the data of the presented study demonstrates that P-Rex2 regulates endothelial barrier dysfunction downstream of TNF- α signaling via activating Rac1. As a result of Rac1

activation, rearrangement of AJs and actin dynamics lead to increased gap formation between adjacent ECs, which in turn increases barrier permeability.

5.4 P-Rex2 Overexpression Triggers Pathological Angiogenesis

Moreover, the present study showed that P-Rex2 promotes *in vitro* angiogenesis via triggering EC migration, *in vitro* sprout formation, and EC activation under inflammatory stimuli. Angiogenesis can occur either physiologically or pathologically. Perturbation of EC metabolism and thus its barrier dysfunction is related to the development of pathological angiogenesis (Goveia et al., 2014). Abnormally growing blood vessels observed in pathological angiogenesis are related to various diseases, including chronic inflammation and cardiovascular diseases (Dvorak, 2005). Inflammation also induces angiogenesis with a mechanism that is not well understood yet.

Angiogenesis requires the migration of ECs, which is controlled by various stimuli and signaling cascades to allow ECs to rearrange the cytoskeleton for migration (Lamalice et al., 2007). It was found in our study that Rac1 GEF P-Rex2 overexpression significantly increased the wound closure rate of ECs and EC sprouting. Although its effect was enhanced in the presence of angiogenic factor VEGF (10 ng/mL) in HUVEC monolayers, the VEGF-induced EC sprouting in HU-ARLT cells could not be observed. Nevertheless, inflammatory cytokine TNF-α (10 ng/mL) increased wound closure rate and EC sprouting in P-Rex2 overexpressing cells. However, P-Rex2 mediated EC migration was attenuated in the presence of Rac1 inhibitor NSC23766. Interestingly, inhibition of Rac1 blocked TNF-α induced cell migration only in P-Rex2 overexpressing cells, indicating the central role of Rac1 in the downstream of P-Rex2 mediated cell migration in response to TNF-α.

It is well-known that the Rho family of GTPases regulates the movement of migratory cells via rearranging actin cytoskeleton dynamics. Ridley *et al.* found that active Rac1 regulates actin filaments into lamellipodia structures for the cell movement, while biological inhibition of Rac1 with N17 mutation prevents observed effects (Ridley et al., 1992). Consistently, Tan *et al.* stated that conditional deletion of Rac1 in primary mice ECs via Cre/Flox approach results in reduced migration, while it is lethal for vascular development *in vivo* (Tan et al., 2008). Our findings showed that activation of Rac1 via P-Rex2 weakens the EC barrier's integrity, thus facilitating migration via downregulating assembly of VE-cadherin and actin at cell-cell junctions. By

inhibiting Rac1 activity, we were able to show that TNF-α induced gap formation between adjacent cells was prevented only in P-Rex2 overexpressing cells, indicating TNF-α-P-Rex2-Rac1-axis in the regulation of EC barrier and supporting the role of P-Rex2 in EC migration. Additionally, Rac1-mediated regulation of angiogenesis includes ROS generation, which also regulates EC migration. Moldovan *et al.* stated the presence of ROS at the lamellipodia structure and decrease at cell migration in response to chemical inhibition of ROS (Moldovan et al., 2006). Additionally, constitutive expression of Rac1 in cultured HUVECs resulted in the loss of integrity via increasing tyrosine phosphorylation of VE-cadherin. The internalization of VE-cadherin was associated with increased ROS production, and the absence of ROS also resulted in a decrease in cell migration (van Wetering et al., 2003). The role of TNF-α both in the Rac1-mediated regulation of actin cytoskeleton dynamics and ROS generation was already established. Our data also confirmed these findings and demonstrated a novel mechanism in which P-Rex2 provides a link between TNF-α and Rac1 in the regulation of ROS-mediated EC barrier dysfunction. Furthermore, during vascular inflammation and angiogenesis, cell adhesion molecules expressed by ECs allow leukocytes to reach tissues across endothelium through the gaps opened between adjacent cells. The process begins with TNF-α, which triggers endothelial activation, thus the expression of intercellular adhesion molecule 1 (ICAM-1), vascular cell adhesion molecule 1 (VCAM-1), and production of IL-6 and IL-8 (Hanada & Yoshimura, 2002; Cook-Mills & Deem, 2005). Consistently, TNF-α upregulated the expression of ICAM-1, VCAM-1, IL-6, and IL-8 in our cell culture models. Additionally, P-Rex2 overexpression alone could upregulate ICAM-1, IL-6, and IL-8 in Hu-ARLT cells, indicating activation of angiogenesis pathways with increased P-Rex2 expression. However, unlike our findings in EC cell line Hu-ARLT, no significant differences was observed in HUVEC, which could caused by a small sample size.

Taken together, the present work demonstrates the angiogenic effects of P-Rex2-mediated activation of Rac1 during vascular inflammation and suggests P-Rex2 as a target for therapeutic approaches against pathological angiogenesis in diseases.

5.5 P-Rex2 Overexpression Triggers TNF-α-induced-NADPH oxidase-dependent ROS Formation

Although ROS is important in regulating various biological functions, uncontrolled production of ROS can lead to endothelial barrier dysfunction. The presented study showed that

P-Rex2 is a regulator of NADPH oxidase-dependent-ROS generation in ECs via activating Rac1 in response to TNF-α. The activation of Rac1 via P-Rex2 stimulated a cellular response through ROS production and altered peripheral assembly of VE-cadherin and actin, which resulted in endothelial barrier dysfunction.

The role of Rac1 in ROS production is a known phenomenon. It was shown by generating Rac1 mutants that the Rac1 activity resulted in excessive ROS generation, weakening the endothelial barrier integrity and increasing stress fibers (van Watering et al., 2002). However, the upstream signaling cascade of Rac1 leading to excessive ROS production, ultimately EC barrier dysfunction, needs to be elucidated. As previously mentioned, it was shown in the presented study that P-Rex2 mediated activation of Rac1 results in barrier disruption. It was found that both pharmacological and biological inhibition of Rac1 prevent P-Rex2-mediated loss of junctional integrity and formation of stress fibers. In line with these findings, constitutive expression of Rac1 accelerated the effects of P-Rex2. Further analyses were performed to determine the contribution of ROS to P-Rex2-Rac1 mediated barrier disruption. In the current work, it was found that intracellular ROS levels significantly increased with P-Rex2 overexpression. Although the effect of TNF-α-induced ROS production was limited. This data can be explained by experimental difficulties in monitoring ROS, which has a short lifetime. Thus, the cell imaging technique was used to confirm our initial findings and analyze the effects of excessive ROS production on the EC barrier. It was found that both TNF-α exposure (concentration-dependent) and P-Rex2 overexpression disrupt the EC barrier via downregulating peripheral VE-cadherin and actin assembly. Moreover, by using ROS scavenger N-Acetyl-L-cysteine (NAC), it was shown that ROS depletion could recover EC barrier loss due to TNF-α and P-Rex2 overexpression, indicating ROS dependent regulation of the EC barrier.

Inhibitors are an important and useful tool to identify the source of ROS and verify the role of biological targets. The ROS scavenger NAC is widely used in the studies; however, it is a general inhibitor against ROS rather than being specific to NADPH oxidases and has toxic effects on cells (Altenhöfer et al., 2015; Teixeira et al., 2017). Whereas, VAS compounds; VAS2870 and VAS3947, are developed as NADPH oxidase specific inhibitors and were verified in cell-free systems, various cell types, tissues, and *in vivo* experiments (Altenhöfer et al., 2012). Until now, inhibition of NOX1, NOX2, NOX4, and NOX5 by VAS2870 were shown (Chocry & Leloup,

2020). In the current study, the concentration-dependent inhibition of NADPH oxidase activity by VAS2870 provided evidence for NADPH-oxidase- dependent ROS regulation controlled by P-Rex2. It was found that NADPH oxidase inhibition reversed P-Rex2-mediated loss of VE-cadherin and actin localization at cell-cell borders, accompanied by a reduction in stress fibers. Interestingly, the NADPH oxidase inhibition failed to prevent TNF-α- induced barrier disruption. However, in the presence of P-Rex2 overexpression, the barrier integrity was protected against TNF-α exposure via NADPH oxidase inhibition. Since P-Rex2 is a GEF activating Rac1 and our findings confirmed P-Rex2-Rac1-mediated loss of the EC barrier, the study demonstrated a novel mechanism modulating VE-cadherin and actin assembly through NADPH oxidase-dependent excessive ROS generation. This occurs through activating Rac1 via P-Rex2 in response to TNF-α and further the binding of active Rac1 to the NADPH-oxidase complex.

5.6 Conclusion

Overall, the presented study demonstrated that activation of Rac1 via P-Rex2 at the downstream of inflammatory signaling leads to EC barrier dysfunction. This occurs through the binding of active Rac1 to the NADPH oxidase complex to trigger excessive ROS production, which rearranges VE-cadherin-based AJs and actin cytoskeleton to open gaps between adjacent cells. As a result, ECs lose their integrity, and barrier permeability increases. Furthermore, activation of Rac1 via P-Rex2 triggers pathological angiogenesis, where EC migration and sprouting increase. In our *in vitro* EC culture models, overexpression of P-Rex2 caused increased endothelial permeability, migration, sprouting, and generation of NADPH oxidase-dependent ROS through Rac1 activation. The pharmacological and biological intervention of Rac1 activation recovered P-Rex2 and TNF-α induced loss of endothelial barrier integrity. In conclusion, in the current study, a novel P-Rex2-Rac1 pathway was revealed in the regulation of EC barrier integrity in response to inflammatory mediators.

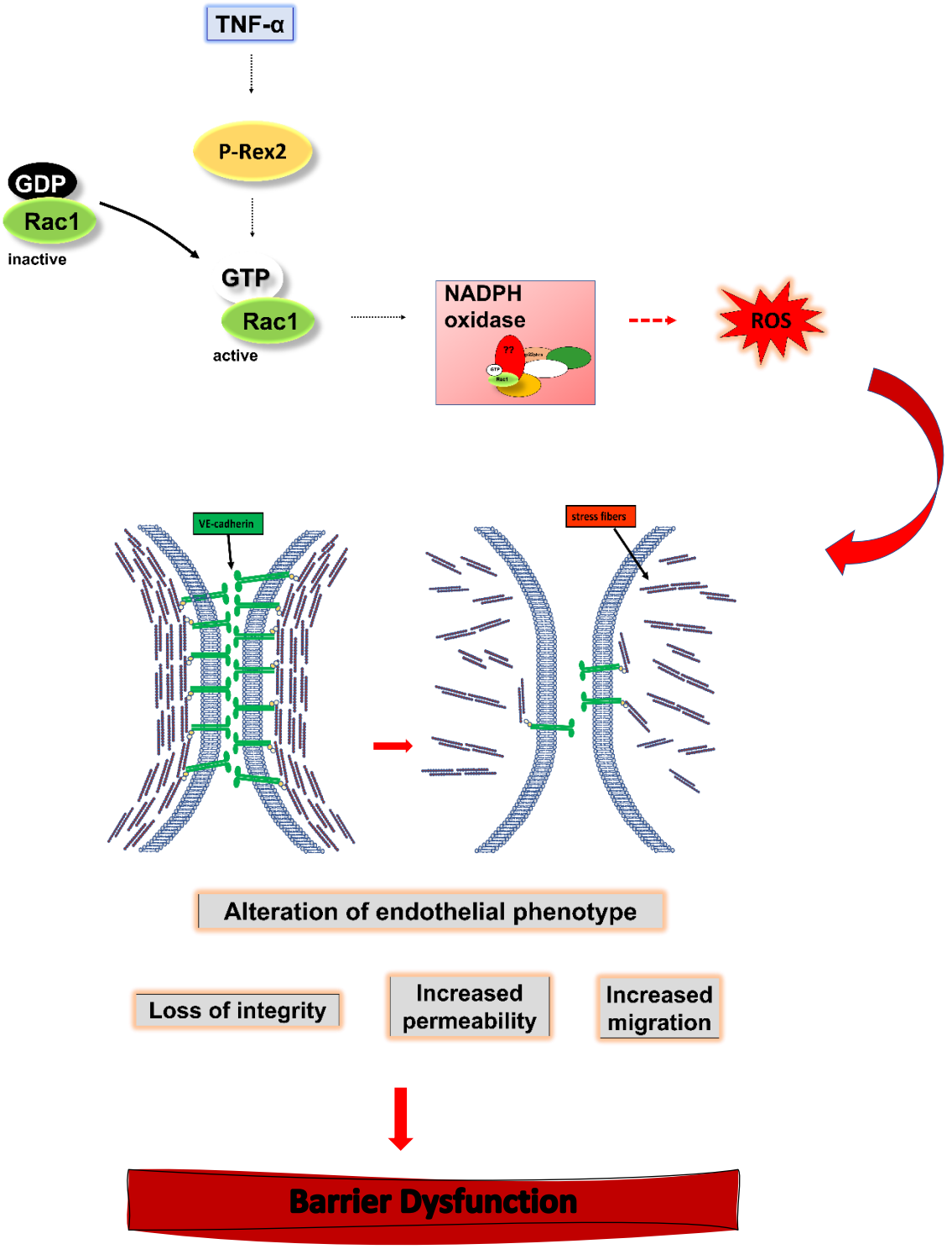

Figure 5.1: Schematic presentation of endothelial barrier dysfunction due to P-Rex2-mediated Rac1 activation in response to TNF-α. This activation directs Rac1 to the NADPH oxidase complex, where it builds an active enzyme complex. The active NADPH oxidase complex generates excessive ROS, which in turn causes gap formation between adjacent ECs via rearranging VE-cadherin-based AJs and actin cytoskeleton. As a result, ECs lose their integrity, barrier permeability and EC migration increase.

5.7 Future Perspective

Endothelial barrier dysfunction, which is mainly related to inflammation and excessive ROS production, plays a crucial role in the progression of various cardiovascular diseases. Thus, prevention of barrier dysfunction or improvement of endothelial function is the focus of therapeutic approaches. However, current treatment approaches are restricted to eliminating and treating underlying risk factors that arise from lifestyle or secondary diseases that might contribute to clinical outcomes (Park & Park, 2015). Available treatments provide only partial recovery on the endothelial barrier and do not sufficient to reverse disease phenotype, only delaying the progression of the diseases. Thus, novel therapeutic approaches are required for an effective treatment.

The findings of the study clearly showed that P-Rex2-mediated activation of Rac1 in EC barrier dysfunction during inflammation. It was found that TNF-α upregulates Rac1-GTP levels in a time-dependent manner. Increased expression of P-Rex2 dramatically enhanced TNF-α induced Rac1 activation, and P-Rex2-mediated activation of Rac1 resulted in reduced integrity, increased permeability, and angiogenesis. Our data provided evidence that the active Rac1 induced barrier dysfunction via NADPH-oxidase-dependent ROS production. In the study, the role of Rac1 in P-Rex2-mediated endothelial barrier disruption was confirmed by generating Rac1 mutants. Our data also showed that TNF-α-induced barrier disruption could be reversed with Rac1 inhibition only with P-Rex2 overexpression, indicating a regulatory pathway at the upstream of Rac1, in which Rac1 is activated in response to TNF-α mediated activation of P-Rex2. However, since P-Rex2 expression has not been downregulated in the study, it is unclear whether other pathways or GEFs involve in TNF-α-induced barrier disruption. Thus, further analysis that downregulates P-Rex2 expression will provide a better understanding.

Additionally, a specific NADPH-oxidase acting at the downstream of P-Rex2-Rac1 could not be determined. The pharmacological inhibition of NADPH-oxidases provided evidence for Rac1-mediated ROS production and pointed out NOX1 and NOX2 since they are the known oxidases activated via active Rac1 in ECs. Since NOX2 is an abundantly expressed form in ECs, it is a strong candidate for Rac1-induced barrier disruption. However, further research that focuses on inhibiting or downregulating NOXs can reveal specific NADPH-oxidase in the P-Rex2-Rac1-NOX axis.

These findings may contribute to the development of novel therapies against pathological conditions caused by endothelial barrier dysfunction. To reveal pathways in the pathogenesis of the diseases is the key step in developing therapeutic strategies. Thus, a better understanding of the inflammatory mediators induced EC barrier dysfunction will further elucidate regulatory mechanisms leading to the pathophysiological conditions and may provide potential therapeutic targets.

6 SUMMARY

The endothelial barrier is formed by tightly integrated endothelial cells (ECs), which loosen their interaction and then recover again in a controlled way to open paracellular gaps for the transport of leukocytes and macromolecules across the endothelium. Endothelial barrier dysfunction occurs when this reversible mechanism is disrupted, and it leads to various pathological conditions due to the accumulation of cells and molecules within the surrounding tissues. The endothelial barrier is stabilized by Ras-related C3 botulinum toxin substrate 1 (Rac1), a member of the Rho family of GTPases. The Rac1 also regulates enzyme complex nicotinamide adenine dinucleotide phosphate (NADPH) oxidase, uncontrolled activation of which leads to over-production of reactive oxygen species (ROS) and thus dysfunction of the endothelial barrier. The guanine nucleotide exchange factors (GEFs) such as phosphatidylinositol-3,4,5-trisphosphate dependent Rac exchange factor 1 (P-Rex1), phosphatidylinositol-3,4,5-trisphosphate dependent Rac exchange factor 2 (P-Rex2), and T-lymphoma invasion and metastasis-inducing protein 1 (Tiam1) control the activity of Rac1 in ECs.

The present study investigated the effects of inflammatory conditions on Rac1 activation to reveal the molecular pathway directing Rac1 towards its role in endothelial barrier dysfunction. Our study demonstrated that P-Rex2 overexpression reduced the integrity of the endothelial barrier by downregulating the assembly of vascular endothelial cadherin (VE-cadherin) Adherens junctions (AJs) and actin at the cell-cell junctions, and TNF-α dramatically enhanced the effects of P-Rex2 on the EC barrier. Consistently, P-Rex2 overexpression resulted in increased barrier permeability. Furthermore, our findings showed that P-Rex2-mediated barrier disruption in response to TNF-α was mediated via Rac1 activation. Under basal conditions, the pharmacological and biological intervention of Rac1 activation using NSC23766 and dominant-negative Rac1 (Rac1-DN) resulted in gap formation, dramatically increased stress fibers, and failed to protect endothelial barrier against TNF-α. In contrast to that, P-Rex2 overexpression directed Rac1 to an opposite role. Inhibition of Rac1 activation in P-Rex2 overexpressing cells recovered endothelial barrier via reassembly of AJs and peripheral actin. Moreover, it was protective against TNF-α induced barrier disruption. Similarly, expression of constitutively active Rac1 (Rac1-CA) was protective for the barrier under basal conditions, but it dramatically enhanced actin stress fibers in P-Rex2 overexpressing ECs, supporting the role of Rac1 in the P-Rex2-mediated EC barrier dysfunction.

In accordance with these findings, P-Rex2 overexpression induced EC migration while triggering *in vitro* sprouting in ECs. Chemical inhibition of Rac1 attenuated EC migration only in the P-Rex2 overexpressing cells, indicating that P-Rex2 mediated EC migration is Rac1-dependent. Additionally, P-Rex2 overexpression significantly upregulated intracellular ROS production in ECs. Inhibition of ROS using ROS scavenger N-Acetyl-L-cysteine (NAC) protected the EC barrier against P-Rex2 mediated loss of VE-cadherin from cell-cell junctions and increased localization of actin at the cell periphery. Interestingly, the NADPH oxidase inhibitor VAS2870 prevented barrier loss caused by P-Rex2 overexpression in a concentration-dependent manner both with and without TNF-α stimuli, indicating that P-Rex2 leads to TNF-α-induced NADPH oxidase-dependent ROS production in ECs.

In conclusion, the data of the presented study demonstrates that P-Rex2 regulates endothelial barrier dysfunction downstream of TNF- α signaling via activating Rac1. As a result of Rac1 activation, NADPH oxidase-dependent excessive ROS production causes rearrangement of AJs and actin dynamics leading to gap formation between adjacent ECs, which in turn increases barrier permeability, endothelial migration, and sprouting. P-Rex2 may offer an important target to prevent inflammation-induced ROS production and endothelial dysfunction. Manipulation of P-Rex2 activity might be a therapeutic approach to maintain barrier stabilization.

7 ZUSAMMENFASSUNG

Die Endothelbarriere wird von eng miteinander verflochtenen Endothelzellen (ECs) gebildet, die ihre Interaktion lockern und sich dann kontrolliert wieder erholen, um parazelluläre Lücken für den Transport von Leukozyten und Makromolekülen durch das Endothel zu öffnen. Wenn dieser reversible Mechanismus gestört ist, kommt es zu einer Dysfunktion der Endothelbarriere, die aufgrund der Ansammlung von Zellen und Molekülen in den umliegenden Geweben zu verschiedenen pathologischen Zuständen führt. Die Endothelbarriere wird durch das mit Ras verwandte C3-Botulinumtoxin-Substrat 1 (Rac1), ein Mitglied der GTPasen der Rho-Familie, stabilisiert. Rac1 reguliert auch den Enzymkomplex Nikotinamid-Adenin-Dinukleotid-Phosphat (NADPH)-Oxidase, dessen unkontrollierte Aktivierung zu einer Überproduktion reaktiver Sauerstoffspezies (ROS) und damit zu einer Funktionsstörung der Endothelbarriere führt. Guaninnukleotid-Austauschfaktoren (GEFs) wie der Phosphatidylinositol-3,4,5-Trisphosphat-abhängige Rac-Austauschfaktor 1 (P-Rex1), der Phosphatidylinositol-3,4,5-Trisphosphat-abhängige Rac-Austauschfaktor 2 (P-Rex2) und das T-Lymphom-Invasions- und Metastasen-induzierende Protein 1 (Tiam1) kontrollieren die Aktivität von Rac1 in ECs.

In der vorliegenden Dissertation wurden die Auswirkungen von Entzündungszuständen auf die Rac1-Aktivierung untersucht, um den molekularen Weg aufzuzeigen, der Rac1 zu seiner Rolle bei der Dysfunktion der endothelialen Barriere führt. Unsere Studie zeigte, dass die Überexpression von P-Rex2 die Integrität der Endothelbarriere durch die Reduzierung des Zusammenbaus von vaskulärem endothelialem Cadherin (VE-Cadherin), Adherens Junctions (AJs) und Aktin an den Zell-Zell-Verbindungen verringert, und dass TNF-α die Auswirkungen von P-Rex2 auf die EC-Barriere dramatisch verstärkt. Dementsprechend führte die Überexpression von P-Rex2 zu einer erhöhten Permeabilität der Barriere. Darüber hinaus zeigten unsere Ergebnisse, dass die P-Rex2-vermittelte Barrierestörung als Reaktion auf TNF-α über die Rac1-Aktivierung vermittelt wird. Unter physiologischen Bedingungen führte die pharmakologische und biologische Intervention der Rac1-Aktivierung mit NSC23766 und dominant-negativem Rac1 (Rac1-DN) zur Gap-Bildung, zu einer dramatischen Zunahme der Stressfasern und zu keinem Schutz der endothelialen Barriere vor TNF-α. Im Gegensatz führte die Überexpression von P-Rex2 dazu, dass Rac1 eine entgegengesetzte Rolle spielte. Die Hemmung der Rac1-Aktivierung in P-Rex2 überexprimierten Zellen führte zur Wiederherstellung der Endothelbarriere durch den Wiederaufbau von AJs und

peripherem Aktin. Darüber hinaus wirkte sie schützend gegen TNF-α-induzierte Barrierestörungen. Ähnlich schützte die Expression von konstitutiv aktivem Rac1 (Rac1-CA) die Barriere unter physiologischen Bedingungen, verstärkte aber die Aktinstressfasern in P-Rex2-überexprimierenden ECs dramatisch, was die Rolle von Rac1 bei der P-Rex2-vermittelten Barrierestörung in ECs unterstützt. In Übereinstimmung mit diesen Erkenntnissen induzierte die Überexpression von P-Rex2 die EC-Migration und löste gleichzeitig die in vitro Sprossung in ECs aus. Die chemische Hemmung von Rac1 schwächte die EC-Migration nur in den P-Rex2-überexprimierenden Zellen ab, was darauf hindeutet, dass die P-Rex2-vermittelte EC-Migration Rac1-abhängig ist. Außerdem führte die Überexpression von P-Rex2 zu einer signifikanten Erhöhung der intrazellulären ROS-Produktion in den ECs. Die Hemmung von ROS durch den ROS-Fänger N-Acetyl-L-Cystein (NAC) schützte die EC-Barriere vor dem durch P-Rex2 vermittelten Verlust von VE-Cadherin an den Zell-Zell-Verbindungen und der verstärkten Lokalisierung von Aktin an der Zellperipherie. Interessanterweise verhinderte der NADPH-Oxidase-Inhibitor VAS2870 den durch die P-Rex2-Überexpression verursachten Barriereverlust in einer dosisabhängigen Weise sowohl mit als auch ohne TNF-α-Stimuli. Dies deutet darauf hin, dass P-Rex2 zu einer TNF-α-induzierten NADPH-Oxidase-abhängigen ROS-Produktion in ECs führt.

Zusammenfassend zeigen die Daten der vorliegenden Studie, dass P-Rex2 die Dysfunktion der endothelialen Barriere stromabwärts von TNF-α-Signalen über die Aktivierung von Rac1 reguliert. Infolge der Rac1-Aktivierung verursacht die von der NADPH-Oxidase abhängige übermäßige ROS-Produktion eine Umstrukturierung der AJs und der Aktin-Dynamik, was zur Bildung von Lücken zwischen benachbarten ECs führt, was wiederum die Barrieredurchlässigkeit, die endotheliale Migration und die Sprossung erhöht. P-Rex2 könnte ein wichtiger Angriffspunkt sein, um die entzündungsbedingte ROS-Produktion und endotheliale Dysfunktion zu verhindern. Außerdem könnte die Manipulation der P-Rex2-Aktivität ein therapeutischer Ansatz zur Aufrechterhaltung der Barrierestabilisierung sein.

8 REFERENCES

1. Abid, M. R., Spokes, K. C., Shih, S.-C., & Aird, W. C. (2007). NADPH oxidase activity selectively modulates vascular endothelial growth factor signaling pathways. *The Journal of biological chemistry*, *282*(48), 35373–35385.

2. Abiko, H., Fujiwara, S., Ohashi, K., Hiatari, R., Mashiko, T., Sakamoto, N., Sato, M., Mizuno, K. (2015). Rho guanine nucleotide exchange factors involved in cyclic-stretch-induced reorientation of vascular endothelial cells. *Journal of Cell Science*, 128, 1683–1695.

3. Abo, A., Pick, E., Hall, A., Totty, N., Teahan, C. G., & Segal, A. W. (1991). Activation of the NADPH oxidase involves the small GTP-binding protein p21rac1. *Nature*, *353*, 668–670.

4. Aghajanian, A., Wittchen, E. S., Allingham, M. J., Garrett, T. A., & Burridge, K. (2008). Endothelial cell junctions and the regulation of vascular permeability and leukocyte transmigration. *Journal of thrombosis and haemostasis JTH*, *6*(9), 1453–1460.

5. Ago, T., Kitazono, T., Ooboshi, H., Iyama, T., Han, Y. H., Takada, J., Wakisaka, M., Ibayashi, S., Utsumi, H., & Iida, M. (2004). Nox4 as the major catalytic component of an endothelial NAD(P)H oxidase. *Circulation*, *109*(2), 227–233.

6. Altenhöfer, S., Kleikers, P. W. M., Radermacher, K. A., Scheurer, P., Rob Hermans, J. J., Schiffers, P., Ho, H., Wingler, K., & Schmidt, H. H. H. W. (2012). The NOX toolbox: validating the role of NADPH oxidases in physiology and disease. *Cellular and molecular life sciences CMLS*, *69*(14), 2327–2343.

7. Altenhöfer, S., Radermacher, K. A., Kleikers, P. W. M., Wingler, K., & Schmidt, H. H. H. W. (2015). Evolution of NADPH Oxidase Inhibitors: Selectivity and Mechanisms for Target Engagement. *Antioxidants & redox signaling*, *23*(5), 406–427.

8. Amado-Azevedo, J., de Menezes, R., X., van Nieuw Amerongen, G., P., van Hinsbergh, V., W., M., Hordijk, P., L. (2018). A functional siRNA screen identifies RhoGTPase-associated genes involved in thrombin-induced endothelial permeability. *PLoS ONE* 13(7): e0201231.

9. Aslam, M., Schluter, K.-D., Rohrbach, S., Rafiq, A., Nazli, S., Piper, H. M., Noll, T., Schulz, R., & Gündüz, D. (2013). Hypoxia-reoxygenation-induced endothelial barrier failure: role of RhoA, Rac1 and myosin light chain kinase. *The Journal of physiology*, *591*(2), 461–473.

10. Aslam, M., Tanislav, C., Troidl, C., Schulz, R., Hamm, C., & Gündüz, D. (2014). cAMP controls the restoration of endothelial barrier function after thrombin-induced hyperpermeability via Rac1 activation. *Physiological reports*, *2*(10).

11. Babior, B. M. (1999). NADPH Oxidase: An Update. *Blood*, *93*(5), 1464–1476.

12. Babior, B. M. (2000). The NADPH Oxidase of Endothelial Cells. *IUBMB Life*, *50*, 267–269.

13. Babior, B. M., Kipnes, R. S., & Curnutte, J. T. (1973). Biological Defense Mechanisms Biological Defense Mechanisms. The Production by Leukocytes of Superoxide, a Potential Bactericidal agent. *The Journal of Clinical Investigation*, *52*, 741–744.

14. Barth, B. M., Stewart-Smeets, S., & Kuhn, T. B. (2009). Proinflammatory cytokines provoke oxidative damage to actin in neuronal cells mediated by Rac1 and NADPH oxidase. *Molecular and cellular neurosciences*, *41*(2), 274–285.

15. Bazzoni, G. (2006). Endothelial tight junctions: permeable barriers of the vessel wall. *Thrombosis and Haemostasis*, *95*(01), 36–42.

16. Beckers, C. M. L., van Hinsbergh, V. W. M., & van Nieuw Amerongen, G. P. (2010). Driving Rho GTPase activity in endothelial cells regulates barrier integrity. *Thrombosis and haemostasis*, *103*(1), 40–55.

17. Bedard, K., & Krause, K.-H. (2007). The NOX family of ROS-generating NADPH oxidases: physiology and pathophysiology. *Physiological reviews*, *87*(1), 245–313.

18. Berger, M. F., Hodis, E., Heffernan, T. P., Deribe, Y. L., Lawrence, M. S., Protopopov, A., Ivanova, E., Watson, I. R., Nickerson, E., Ghosh, P., Zhang, H., Zeid, R., Ren, X., Cibulskis, K., Sivachenko, A. Y., Wagle, N., Sucker, A., Sougnez, C., Onofrio, R., Ambrogio, L., Auclair, D., Fennell, T., Carter, S. L., Drier, Y., Stojanov, P., Singer, M. A., Voet, D., Jing, R., Saksena, G., Barretina, J., Ramos, A. H., Pugh, T. J., Stransky, N., Parkin, M., Winckler, W., Mahan, S., Ardlie, K., Baldwin, J., Wargo, J., Schadendorf, D., Meyerson, M., Gabriel, S. B., Golub, T. R., Wagner, S. N., Lander, E. S., Getz, G., Chin, L., & Garraway, L. A. (2012). Melanoma genome sequencing reveals frequent PREX2 mutations. *Nature*, *485*(7399), 502–506.

19. Birukova, A. A., Zagranichnaya, T., Alekseeva, E., Bokoch, G. M., & Birukov, K. G. (2008). Epac/Rap and PKA are novel mechanisms of ANP-induced Rac-mediated pulmonary endothelial barrier protection. *Journal of cellular physiology*, *215*(3), 715–724.

20. Bogatcheva, N. V., & Verin, A. D. (2008). The role of cytoskeleton in the regulation of vascular endothelial barrier function. *Microvascular research*, *76*(3), 202–207.

21. Bonetti, P. O., Lerman, L. O., & Lerman, A. (2003). Endothelial dysfunction: a marker of atherosclerotic risk. *Arteriosclerosis, thrombosis, and vascular biology*, *23*(2), 168–175.

22. Boueiz, A., & Hassoun, P. M. (2009). Regulation of endothelial barrier function by reactive oxygen and nitrogen species. *Microvascular research*, *77*(1), 26–34.

23. Bretón-Romero, R., & Lamas, S. (2014). Hydrogen peroxide signaling in vascular endothelial cells. *Redox biology*, *2*, 529–534.

24. Brown, D. I., & Griendling, K. K. (2009). Nox proteins in signal transduction. *Free radical biology & medicine*, *47*(9), 1239–1253.

25. Buchsbaum, R. J., Connolly, B. A., & Feig, L. A. (2002). Interaction of Rac exchange factors Tiam1 and Ras-GRF1 with a scaffold for the p38 mitogen-activated protein kinase cascade. *Molecular and cellular biology*, *22*(12), 4073–4085.

26. Burtenshaw, D., Kitching, M., Redmond, E. M., Megson, I. L., & Cahill, P. A. (2019). Reactive Oxygen Species (ROS), Intimal Thickening, and Subclinical Atherosclerotic Disease. *Frontiers in cardiovascular medicine*, *6*, 89.

27. Cai, H., & Harrison, D. G. (2000). Endothelial Dysfunction in Cardiovascular Diseases: The Role of Oxidant Stress. *Circulation research*, *87*, 840–844.

28. Cain, R. J., Vanhaesebroeck, B., & Ridley, A. J. (2010). The PI3K p110alpha isoform regulates endothelial adherens junctions via Pyk2 and Rac1. *The Journal of cell biology*, *188*(6), 863–876.

29. Campeau, E., Ruhl, V. E., Rodier, F., Smith, C. L., Rahmberg, B. L., Fuss, J. O., Campisi, J., Yaswen, P., Cooper, P. K., & Kaufman, P. D. (2009). A versatile viral system for expression and depletion of proteins in mammalian cells. *PloS one*, *4*(8), e6529.

30. Carlier, M. F., & Pantaloni, D. (1997). Control of Actin Dynamics in Cell Motility. *Journal of molecular biology*, *269*(4), 459–467.

31. Cash, J., N., Sharma, P., V., Tesmer, J., J., G. (2019). Structural and biochemical characterization of the pleckstrin homology domain of the RhoGEF P-Rex2 and its regulation by PIP3. *Journal of Structural Biology*, X 1, 100001.

32. Chen, X., Pan, M., Han, L., Lu, H., Hao, X., & Dong, Q. (2013). miR-338-3p suppresses neuroblastoma proliferation, invasion and migration through targeting PREX2a. *FEBS letters*, *587*(22), 3729–3737.

33. Cheng, G., Cao, Z., Xu, X., Meir, E. G., & Lambeth, J. (2001). Homologs of gp91 phox cloning and tissue expression of Nox3, Nox4, and Nox5. *Gene*, *269*(1-2), 131–140.

34. Cheng, G., Diebold, B. A., Hughes, Y., & Lambeth, J. D. (2006). Nox1-dependent reactive oxygen generation is regulated by Rac1. *The Journal of biological chemistry*, *281*(26), 17718–17726.

35. Chistiakov, D. A., Orekhov, A. N., & Bobryshev, Y. V. (2015). Endothelial Barrier and Its Abnormalities in Cardiovascular Disease. *Frontiers in physiology*, *6*, 365.

36. Chocry, M., & Leloup, L. (2020). The NADPH Oxidase Family and Its Inhibitors. *Antioxidants & redox signaling*, 10;33(5), 332-353.

37. Connolly, B. A., Rice, J., Feig, L. A., & Buchsbaum, R. J. (2005). Tiam1-IRSp53 complex formation directs specificity of rac-mediated actin cytoskeleton regulation. *Molecular and cellular biology*, *25*(11), 4602–4614.

38. Cook, D. R., Rossman, K. L., & Der, C. J. (2014). Rho guanine nucleotide exchange factors: regulators of Rho GTPase activity in development and disease. *Oncogene*, *33*(31), 4021–4035.

39. Cook-Mills, J. M., & Deem, T. L. (2005). Active participation of endothelial cells in inflammation. *Journal of leukocyte biology*, *77*(4), 487–495.

40. Cully, M., You, H., Levine, A. J., & Mak, T. W. (2006). Beyond PTEN mutations: the PI3K pathway as an integrator of multiple inputs during tumorigenesis. *Nature reviews. Cancer*, *6*(3), 184–192.

41. Deng, R., Li, F., Wu, H., Wang, W.-Y., Dai, L., Zhang, Z.-R., & Fu, J. (2018). Anti-inflammatory Mechanism of Geniposide: Inhibiting the Hyperpermeability of Fibroblast-Like Synoviocytes via the RhoA/p38MAPK/NF-κB/F-Actin Signal Pathway. *Frontiers in pharmacology*, *9*, 105.

42. Dominguez, R., & Holmes, K. C. (2011). Actin structure and function. *Annual review of biophysics*, *40*, 169–186.

43. Donald, S., Hill, K., Lecureuil, C., Barnouin, R., Krugmann, S., John Coadwell, W., Andrews, S. R., Walker, S. A., Hawkins, P. T., Stephens, L. R., & Welch, H. C. E. (2004). P-Rex2, a new guanine-nucleotide exchange factor for Rac. *FEBS letters*, *572*(1-3), 172–176.

44. Dröge, W. (2002). Free radicals in the physiological control of cell function. *Physiological reviews*, *82*(1), 47–95.

45. Du, X.-L., Edelstein, D., Rossetti, L., Fantus, I. G., Goldberg, H., Ziyadeh, F., Wu, J., & Brownlee, M. (2000). Hyperglycemia-induced mitochondrial superoxide overproduction activates the hexosamine pathway and induces plasminogen activator inhibitor-1 expression by increasing Sp1 glycosylation. *Proceedings of the National Academy of Sciences*, *97*(22), 12222–12226.

46. Dudek, S. M., & Garcia, J. G. N. (2001). Cytoskeletal regulation of pulmonary vascular permeability. *J Appl Physiol*, *91*, 1487–1500.

47. Dull, T., Zufferey, R., Kelly, M., Nguyen, R. J. M., Trono, D., Naldini, & Luigi (1998). A Third-Generation Lentivirus Vector with a Conditional Packaging System. *journal of virology*, *72*(11), 8463–8471.

48. Dupré-Crochet, S., Erard, M., & Nüβe, O. (2013). ROS production in phagocytes: why, when, and where? *Journal of leukocyte biology*, *94*(4), 657–670.

49. Dvorak, H. F. (2005). Angiogenesis: update 2005. *Journal of thrombosis and haemostasis JTH*, *3*(8), 1835–1842.

50. Dworakowski, R., Alom-Ruiz, S. P., & Shah, A. M. (2008). NADPH oxidase-derived reactive oxygen species in the regulation of endothelial phenotype. *Pharmacological reports PR*, *60*, 21–28.

51. Edens, W. A., Sharling, L., Cheng, G., Shapira, R., Kinkade, J. M., Lee, T., Edens, H. A., Tang, X., Sullards, C., Flaherty, D. B., Benian, G. M., & Lambeth, J. D. (2001). Tyrosine cross-linking of extracellular matrix is catalyzed by Duox, a multidomain oxidase/peroxidase with homology to the phagocyte oxidase subunit gp91phox. *The Journal of cell biology*, *154*(4), 879–891.

52. Eriksson, A., Cao, R., Roy, J., Tritsaris, K., Wahlestedt, C., Dissing, S., Thyberg, J., & Cao, Y. (2003). Small GTP-binding protein Rac is an essential mediator of vascular endothelial growth factor-induced endothelial fenestrations and vascular permeability. *Circulation*, *107*(11), 1532–1538.

53. Fine, B., Hodakoski, C., Koujak, S., Su, T., Saal, L. H., Maurer, M., Hopkins, B., Keniry, M., Sulis, M. L., Mense, S., Hibshoosh, H., & Parsons, R. (2009). Activation of the PI3K pathway in cancer through inhibition of PTEN by exchange factor P-REX2a. *Science (New York, N.Y.)*, *325*(5945), 1261–1265.

54. Finkel, T. (2011). Signal transduction by reactive oxygen species. *The Journal of cell biology*, *194*(1), 7–15.

55. Franses, J. W., Drosu, N. C., Gibson, W. J., Chitalia, V. C., & Edelman, E. R. (2013). Dysfunctional endothelial cells directly stimulate cancer inflammation and metastasis. *International journal of cancer*, *133*(6), 1334–1344.

56. Frey, R. S., Ushio-Fukai, M., & Malik, A. B. (2009). NADPH oxidase-dependent signaling in endothelial cells: role in physiology and pathophysiology. *Antioxidants & redox signaling*, *11*(4), 791–810.

57. Garrett, T. A., van Buul, J. D., & Burridge, K. (2007). VEGF-induced Rac1 activation in endothelial cells is regulated by the guanine nucleotide exchange factor Vav2. *Experimental cell research*, *313*(15), 3285–3297.

58. Gavard, J., & Gutkind, J. S. (2006). VEGF controls endothelial-cell permeability by promoting the beta-arrestin-dependent endocytosis of VE-cadherin. *Nature cell biology*, *8*(11), 1223–1234.

59. Gavard, J., Patel, V., & Gutkind, J. S. (2008). Angiopoietin-1 prevents VEGF-induced endothelial permeability by sequestering Src through mDia. *Developmental cell*, *14*(1), 25–36.

60. Gogolla, N., Caroni, P., Lüthi, A., & Herry, C. (2009). Perineuronal nets protect fear memories from erasure. *Science (New York, N.Y.)*, *325*(5945), 1258–1261.

61. Goveia, J., Stapor, P., & Carmeliet, P. (2014). Principles of targeting endothelial cell metabolism to treat angiogenesis and endothelial cell dysfunction in disease. *EMBO molecular medicine*, *6*(9), 1105–1120.

62. Groeneveld, A. (2002). Vascular pharmacology of acute lung injury and acute respiratory distress syndrome. *Vascular Pharmacology*, *39*(4-5), 247–256.

63. Gulino-Debrac, D. (2013). Mechanotransduction at the basis of endothelial barrier function. *Tissue barriers*, *1*(2), e24180.

64. Gündüz, D., Klewer, M., Bauer, P., Tanislav, C., Sedding, D., Rohrbach, S., Schulz, R., & Aslam, M. (2015). Compound C inhibits in vitro angiogenesis and ameliorates thrombin-induced endothelial barrier failure. *European journal of pharmacology*, *768*, 165–172.

65. Gündüz, D., Thom, J., Hussain, I., Lopez, D., Härtel, F. V., Erdogan, A., Grebe, M., Sedding, D., Piper, H. M., Tillmanns, H., Noll, T., & Aslam, M. (2010). Insulin stabilizes microvascular endothelial barrier function via phosphatidylinositol 3-kinase/Akt-mediated Rac1 activation. *Arteriosclerosis, thrombosis, and vascular biology*, *30*(6), 1237–1245.

66. Guo, B., Liu, L., Yao, J., Ma, R., Chang, D., Li, Z., Song, T., & Huang, C. (2014). miR-338-3p suppresses gastric cancer progression through a PTEN-AKT axis by targeting P-REX2a. *Molecular cancer research MCR*, *12*(3), 313–321.

67. Guzik, T. J., Sadowski, J., Kapelak, B., Jopek, A., Rudzinski, P., Pillai, R., Korbut, R., & Channon, K. M. (2004). Systemic regulation of vascular NAD(P)H oxidase activity and nox isoform expression in human arteries and veins. *Arteriosclerosis, thrombosis, and vascular biology*, *24*(9), 1614–1620.

68. Hanada, T., & Yoshimura, A. (2002). Regulation of cytokine signaling and inflammation. *Cytokine & Growth Factor Reviews*, *13*, 413–421.

69. Hasan, S. S., & Siekmann, A. F. (2015). The same but different: signaling pathways in control of endothelial cell migration. *Current opinion in cell biology*, *36*, 86–92.

70. Hodakoski, C., Hopkins, B. D., Barrows, D., Mense, S. M., Keniry, M., Anderson, K. E., Kern, P. A., Hawkins, P. T., Stephens, L. R., & Parsons, R. (2014). Regulation of PTEN inhibition by the pleckstrin homology domain of P-REX2 during insulin signaling and glucose homeostasis. *Proceedings of the National Academy of Sciences of the United States of America*, *111*(1), 155–160.

71. Holmström, K. M., & Finkel, T. (2014). Cellular mechanisms and physiological consequences of redox-dependent signalling. *Nature reviews. Molecular cell biology*, *15*(6), 411–421.

72. Hotulainen, P., & Lappalainen, P. (2006). Stress fibers are generated by two distinct actin assembly mechanisms in motile cells. *The Journal of cell biology*, *173*(3), 383–394.

73. Imhof, B. A., & Aurrand-Lions, M. (2006). Angiogenesis and inflammation face off. *nature medicine*, *12*(2), 171–172.

74. Kawahara, T., & Lambeth, J. D. (2008). Phosphatidylinositol (4,5)-bisphosphate Modulates Nox5 Localization via an N-Terminal Polybasic Region. *Molecular Biology of the Cell*, *19*, 4020–4031.

75. Kim, H., Hwang, J.-S., Woo, C.-H., Kim, E.-Y., Kim, T.-H., Cho, K.-J., Seo, J.-M., Lee, S.-S., & Kim, J.-H. (2008). TNF-α-induced up-regulation of intercellular adhesion molecule-1 is regulated by a Rac-ROS-dependent cascade in human airway epithelial cells. *Experimental and Molecular Medicine*, *40*(2), 167–175.

76. Kim, Y.-W., West, X. Z., & Byzova, T. V. (2013). Inflammation and oxidative stress in angiogenesis and vascular disease. *Journal of molecular medicine*, *91*(3), 323–328.

77. Knezevic, I. I., Predescu, S. A., Neamu, R. F., Gorovoy, M. S., Knezevic, N. M., Easington, C., Malik, A. B., & Predescu, D. N. (2009). Tiam1 and Rac1 are required for platelet-activating factor-induced endothelial junctional disassembly and increase in vascular permeability. *The Journal of biological chemistry*, *284*(8), 5381–5394.

78. Koestler, S. A., Rottner, K., Lai, F., Block, J., Vinzenz, M., & Small, J. V. (2009). F- and G-actin concentrations in lamellipodia of moving cells. *PloS one*, *4*(3), e4810.

79. Komarova, Y. A., Kruse, K., Mehta, D., & Malik, A. B. (2017). Protein Interactions at Endothelial Junctions and Signaling Mechanisms Regulating Endothelial Permeability. *Circulation research*, *120*(1), 179–206.

80. Konior, A., Schramm, A., Czesnikiewicz-Guzik, M., & Guzik, T. J. (2014). NADPH oxidases in vascular pathology. *Antioxidants & redox signaling*, *20*(17), 2794–2814.

81. Kumar, P., Shen, Q., Pivetti, C. D., Lee, E. S., Wu, M. H., & Yuan, S. Y. (2009). Molecular mechanisms of endothelial hyperpermeability: implications in inflammation. *Expert reviews in molecular medicine*, *11*, e19.

82. Küppers, V., Vockel, M., Nottebaum, A. F., & Vestweber, D. (2014). Phosphatases and kinases as regulators of the endothelial barrier function. *Cell and tissue research*, *355*(3), 577–586.

83. Lamalice, L., Le Boeuf, F., & Huot, J. (2007). Endothelial cell migration during angiogenesis. *Circulation research*, *100*(6), 782–794.

84. Li, J.-M., & Shah, A. M. (2002). Intracellular localization and preassembly of the NADPH oxidase complex in cultured endothelial cells. *The Journal of biological chemistry*, *277*(22), 19952–19960.

85. Li, J.-M., & Shah, A. M. (2004). Endothelial cell superoxide generation: regulation and relevance for cardiovascular pathophysiology. *American journal of physiology. Regulatory, integrative and comparative physiology*, *287*(5), R1014-30.

86. Liao, Z., Cao, C., Wang, J., Huxley, V. H., Baker, O., Weisman, G. A., & Erb, L. (2014). The P2Y2 Receptor Interacts with VE-Cadherin and VEGF Receptor-2 to Regulate Rac1 Activity in Endothelial Cells. *Journal of biomedical science and engineering*, *7*(14), 1105–1121.

87. Lissanu Deribe, Y. (2016). Interplay between PREX2 mutations and the PI3K pathway and its effect on epigenetic regulation of gene expression in NRAS-mutant melanoma. *Small GTPases*, *7*(3), 178–185.

88. Lissanu Deribe, Y., Shi, Y., Rai, K., Nezi, L., Amin, S. B., Wu, C. C., Akdemir, K. C., Mahdavi, M., Peng, Q., Chang, Q. E., Hornigold, K., Arold, S. T., Welch, H. C. E., Garraway, L. A., & Chin, L. (2016). Truncating PREX2 mutations activate its GEF activity and alter gene expression regulation in NRAS-mutant melanoma. *Proceedings of the National Academy of Sciences of the United States of America*, *113*(9), E1296-305.

89. Liu, H., Yu, X., Yu, S., & Kou, J. (2015). Molecular mechanisms in lipopolysaccharide-induced pulmonary endothelial barrier dysfunction. *International immunopharmacology*, *29*(2), 937–946.

90. Liu, Y., Collins, C., Kiosses, W. B., Murray, A. M., Joshi, M., Shepherd, T. R., Fuentes, E. J., & Tzima, E. (2013). A novel pathway spatiotemporally activates Rac1 and redox signaling in response to fluid shear stress. *The Journal of cell biology*, *201*(6), 863–873.

91. Machin, P., A., Tsonou, E., Hornigold, D., C., Welch, H., C., E. (2021). Rho Family GTPases and Rho GEFs in Glucose Homeostasis. *Cells*, 10, 915.

92. Manser, E., Loo, T. H., Koh, C. G., Zhao, Z. S., Chen, X. Q., Tan, L., Tan, I., Leung, T., & Lim, L. (1998). PAK Kinases Are Directly Coupled to the PIX Family of Nucleotide Exchange Factors. *Molecular cell*, *1*, 183–192.

93. Marcos-Ramiro, B., García-Weber, D., & Millán, J. (2014). TNF-induced endothelial barrier disruption: beyond actin and Rho. *Thrombosis and haemostasis*, *112*(6), 1088–1102.

94. Marei, H., Carpy, A., Macek, B., & Malliri, A. (2016a). Proteomic analysis of Rac1 signaling regulation by guanine nucleotide exchange factors. *Cell cycle (Georgetown, Tex.)*, *15*(15), 1961–1974.

95. Marei, H., Carpy, A., Woroniuk, A., Vennin, C., White, G., Timpson, P., Macek, B., & Malliri, A. (2016b). Differential Rac1 signalling by guanine nucleotide exchange factors implicates FLII in regulating Rac1-driven cell migration. *Nature communications*, *7*, 10664.

96. Marei, H., & Malliri, A. (2017). GEFs: Dual regulation of Rac1 signaling. *Small GTPases*, *8*(2), 90–99.

97. McKenzie, J. A. G., & Ridley, A. J. (2007). Roles of Rho/ROCK and MLCK in TNF-alpha-induced changes in endothelial morphology and permeability. *Journal of cellular physiology*, *213*(1), 221–228.

98. Mehta, D., & Malik, A. B. (2006). Signaling mechanisms regulating endothelial permeability. *Physiological reviews*, *86*(1), 279–367.

99. Meng, D., Lv, D.-D., & Fang, J. (2008). Insulin-like growth factor-I induces reactive oxygen species production and cell migration through Nox4 and Rac1 in vascular smooth muscle cells. *Cardiovascular research*, *80*(2), 299–308.

100. Mense, S. M., Barrows, D., Hodakoski, C., Steinbach, N., Schoenfeld, D., Su, W., Hopkins, B. D., Su, T., Fine, B., Hibshoosh, H., & Parsons, R. (2015). PTEN inhibits PREX2-catalyzed activation of RAC1 to restrain tumor cell invasion. *Science signaling*, *8*(370), ra32.

101. Moldovan, L., Mythreye, K., Goldschmidt-Clermont, P. J., & Satterwhite, L. L. (2006). Reactive oxygen species in vascular endothelial cell motility. Roles of NAD(P)H oxidase and Rac1. *Cardiovascular research*, *71*(2), 236–246.

102. Monaghan-Benson, E., & Burridge, K. (2009). The regulation of vascular endothelial growth factor-induced microvascular permeability requires Rac and reactive oxygen species. *The Journal of biological chemistry*, *284*(38), 25602–25611.

103. Montezano, A. C., Burger, D., Ceravolo, G. S., Yusuf, H., Montero, M., & Touyz, R. M. (2011). Novel Nox homologues in the vasculature: focusing on Nox4 and Nox5. *Clinical science (London, England 1979)*, *120*(4), 131–141.

104. Mumbengegwi, D. R., Li, Q., Li, C., Bear, C. E., & Engelhardt, J. F. (2008). Evidence for a superoxide permeability pathway in endosomal membranes. *Molecular and cellular biology*, *28*(11), 3700–3712.

105. Muñoz-Chápuli, R., Quesada, A. R., & Angel Medina, M. (2004). Angiogenesis and signal transduction in endothelial cells. *Cellular and molecular life sciences CMLS*, *61*(17), 2224–2243.

106. Naikawadi, R. P., Cheng, N., Vogel, S. M., Qian, F., Wu, D., Malik, A. B., & Ye, R. D. (2012). A critical role for phosphatidylinositol (3,4,5)-trisphosphate-dependent Rac exchanger 1 in endothelial junction disruption and vascular hyperpermeability. *Circulation research*, *111*(12), 1517–1527.

107. Naldini, L., Blomer, U., Gallay, P., Ory, D., Mulligan, R., Gage, F. H., Inder, M. V., & Trono, D. (1996). In Vivo Gene Delivery and Stable Transduction of Nondividing Cells by a Lentiviral Vector. *Science (New York, N.Y.)*, *272*(5259), 263–267.

108. Niu, J., Profirovic, J., Pan, H., Vaiskunaite, R., & Voyno-Yasenetskaya, T. (2003). G Protein betagamma subunits stimulate p114RhoGEF, a guanine nucleotide exchange factor for RhoA and Rac1: regulation of cell shape and reactive oxygen species production. *Circulation research*, *93*(9), 848–856.

109. Noria, S., Xu, F., McCue, S., Jones, M., Gotlieb, A. I., & Langille, B. L. (2004). Assembly and Reorientation of Stress Fibers Drives Morphological Changes to Endothelial Cells Exposed to Shear Stress. *American Journal of Pathology*, *164*(4), 1211–1223.

110. Oakley, F. D., Abbott, D., Li, Q., Engelhardt, & John F. (2009). Signaling Components of Redox Active Endosomes: The Redoxosomes. *Antioxidants & redox signaling*, *11*(6), 1313-1333.

111. Pandiella, A., & Montero, J. C. (2013). Molecular pathways: P-Rex in cancer. *Clinical cancer research an official journal of the American Association for Cancer Research*, *19*(17), 4564–4569.

112. Papaharalambus, C. A., & Griendling, K. K. (2007). Basic mechanisms of oxidative stress and reactive oxygen species in cardiovascular injury. *Trends in cardiovascular medicine*, *17*(2), 48–54.

113. Park, K.-H., & Park, W. J. (2015). Endothelial Dysfunction: Clinical Implications in Cardiovascular Disease and Therapeutic Approaches. *Journal of Korean medical science*, *30*(9), 1213–1225.

114. Pearlstein, D. P., Ali, M. H., Mungai, P. T., Hynes, K. L., Gewertz, B. L., & Schumacker, P. T. (2002). Role of mitochondrial oxidant generation in endothelial cell responses to hypoxia. *Arteriosclerosis, thrombosis, and vascular biology*, *22*(4), 566–573.

115. Pellegrin, S., & Mellor, H. (2007). Actin stress fibres. *Journal of cell science*, *120*(Pt 20), 3491–3499.

116. Petrache, I., Verin, A. D., Crow, M. T., Birukova, A., Liu, F., & Garcia, J. G. (2001). Differential effect of MLC kinase in TNF-alpha-induced endothelial cell apoptosis and barrier dysfunction. *American journal of physiology. Lung cellular and molecular physiology*, *280*(6), L1168-78.

117. Potente, M., Gerhardt, H., & Carmeliet, P. (2011). Basic and therapeutic aspects of angiogenesis. *Cell*, *146*(6), 873–887.

118. Prasain, N., & Stevens, T. (2009). The actin cytoskeleton in endothelial cell phenotypes. *Microvascular research*, *77*(1), 53–63.

119. Prieto-Bermejo, R., & Hernández-Hernández, A. (2017). The Importance of NADPH Oxidases and Redox Signaling in Angiogenesis. *Antioxidants (Basel, Switzerland)*, *6*(2).

120. Qiao, J., Holian, O., Lee, B.-S., Huang, F., Zhang, J., & Lum, H. (2008). Phosphorylation of GTP dissociation inhibitor by PKA negatively regulates RhoA. *American journal of physiology. Cell physiology*, *295*(5), C1161-8.

121. Ray, R., & Shah, A. M. (2005). NADPH oxidase and endothelial cell function. *Clinical science (London, England 1979)*, *109*(3), 217–226.

122. Ridley, A., Paterson, H. F., Johnston, C. L., Diekmann, D., & Hall, A. (1992). The small GTP-binding protein Rac regulates growth factor-induced membrane ruffling. *Cell*, *70*, 401–410.

123. Rosenfeldt, H., Vázquez-Prado, J., & Gutkind, J. S. (2004). P-REX2, a novel PI-3-kinase sensitive Rac exchange factor. *FEBS letters*, *572*(1-3), 167–171.

124. Rossman, K. L., Der, C. J., & Sondek, J. (2005). GEF means go: turning on RHO GTPases with guanine nucleotide-exchange factors. *Nature reviews. Molecular cell biology*, *6*(2), 167–180.

125. Sawada, N., Li, Y., & Liao, J. K. (2010). Novel aspects of the roles of Rac1 GTPase in the cardiovascular system. *Current opinion in pharmacology*, *10*(2), 116–121.

126. Schlegel, N., & Waschke, J. (2014). cAMP with other signaling cues converges on Rac1 to stabilize the endothelial barrier- a signaling pathway compromised in inflammation. *Cell and tissue research*, *355*(3), 587–596.

127. Schröder, K. (2010). Isoform specific functions of Nox protein-derived reactive oxygen species in the vasculature. *Current opinion in pharmacology*, *10*(2), 122–126.

128. Sena, L. A., & Chandel, N. S. (2012). Physiological roles of mitochondrial reactive oxygen species. *Molecular cell*, *48*(2), 158–167.

129. Shao, M., Yue, Y., Sun, G.-Y., You, Q.-H., Wang, N., & Zhang, D. (2013). Caveolin-1 regulates Rac1 activation and rat pulmonary microvascular endothelial hyperpermeability induced by TNF-α. *PloS one*, *8*(1), e55213.

130. Singleton, P. A., Dudek, S. M., Chiang, E. T., & Garcia, J. G. N. (2005). Regulation of sphingosine 1-phosphate-induced endothelial cytoskeletal rearrangement and barrier enhancement by S1P1 receptor, PI3 kinase, Tiam1/Rac1, and alpha-actinin. *FASEB journal official publication of the Federation of American Societies for Experimental Biology*, *19*(12), 1646–1656.

131. Soga, N., Namba, N., McAllister, S., Cornelius, L., Teitelbaum, S. L., Dowdy, S. F., Kawamura, J., & Hruska, K. A. (2001). Rho family GTPases regulate VEGF-stimulated endothelial cell motility. *Experimental cell research*, *269*(1), 73–87.

132. Spindler, V., Schlegel, N., & Waschke, J. (2010). Role of GTPases in control of microvascular permeability. *Cardiovascular research*, *87*(2), 243–253.

133. Steven, S., Frenis, K., Oelze, M., Kalinovic, S., Kuntic, M., Bayo Jimenez, M. T., Vujacic-Mirski, K., Helmstädter, J., Kröller-Schön, S., Münzel, T., & Daiber, A. (2019). Vascular Inflammation and Oxidative Stress: Major Triggers for Cardiovascular Disease. *Oxidative medicine and cellular longevity*, *2019*, 7092151.

134. Suh, Y. A., Arnold, R. S., Lassegue, B., Shi, J., Xu, X., Sorescu, D., Chung, A. B., Griendling, K. K., & Lambeth, J. D. (1999). Cell transformation by the superoxide generating oxidase Mox1. *Nature*, *401*, 79–82.

135. Sukriti, S., Tauseef, M., Yazbeck, P., & Mehta, D. (2014). Mechanisms regulating endothelial permeability. *Pulmonary circulation*, *4*(4), 535–551.

136. Tan, W., Palmby, T. R., Gavard, J., Amornphimoltham, P., Zheng, Y., & Gutkind, J. S. (2008). An essential role for Rac1 in endothelial cell function and vascular development. *FASEB journal official publication of the Federation of American Societies for Experimental Biology*, *22*(6), 1829–1838.

137. Teixeira, G., Szyndralewiez, C., Molango, S., Carnesecchi, S., Heitz, F., Wiesel, P., & Wood, J. M. (2017). Therapeutic potential of NADPH oxidase 1/4 inhibitors. *British journal of pharmacology*, *174*(12), 1647–1669.

138. Tojkander, S., Gateva, G., & Lappalainen, P. (2012). Actin stress fibers--assembly, dynamics and biological roles. *Journal of cell science*, *125*(Pt 8), 1855–1864.

139. Turrens, J. F. (2003). Mitochondrial formation of reactive oxygen species. *The Journal of physiology*, *552*(Pt 2), 335–344.

140. Ushio-Fukai, M. (2006). Redox signaling in angiogenesis: role of NADPH oxidase. *Cardiovascular research*, *71*(2), 226–235.

141. van Buul, J. D., Geerts, D., & Huveneers, S. (2014). Rho GAPs and GEFs: controling switches in endothelial cell adhesion. *Cell adhesion & migration*, *8*(2), 108–124.

142. van der Vliet, A., & Cross, C. E. (2000). Oxidants, Nitrosants, and the Lung. *THE AMERICAN JOURNAL OF MEDICINE*, *109*, 398–421.

143. van Nieuw Amerongen, G. P., Draijer, R., Vermeer, M. A., van Hinsbergh, & Victor W. M. (1998). Transient and Prolonged Increase in Endothelial Permeability Induced by Histamine and Thrombin. *Circulation research*, *83*(11), 1115–1123.

144. van Nieuw Amerongen, G. P., Koolwijk, P., Versteilen, A., & van Hinsbergh, V. W. M. (2003). Involvement of RhoA/Rho kinase signaling in VEGF-induced endothelial cell

migration and angiogenesis in vitro. *Arteriosclerosis, thrombosis, and vascular biology*, *23*(2), 211–217.

145. van Watering, S., van Buul, J. D., Quik, S., Mul, F. P. J., Anthony, E. C., Klooster, J.-P. ten, Collard, J. G., & Hordijk, P. L. (2002). Reactive oxygen species mediate Rac-induced loss of cell-cell adhesion in primary human endothelial cells. *Journal of cell science*, *115*, 1837–1846.

146. van Wetering, S., van den Berk, N., van Buul, J. D., Mul, F. P. J., Lommerse, I., Mous, R., Klooster, J.-P. ten, Zwaginga, J.-J., & Hordijk, P. L. (2003). VCAM-1-mediated Rac signaling controls endothelial cell-cell contacts and leukocyte transmigration. *American journal of physiology. Cell physiology*, *285*(2), C343-52.

147. 1Vandenbroucke, E., Mehta, D., Minshall, R., & Malik, A. B. (2008). Regulation of endothelial junctional permeability. *Annals of the New York Academy of Sciences*, *1123*, 134–145.

148. Vargas, J. E., Chicaybam, L., Stein, R. T., Tanuri, A., Delgado-Cañedo, A., & Bonamino, M. H. (2016). Retroviral vectors and transposons for stable gene therapy: advances, current challenges and perspectives. *Journal of translational medicine*, *14*(1), 288.

149. Vouret-Craviari, V., Boquet, P., Pouysse´gur, J., & van Obberghen-Schilling, E. (1998). Regulation of the Actin Cytoskeleton by Thrombin in Human Endothelial Cells: Role of Rho Proteins in Endothelial Barrier Function. *Molecular Biology of the Cell*, *9*, 2639–2653.

150. Wang, H., Fotheringham, L., Wittchen, E. S., & Hartnett, M. E. (2015). Rap1 GTPase Inhibits Tumor Necrosis Factor-α-Induced Choroidal Endothelial Migration via NADPH Oxidase- and NF-κB-Dependent Activation of Rac1. *The American journal of pathology*, *185*(12), 3316–3325.

151. Welch, H. C. E. (2015). Regulation and function of P-Rex family Rac-GEFs. *Small GTPases*, *6*(2), 49–70.

152. Welch, H. C. E., Coadwell, W. J., Ellson, C. D., Ferguson, G. J., Andrews, S. R., Erdjument-Bromage, H., Tempst, P., Hawkins, P. T., & Stephens, L. R. (2002). P-Rex1, a PtdIns(3,4,5)P3- and Gβγ-Regulated Guanine-Nucleotide Exchange Factor for Rac. *Cell*, *108*, 809–821.

153. Wildenberg, G. A., Dohn, M. R., Carnahan, R. H., Davis, M. A., Lobdell, N. A., Settleman, J., & Reynolds, A. B. (2006). p120-catenin and p190RhoGAP regulate cell-cell adhesion by coordinating antagonism between Rac and Rho. *Cell*, *127*(5), 1027–1039.

154. Wójciak-Stothard, B., Entwistle, A., Garg, R., & Ridley, A. J. (1998). Regulation of TNF-α-induced reorganization of the actin cytoskeleton and cell-cell junctions by Rho, Rac, and Cdc42 in human endothelial cells. *Journal of cellular physiology*, *176*, 150–165.

155. Wolczyk, D., Zaremba-Czogalla, M., Hryniewicz-Jankowska, A., Tabola, R., Grabowski, K., Sikorski, A. F., & Augoff, K. (2016). TNF-α promotes breast cancer cell migration and

enhances the concentration of membrane-associated proteases in lipid rafts. *Cellular oncology (Dordrecht)*, *39*(4), 353–363.

156. Xu, S.-Q., Mahadev, K., Wu, X., Fuchsel, L., Donnelly, S., Scalia, R. G., & Goldstein, B. J. (2008). Adiponectin protects against angiotensin II or tumor necrosis factor alpha-induced endothelial cell monolayer hyperpermeability: role of cAMP/PKA signaling. *Arteriosclerosis, thrombosis, and vascular biology*, *28*(5), 899–905.

157. Yamagishi, S. I., Edelstein, D., Du, X. L., Kaneda, Y., Guzmán, M., & Brownlee, M. (2001). Leptin induces mitochondrial superoxide production and monocyte chemoattractant protein-1 expression in aortic endothelial cells by increasing fatty acid oxidation via protein kinase A. *The Journal of biological chemistry*, *276*(27), 25096–25100.

158. Yuan, S. Y., Shen, Q., Rigor, R. R., & Wu, M. H. (2012). Neutrophil transmigration, focal adhesion kinase and endothelial barrier function. *Microvascular research*, *83*(1), 82–88.

159. Zhang, C. (2008). The role of inflammatory cytokines in endothelial dysfunction. *Basic research in cardiology*, *103*(5), 398–406.

160. Zhang, D. X., & Gutterman, D. D. (2007). Mitochondrial reactive oxygen species-mediated signaling in endothelial cells. *American journal of physiology. Heart and circulatory physiology*, *292*(5), H2023-31.

161. Zhou, K., Wang, Y., Gorski, J. L., Nomurai, N., Collard, J., & Bokoch, G. M. (1998). Guanine Nucleotide Exchange Factors Regulate Specificity of Downstream Signaling from Rac and Cdc42. *The Journal of biological chemistry*, *273*(27), 16782–16786.

9 MATERIALS

9.1 Chemicals and Consumables

Chemical/consumable	Manufacturer
Acrylamide/Bisacrylamide (1:19) (40%; wt/vol)	SERVA Electrophoresis GmbH; Germany
Acetic acid	Merck; Darmstadt, Germany
Agarose gel powder	Sigma-Aldrich; Steinheim, Germany
Ammonium peroxydisulfate	Sigma-Aldrich; Steinheim, Germany
Ampicillin	Carl Roth; Karlsruhe, Germany
Bovine serum albumin	ThermoFisher Scientific; Waltham, USA
Bromophenol blue	Sigma-Aldrich; Steinheim, Germany
Calcium chloride	Merck; Darmstadt, Germany
Cell culture flasks	BD; Heidelberg, Germany
Cell culture plates	BD; Heidelberg, Germany
Cell scraper	Greiner; Nürtingen, Germany
Coomassie Brilliant Blue R250	Sigma-Aldrich; Steinheim, Germany
DAPI (4′,6-Diamidin-2-phenylindol)	Life Technologies; Carlsbad, USA
DCF-DA	Invitrogen™; Waltham, USA
Dimethyl sulfoxide	Sigma-Aldrich; Steinheim, Germany
Dithiothreitol (DTT)	Amersham Pharmacia, UK
DMEM	Gibco; Karlsruhe, Germany
DNA ladder (Fermentas GeneRuler 1 kb)	ThermoFisher Scientific; Waltham, USA

DNA gel loading dye (6X)	ThermoFisher Scientific; Waltham, USA
DNase/RNase free distilled water	Gibco; Karlsruhe, Germany
dNTP's	ThermoFisher Scientific; Waltham, USA
ECL solution	Bio-Rad; Hercules, USA
EDTA	Carl Roth; Karlsruhe, Germany
Endothelial cell growth medium	PromoCell; Heidelberg, Germany
Eppendorf tubes	Eppendorf; Hamburg, Germany
Ethanol	Carl Roth; Karlsruhe, Germany
Falcon tubes	BD; Heidelberg, Germany
FCS	PAA; Pasching, Austria
Filter papers	Biotech-Fischer; Reiskirchen, Germany
GelRed® Nucleic acid gel stain	Biotium; Fremont, USA
Gentamycin	Sigma-Aldrich; Steinheim, Germany
Glass cover slips	Menzel; Braunschweig, Germany
Glycerol (100%)	Sigma-Aldrich; Steinheim, Germany
Glycine	Carl Roth; Karlsruhe, Germany
HBSS	Gibco; Karlsruhe, Germany
HEPES	Merck; Darmstadt, Germany
Hydrogen chloride	Merck; Darmstadt, Germany
Isopropanol	Carl Roth; Karlsruhe, Germany
Kanamycin	Carl Roth; Karlsruhe, Germany
L-Glutamine [200mM]	Gibco; Karlsruhe, Germany
LB agar growth medium	Carl Roth; Karlsruhe, Germany

LB broth growth medium	Carl Roth; Karlsruhe, Germany
Magnesium chloride	Merck; Darmstadt, Germany
Magnesium sulfate	Merck; Darmstadt, Germany
Matrigel matrix	BD Bioscience; Heidelberg, Germany
Methanol	Merck; Darmstadt, Germany
Millipore water	Millipore; Eschborn, Germany
Milk powder	Sigma-Aldrich; Steinheim, Germany
Molecular weight marker	Sigma-Aldrich; Steinheim, Germany
MTT	Sigma-Aldrich; Steinheim, Germany
Nitrocellulose membrane	Schleicher und Schuell; Dassel, Germany
Non-fat milk powder	Sigma-Aldrich; Steinheim, Germany
Nonidet P-40	Sigma-Aldrich; Steinheim, Germany
Parafilm	American National; Greenwich, USA
Paraformaldehyde	Sigma-Aldrich; Steinheim, Germany
PBS	Life Technologies; Carlsbad, USA
Penicillin/streptomycin	Gibco; Karlsruhe, Germany
Pipette tips	Eppendorf AG; Hamburg, Germany
PMSF	Sigma-Aldrich; Steinheim, Germany

Proteinase K	Sigma-Aldrich; Steinheim, Germany
RNaseZAP®	Sigma-Aldrich; Steinheim, Germany
Serological pipettes	Sigma-Aldrich; Steinheim, Germany
Sodium bicarbonate	Carl Roth; Karlsruhe, Germany
Sodium chloride	Carl Roth; Karlsruhe, Germany
Sodium dodecyl sulfate	Sigma-Aldrich; Steinheim, Germany
Sodium fluoride	Sigma-Aldrich; Steinheim, Germany
Sodium hydroxide	Carl Roth; Karlsruhe, Germany
Sodium orthovanadate	Sigma-Aldrich; Steinheim, Germany
Sterile filters (0.22 µm)	Sartorius; Goettingen, Germany
Streptomycin	Carl Roth; Karlsruhe, Germany
Syringes	BD Bioscience; Heidelberg, Germany
TEMED	Sigma-Aldrich; Steinheim, Germany
Tris	Sigma-Aldrich; Steinheim, Germany
Tris base	Carl Roth; Karlsruhe, Germany
Triton X-100	Sigma-Aldrich; Steinheim, Germany
Trypan blue (4%)	Gibco; Karlsruhe, Germany
Tween 20	Sigma-Aldrich; Steinheim, Germany
Opti-MEM reduced serum medium	Gibco; Karlsruhe, Germany

β-mercaptoethanol	Sigma-Aldrich; Steinheim, Germany
Trizol	Sigma-Aldrich; Steinheim, Germany

9.2 Antibodies

Antibodies	**Manufacturer**
P-Rex2	Thermo Fisher Scientific; Waltham, USA
V5 tag	Invitrogen™; Waltham, USA
GAPDH	Cell Signaling Technologies; Frankfurt am Main, Germany
Rac1	Thermo Fisher Scientific; Waltham, USA
Histidine tag	Thermo Fisher Scientific; Waltham, USA
VE-cadherin (CD144)	BD Bioscience; Heidelberg, Germany
Alexa Fluor® 488 (FITC)	Thermo Fisher Scientific; Waltham, USA
Anti-Rabbit IgG, HRP-linked	Santa-Cruz Biotechnology; Heidelberg, Germany
Anti-Mouse IgG, HRP-linked	Santa-Cruz Biotechnology; Heidelberg, Germany

9.3 Enzymes and Inhibitors

Enzyme/Inhibitor	**Manufacturer**
Benzonase®	Merck; Darmstadt, Germany
Collagenase II	PAA Labs.; Pasching, Austria
cOmplete™ Protease Inhibitor Cocktail	Roche; Mannheim, Germany
Trypsin-EDTA	Gibco; Karlsruhe, Germany
AgeI-HF	New England Biolabs; Frankfurt, Germany
PvuI	New England Biolabs; Frankfurt, Germany
SacII	New England Biolabs; Frankfurt, Germany

9.4 Kits

Kit	Manufacturer
2x SYBR Green qPCR Master Mix	Bimake; Houston, USA
Active Rac1 Pull-Down and detection kit	Thermo Fisher Scientific; Waltham, USA
All-in-One cDNA Synthesis SuperMix	Bimake; Houston, USA
Direct-zol RNA Miniprep Plus	Zymo Research; Irvine, USA
Dynabeads® Protein G	Thermo Fisher Scientific; Waltham, USA
Gateway™ LR Clonase™ II Enzyme mix	Invitrogen™; Waltham, USA
jetPRIME® Transfection Reagent	PolyPlus Transfection; Illkirch, France
Pierce™ BCA Protein Assay Kit	Thermo Fisher Scientific; Waltham, USA
Plasmid Miniprep Kit I	peqGOLD, Avantor; Leighton Buzzard, UK
PureLink™ HiPure Plasmid Midiprep Kit	Invitrogen™; Waltham, USA
QIAquick Gel Extraction Kit	QIAGEN; Hilden, Germany
Quick Start™ Bradford Protein Assay Kit 2	Bio-Rad; Hercules, USA
ViraPower™ Lentiviral Packaging Mix	Invitrogen™; Waltham, USA

9.5 Plasmids

Plasmid	Provider
pcDNA3.1/nV5-DEST	Invitrogene, 12290010
pENTR-D-TOPO	Invitrogene, K2400-20
pENTR-Rac1-CA	Dr. Muhammad Aslam
pENTR-Rac1-DN	Dr. Muhammad Aslam
pENTR-Rac1-WT	Dr. Muhammad Aslam
pLenti-CMV-Blast-DEST	Addgene, #17451
pLenti-CMV-Puro-DEST	Addgene, #17452
PREX2 pcdna3.1 V5/his	Addgene, #41555
R777-E189 Hs.PREX2	Addgene, #70473

9.6 Equipments

Equipment	Manufacturer
Agarose gel electrophoresis system	Thermo Scientific; Waltham, USA
Autoclave	HMC Europe; Tüssling, Germany
Blotting chambers	Bio-Rad; Hercules, USA
Cell culture inserts	Thermo Scientific; Waltham, USA
Centrifuge (Beckman Allegra 64R)	Beckman Coulter Life Sciences; Krefeld, Germany
Centrifuge (cold-Sigma 1-15K)	Sigma-Aldrich; Steinheim, Germany
Centrifuge (Hettich® MIKRO 120)	Hettich Lab; Tuttlingen, Germany
Centrifuge (mini)	IKA; Staufen, Germany
Centrifuge (Rotanta 460 R)	Hettich Lab; Tuttlingen, Germany
Centrifuge (Sigma 6-16KS)	Sigma-Aldrich; Steinheim, Germany
CFX-96™ Real-time PCR system	Bio-Rad; Hercules, USA
ChemiDoc™ MP imaging systems	Bio-Rad; Hercules, USA
Fluorescence Microscope	Biorevo, KEYENCE; Neu-Isenburg, Germany
Heater (Präzitherm)	Harry Gestigkeit GmbH; Düsseldorf, Germany
Hemocytometer	Thermo Fisher Scientific; Waltham, USA
Incubators	Heraeus; Hanau, Germany
Laminar flow hood	Heraeus; Hanau, Germany
Light Microscope	Leica Microsystems; Wetzlar, Germany
Magnet stirrer	Jahnke und Kunkel; Staufen, Germany
Magnetic Stand	Ambion; Waltham, USA
Microplate reader Infinite 200	Tecan; Männedorf, Switzerland
MicroPulser Electroporator	Bio-Rad; Hercules, USA
Nanodrop 1000 spectrophotometer	Thermo Fisher Scientific; Waltham, USA
Permeability assay; IPC	Ismatech; Wertheim, Germany
Permeability assay; Specord s 600	Analytik Jena; Jena, Germany
pH-Meter	WTW; Weinheim, Germany
Power supply	Biometra; Goettingen, Germany
Scale	Sartorius; Göttingen, Germany

SDS-PAGE apparatus	Bio-Rad; Hercules, USA
Thermal cycler	Biometra; Goettingen, Germany
Thermo Shaker	Biometra; Goettingen, Germany
Vortex	Heidolph Instruments; Schwabach, Germany
Water bath	Julabo; Seelbach, Germany
Water demineralization unit	Millipore; Eschborn, Germany

9.7 Software

Software	**Manufacturer**
BioRad CFX Manager	Bio-Rad; Hercules, USA
Cell D	Olympus Life Science; Waltham, USA
CellSens Dimensions	Olympus Life Science; Waltham, USA
Graph Pad Prism	GraphPad Software; San Diego, USA
Image J	Wayne Rasband; NIH, USA
Image Lab	Bio-Rad; Hercules, USA
Microsoft Office 2010	Microsoft; Redmond, USA
Quantity one ® 1-D analysis software	Bio-Rad; Hercules, USA
SnapGene by Dotmatics	GSL Biotech LLC; San Diego, USA

10 LIST OF ABBREVIATIONS

α	Alpha
β	Beta
βγ	Beta-gamma
β-PIX	Beta-p21-activated Kinase (PAK)-interacting Exchange Factor
Δ	Delta
µ	Micro
µg	Micro gram
µL	Micro liter
$^{\circ}C$	Degree Celsius
AJ	Adherens Junction
Akt	Serine/threonine-specific protein kinase B
APS	Ammonium Persulfate
BCA	Bicinchoninic Acid
bp	Base pairs
BSA	Bovine Serum Albumin
$CaCl_2$	Calcium Chloride
cAMP	Cyclic Adenosine 3′,5′-monophosphate
Cdc42	Cell division control Protein 42 Homolog
cDNA	Complementary DNA
CFU	Colony Forming Unit
CO_2	Carbon Dioxide
CRISPR	Clustered Regularly Interspaced Short Palindromic Repeats
Ct	Cycle Threshold
CYP	Cytochrome P450
DAPI	4′,6-diamidino-2-phenylindole
DCF-DA	2',7'-dichlorofluorescein Diacetate
DEP	Disheveled, EGL-10, and Pleckstrin homology
DH	Diffuse B-cell Lymphoma Homology

dH_2O	Deionized Water
DMEM	Dulbecco's Modified Eagle Medium
DMSO	Dimethyl Sulfoxide
DNA	Deoxyribonucleic Acid
Dox	Doxycycline
DTT	1,4 -Dithiothreitol
DUOX	Dual Oxidase
EC	Endothelial Cell
E-cadherin	Epithelial Cadherin
ECL	Chemiluminescence
E.coli	*Escherichia coli*
ECM	Extracellular Matrix
EDTA	Ethylenediaminetetraacetic Acid
eNOS	Endothelial Nitric Oxide Synthase
et al.	et alia
F-actin	Filamentous Actin
$FADH_2$	Dihydroflavine-Adenine Dinucleotide
FBS	Fetal Bovine Serum
FCS	Fetal Calf Serum
Fig.	Figure
FITC	Fluorescein-5-isothiocyanate
FLII	Flightless-1 Homolog
g	Gram
GAP	GTPase Activating Protein
G-actin	Globular Actin
GAPDH	Glyceraldehyde-3-phosphate Dehydrogenase
GDI	GDP Dissociation Inhibitor
GDP	Guanosine Diphosphate
GEFs	Guanine Nucleotide Exchange Factors
GFP	Green Fluorescent Protein

GST	Glutathione S-transferase
GTP	Guanosine Triphosphate
h	Hour
HA	Hemagglutinin
HBSS	Hank's Balanced Salt Solution
HCl	Hydrogen Chloride
HEK-293	Human Embryonic Kidney Cells 293
HEPES	N-2-hydroxyethyl Piperazine-N'-2-ethane Sulfonic Acid
HIV	Human Immunodeficiency Virus
His	Histidine
HRP	Horse Radish Peroxidase
Hsp90	Heat Shock Protein 90
HUVECs	Human Umbilical Vein Endothelial Cells
H_2O	Water
H_2O_2	Hydrogen Peroxide
ICAM-1	Intercellular Cell Adhesion Molecule 1
IFN-γ	Interferon-gamma
IgG	Immunglobulin G
IL	Interleukin
IL-1β	Interleukin-1 Beta
IP	Immunoprecipitation
IP4P	Inositol Polyphosphate-4 Phosphatase
IU	International Unit
KCl	Potassium Chloride
kDa	Kilo Dalton
KH_2PO_4	Potassium Dihydrogen Phosphate
L	Liter
LB	Lysogeny Broth
LTRs	Long Terminal Repeats
M	Molar

min	Minute
mg	Milligram
$MgCl_2$	Magnesium Chloride
$MgSO_4$	Magnesium Sulfate
mL	Milliliter
MLC	Myosin Light Chains
MLCK	Myosin Light Chain Kinase
MLCP	Myosin Light Chain Phosphates
mM	Millimolar
MnSOD	Mitochondrial Superoxide Dismutase
mRNA	Messenger RNA
NAC	N-Acetyl-L-cysteine
NaCl	Sodium Chloride
NADH	Nicotinamide Adenine Dinucleotide
NADPH	Nicotinamide Adenine Dinucleotide Phosphate
NaF	Sodium Fluoride
ng	Nanogram
$NO\cdot$	Nitrite Oxide
NOX	Nicotinamide Adenine Dinucleotide Phosphate Oxidase
NP-40	Nonyl Phenoxypolyethoxylethanol
ns	Not Significant
ORF	Open Reading Frame
$O_2^{-}\cdot$	Superoxide
$\cdot OH$	Hydroxyl Radicals
$ONOO^{\cdot-}$	Peroxynitrite
PAF	Platelet-activating Factor
PAK1	p21-activated Kinase 1
PBD	p21-binding Domain
PBS	Phosphate Buffered Saline
PCR	Polymerase Chain Reaction

PDZ	Postsynaptic density protein of 95 kDa (PSD95), *Drosophila* disc large tumor suppressor (DlgA), and Zonula occludens-1 protein (Zo-1)
PFA	Paraformaldehyde
PI3K	Phosphoinositide-3-kinase
PIP_2	Phosphatidylinositol 4,5-bisphosphate
PIP_3	Phosphatidylinositol-3,4,5-trisphosphat
pH	Power of Hydrogen
PH	Pleckstrin Homology
PKA	Protein Kinase A
PMSF	Phenylmethylsulphonyl Fluoride
P-Rex1	Phosphatidylinositol-3,4,5-Trisphosphate Dependent Rac Exchange Factor 1
P-Rex2	Phosphatidylinositol-3,4,5-Trisphosphate Dependent Rac Exchange Factor 2
PTEN	Phosphatase and Tensin Homolog on Chromosome 10
PVDF	Polyvinylidene Fluoride
P2Y2R	Gq protein-coupled P2Y2 Nucleotide Receptor
q-PCR	Quantitative Real Time Polymerase Chain Reaction
Rac1	Ras-related C3 Botulinum Toxin Substrate 1
Rac1-CA	Constitutively Active Rac1
Rac1-DN	Dominant Negative Rac1
RE	Restriction Enzyme
RhoA	Ras Homolog Family Member A
RNA	Ribonucleic Acid
ROCK	Rho-associated Kinase
ROS	Reactive Oxygen Species
RT	Room Temperature
SDS	Sodium Dodecyl Sulfate
SDS-PAGE	Sodium Dodecyl Sulfate–Polyacrylamide Gel Electrophoresis
sec	Second
S.E.M.	Standard Error of the Mean

siRNA	Small-interfering RNA
S1P	Sphingosine-1-phosphate
TAE	Tris base, Acetic acid and EDTA
TBS	Tris Buffered Saline
TBS-T	Tris Buffered Saline with Tween
TE	Tris-EDTA
TEM	Trans-endothelial Migration
TEMED	Tetramethylethylenediamine
Tiam1	T-cell Lymphoma Invasion and Metastasis 1
TJs	Tight Junctions
TNF-α	Tumor Necrosis Factor-alpha
TRITC	Tetramethyl Rhodamine
V	Volt
Vav2	Vav Guanine Nucleotide Exchange Factor 2
VCAM-1	Vascular Cell Adhesion Molecule-1
VE-cadherin	Vascular Endothelial Cadherin
VEGF	Vascular Endothelial Growth Factor
VEGFR	Vascular Endothelial Growth Factor Receptor
vol./vol.	Volume / Volume
WB	Western Blot
wt./vol.	Weight / Volume
WT	Wild Type
XO	Xanthine Oxidase
x g	Times Gravity (Relative Centrifugal Force (RCF))

11 ACKNOWLEDGMENT

First, I would like to thank my supervisor, Dr. Muhammed Aslam, for allowing me to conduct research as a Ph.D. student in his group. I have appreciated his scientific guidance in my thesis and his support in teaching me the required techniques for my research. Additionally, I am grateful to Dr. Christian Troidl and Prof. Christian Hamm for the chance to work as a part of the Experimental Cardiology group.

I would like to especially thank Dr. Christoph Lipps for much helpful advice and scientific assistance. I am deeply grateful to Prof. Dr. Dagmar Wirth for her valuable support in providing endothelial cell line Hu-ARLT. Special thanks to Daniela Reitz and Henrike Thomas for always being willing to help and for their valuable support for performing cell culture experiments. I also would like to thank Behnoush, Antje, Sabine, and Stefi for their assistance and support. I am grateful to Julia for her valuable support every time I need it. I also would like to thank Hifza Idrees for her good fellowship and support.

Lastly, I am deeply grateful to my friends and dear family for their constant support and presence whenever I need them. I especially would like to thank to Edibe, Selin, Cemile, Sebnem, and Ipek for their continuous support and understanding. Dear Dogan, I am so grateful to have you in my life and for your support in letting me through all the difficulties.

Sevgili ailem, sizin desteğiniz, güveniniz ve sevginiz olmadan ilerlemem mümkün değildi. Maddi manevi her zaman yanımda olduğunuz için size sonsuz teşekkür ediyorum. Aramızdaki mesafeye rağmen kendimi hiç yalnız hissettirmediniz. Siz benim hayattaki en büyük şansımsınız, sizi çok seviyorum ve hep minnettar olacağım.

Neslihan Sevinç

Gießen, 2022